Computational methods for identifying biomarkers of cognitive decline in Parkinson`s Disease using Quantitative EEG

Inauguraldissertation

zur

Erlangung der Würde eines Doktors der Philosophie

vorgelegt der

Philosophisch-Naturwissenschaftlichen Fakultät

der Universität Basel

von

MENORCA CHATURVEDI

von **Indien**

Basel, 2020

Genehmigt von der Philosophisch-Naturwissenschaftlichen Fakultät
auf Antrag von

Faculty Representative: Prof. Dr. Volker Roth

Thesis advisor: Prof. Dr. Peter Fuhr

Co-Referee: Prof. Dr. Stephan Ruegg

Basel, den 17. Dec 2019

Prof. Dr. Martin Spiess, Dekan

Abstract

Neurological disorders are the leading cause of disability and the second leading cause of death worldwide. Among these diseases, neurodegenerative disorders constitute a considerable segment, the two most common ones being Alzheimer's (AD) and Parkinson's disease (PD), which are also the leading causes of dementia. Dementia is a severe burden on the quality of life of the patients and their caregivers. As there is still no cure for the cause of neurodegenerative diseases, dementia due to AD and PD can only be treated symptomatically to some extent. For any potential clinical studies aiming at finding curative agents for neurodegenerative dementias, it is critical to intervene at a very early stage of the disease, when a substantial part of neurons are still alive and can be preserved. Moreover, symptomatic interventions by lifestyle change or drug application are likely more effective when applied early in the disease course. For these reasons, new approaches to assess the risk of dementia in cognitively healthy or only mildly affected patients is essential.

This thesis focusses on finding potential diagnostic and prognostic biomarkers of cognitive decline in Parkinson's disease patients, extensively investigating patterns in brain waves through electroencephalogram (EEG) recordings. In a real-world clinical study at one centre, it is common to have data from a limited number of patients. However, due to the nature of EEG data, the number of features extracted can be much higher than the number of patients, resulting in sparse data requiring suitable analysis methods. The different studies carried out for this project aimed at feature selection – both, for distinguishing PD patients from healthy controls as well as PD patients with Mild Cognitive Impairment from those without, and investigating the association of EEG features with cognitive tests. Through a collaboration, it was also possible to evaluate EEG as a potential marker for patients at the prodromal stage or before there are enough symptoms to have a clear clinical diagnosis of Parkinson's disease.

The first significant outcome of this thesis was identifying optimal methods for feature selection and using penalized regression for shortlisting EEG spectral power features to classify PD patients from healthy individuals using high-density as well as standard 10-20 EEG recording systems. This was also tested on some prodromal PD patients. Theta spectral power came out as an important feature in both studies and was highly associated with dopamine depletion in the brain, as seen with DaTscan imaging on a subset of prodromal and PD patients. Another outcome was finding connectivity measures in delta and theta bands to be of high importance in identifying PD patients with Mild Cognitive Impairment and finding correlations between memory and connectivity in the theta band, attention and connectivity in the beta band. On following up on a subset of these patients for 5 years, theta spectral power and connectivity were found to have the strongest association with the change in cognition, in line with our hypothesis based on all the baseline studies. Our data suggest that theta activity can be a diagnostic marker for PD and prognostic marker for cognitive decline in Parkinson's disease, eventually leading to dementia.

Abbreviations

AD- Alzheimer's disease

AUC = area under the curve

CI-OCS - change index in overall cognitive score

DAT - dopamine active transporter

EEG – Electroencephalogram

fMRI – functional MRI

GP- Global spectral power

HR-PD_{EEG+} - individuals with high risk for motor Parkinson's disease and similarity in EEG pattern of Parkinson's disease patients

HR-PD_{EEG-} individuals with high risk for motor Parkinson's disease without similarity in EEG pattern of Parkinson's disease patients

LASSO – least absolute shrinkage and selection operator

LED- Levodopa equivalent dosage

LR+ / LR- positive and negative likelihood ratio

MCI – Mild Cognitive Impairment

MMSE – Mini Mental State Examination

PD – Parkinson's disease

PET- positron emission tomography

PLI – Phase Lag Index

ROC- Receiver Operator Curve

SN - substantia nigra

SPECT - single-photon emission computed tomography

TCS- Transcranial Sonography

Acknowledgements

The past few years have been an incredible journey, full of growth, challenges and learning; learning not only in terms of expanding my knowledge but to be more persistent, resilient and immensely patient. For this, I have several people to thank for their support, guidance and patience.

Thanks to Prof. Dr. Peter Fuhr and Prof. Dr. Ute Gschwandtner for giving me the opportunity to work with them in the first place, on an entirely new topic for me, when I was new to Basel. Little did I know that this would turn out to be such a long association, one that would constitute a highly significant part of my life. A big thank you to Prof. Dr. Volker Roth for accepting me into his group and for giving consistent guidance, support and for being there whenever I needed help. Thank you for your patience and for teaching me so much on a personal and professional level. People make all the difference, whether it is about adjusting to a new city or working in a team. I am thankful to all my colleagues, especially Dr. Antonia Meyer and Dr. Vitalli Kozak for always being around, helping me out and being part of my Basel experience. I learnt a lot from my former colleagues, Dr. Habib Bousleiman, Dr. Ronan Zimmermann, Dr. Jan Guy Bogaarts, Dr. Rainer Nehring, and am thankful to the rest of the members of the Neurology and Informatics Departments for the congenial work atmosphere.

Thank you Dr. Stephan Ruegg, Dr. Florian Hatz, Dr. Martin Hardmeier, Sebastian Keller, Dr. Dinu Kauffmann, Damien Murezan, Dr. Sonali Parbhoo, Dr. Luigi Cannavacciuolo, Anna Adornetto, Ivana Handabaka, Selina Beltrani, Ketevan Toloraia, Christian Saleh, and everyone else from the BMDA group for your ideas, empathy, support and fun conversations.

A hugely enriching part of my PhD experience has been participating in numerous conferences, transferable skills workshops, seminars and other events for my professional and personal development. For this, I'm genuinely grateful to the University of Basel for offering transferable skills courses every semester, providing travel support for conferences, organizing lunch talks for PhD researchers via the AvuBa, offering start-up courses/workshops via the Innovation Office and for several other opportunities like writing for SciFive, the official blog.

Basel has provided me with a vast support system and has helped me expand my network enormously. I'm so grateful to my friends and flatmates, especially Debi, Kathi but also Helen and Sarah for always listening to me patiently, indulging in various Swiss and non-Swiss experiences with me and attempting to teach me German/Swiss German! I'm especially grateful to my friends from Germany and India, now spread all over the world, who are always only a phone call away and have never stopped being supportive or making me feel included, irrespective of how far we may be or how often (or not) we meet. Thank you Sonanki, Upasana, Benazir, Anuja, Monitha, Vishal, Sankalp for your constant encouragement and Pranika, Anna for making my stay more memorable. I'm also glad to have been part of various organizations in Basel, attend events regularly to stay updated with trends in the healthcare industry and meet some wonderful people along the way. Marini, thank you for helping me through a challenging phase.

Perhaps the people I am and will be the most grateful for, always, are my family. My parents have taught me the true meaning of being patient and resilient and have never given up, no matter how hard the situation might be and how stressed, anxious or even impatient I may have been. From constantly trying to understand my research to being supportive in my most anxiety ridden and confusing days and never failing to call to ask how I'm doing; they have always been there for me and I'm beyond thankful for having them and my brother in my life.

My personal motivation and purpose have always been: continuous growth and impacting people's lives via healthcare and education. This entire PhD experience has contributed to my growth and learning. I now look forward to taking this further and working towards impactful change in society. I hope to inspire many others the same way as so many of you have inspired and influenced me, whether or not you may have realized. Thank you yet again.

Table of Contents

Abstract **1**

Abbreviations **2**

Acknowledgements **3**

1. Introduction **7**

1.1 Neurodegeneration and biomarkers 7
1.2 Applications of machine learning in neurodegeneration 9
1.3 Synchronization in the brain 10
1.4 Motivation and aim of the thesis 12
1.5 Outline 14
1.6 List of Publications 15

2. Parkinson's disease **16**

2.1 Disease progression 16
2.2 Cognitive decline and dementia 20
2.3 Current diagnostic methods for Parkinson's disease 21

3.QEEG features as biomarkers for cognitive decline in Parkinson's disease **27**

3.1 Neurophysiology underlying generation of EEG signals 27
3.2 Slowing of EEG in Parkinson's disease 28
3.3 EEG connectivity in Parkinson's disease patients 29
3.4 EEG features in Parkinson's disease dementia patients 30

4.Computational methods for Brain Signal Analysis **31**

4.1 EEG Recording and processing 31
4.1.1 EEG Features 34
4.2 Machine learning and statistical methods for analysing EEG data 35
4.2.1 The importance of sample size 36
4.2.2 Supervised learning methods 36
Linear regression for regression problems 37
Logistic Regression 38
Penalized regression for classification of sparse data 40
Decision Trees 40
Random Forest 42
Support Vector Machines 44
4.2.3 Cross- Validation 45

5. Diagnostic value of EEG in early Parkinson's disease **47**

5.1 Machine learning in high-density QEEG feature selection for classification 48
5.1.1 Introduction 48
5.1.2 Methods 49
5.1.3 Results 51

5.1.4 Discussion 57
5.2 Feature selection combining QEEG and neuropsychological measures 58
5.2.1 Introduction 58
5.2.2 Methods 58
5.2.3 Results 59
5.2.4 Conclusion 64
5.3 Visuospatial Ability and EEG Slowing in Patients with Parkinson's disease 65
5.3.1 Introduction 65
5.3.2 Materials and Methods 66
5.3.3 Results 68
5.3.4 Discussion 75

6. Predictive value of EEG in prodromal Parkinson's disease patients 80

6.1 Introduction 80
6.2 Materials and methods 81
6.3 Results 85
6.3.1 Differentiation between controls and Parkinson's diseasewith EEG 87
6.3.2 Association between disease-specific EEG pattern and 123I-FP-CIT-SPECT 89
6.3.3 Association between baseline risk and prodromal marker profile and EEG 90
6.3.4 Prediction of motor worsening after two years by EEG 90
6.3.5 Prediction of prodromal Parkinson's disease stage at the time of follow-up 91
6.3.6 Association between EEG and cognitive function 91
6.4 Discussion 92
6.5 Supplementary tables 96

7. EEG Connectivity in Mild Cognitive Impairment 98

7.1 Introduction 98
7.2 Methods 98
7.3 Results 102
7.3.1 Participant characteristics 102
7.3.2 EEG features in PD-MCI and non-MCI patients 103
7.3.3 Classifying PD patients according to MCI using PLI and spectral measures 104
7.3.4 Correlation of Cognitive domains and EEG features 109
7.4 Discussion 112

8. Theta as a potential prognostic marker 114

8.1 Theta spectral power as a predictor of cognitive decline at 3 years 114
8.2 Theta Global PLI and spectral power as predictors of cognitive decline at 5 years . 118

9. Integrated discussion and conclusion 123

9.1 Technical considerations 123
9.2 Clinical implications and challenges 125
9.3 Significance for patients and future direction 131

REFERENCES 132

1. Introduction

1.1 Neurodegeneration and biomarkers

Neurons are the building blocks of the nervous system, which includes the brain and spinal cord. The human brain consists of about 120 billion neurons (Herculano-Houzel, 2009) that can interact, collectively generating complex human behaviours, from sensorimotor response to consciousness. Since neurons do not replace themselves, the body, in the event of damage or death of neurons, cannot replace them. This leads to disorders spanning from movement (such as ataxias), to mental functioning (such as dementias). Neurodegeneration is defined by the progressive loss of structure or function of neurons that also includes the death of neurons (Heemels, 2016). Examples of neurodegenerative diseases include Parkinson's, Alzheimer's, and Huntington's diseases. Neurodegenerative disorders are becoming even more prevalent now, as the ageing population grows. According to the 2019 United Nations report on world population ageing (United Nations, Department of Economic and Social Affairs, Population Division., 2019), the world's population is expected to grow by 10% to 8.5 billion in 2030 and by 2050, one in 6 people worldwide are projected to be aged over 65 (16%), in comparison to one in 11 in 2019 (9%). Ageing has been linked to neurodegeneration due to some observed changes, but the process is especially influenced by factors like genetics, environment and accumulation of certain proteins, lysosomes in the brain.

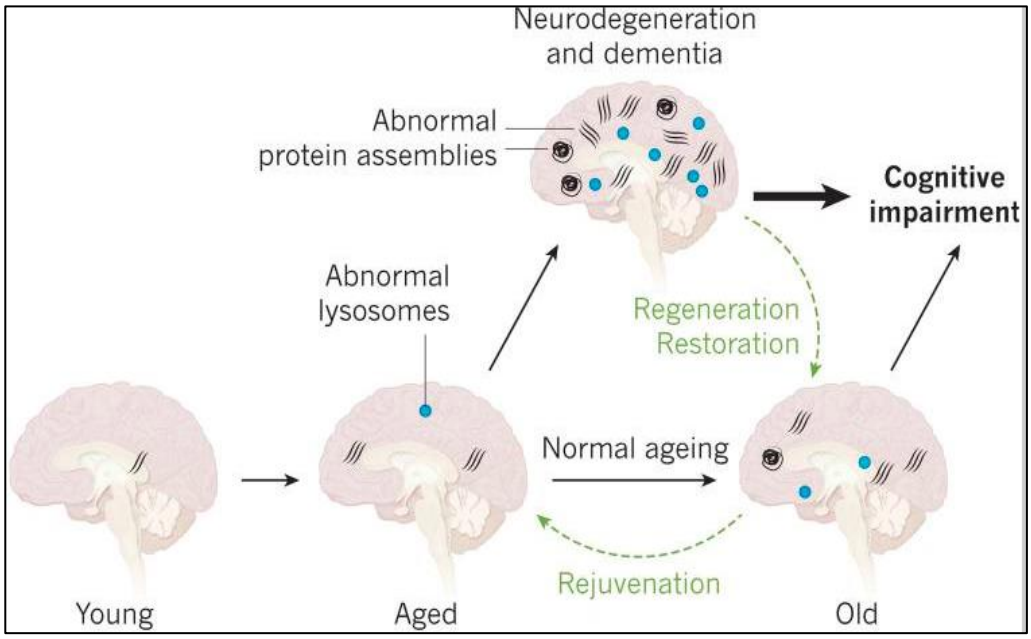

Figure 1.1: Ageing, neurodegeneration and brain rejuvenation (Wyss-Coray, 2016). Aged brains become highly prone to neurodegenerative diseases in which the same lesions amass as those that are found in old brains in smaller numbers. The relationship between such lesions and cognitive impairment is often blurred and normal ageing, neurodegeneration, and dementia can overlap. The concept of rejuvenation posits that old brains are malleable and that aspects of the ageing process can be reversed

to a younger stage. If this can be achieved, it might also be possible to slow or reverse neurodegeneration and cognitive impairment.

Neurodegeneration can begin at any point during an individual's lifespan and progress for several years before becoming clinically manifest (Savica *et al.*, 2010; Reiman *et al.*, 2012). This poses a significant obstacle for research into prevention and delays treatment. Although treatments may help relieve some of the physical or mental symptoms associated with neurodegenerative diseases, there is currently no way to slow disease progression and no known cures. As cognitive decline is a common symptom, leading up to dementia in many cases, any methods of early diagnosis and monitoring would be crucial for improving people's quality of life.

It has long been known that keeping track of certain measures of health can facilitate preventive medicine. These measures, known as biomarkers, could vary from blood pressure, cholesterol levels to antibodies and more tests of the blood and tissue, that could help in preventing and detecting events like heart attacks, stroke or other conditions like autoimmune diseases. A biomarker is defined as any substance, structure or process that can be measured in the body or its products and influence or predict the incidence of outcome or disease (WHO International Programme on Chemical Safety Biomarkers in Risk Assessment: Validity and Validation, 2001; Strimbu and Tavel, 2010). Biomarkers can be classified into four main types: diagnostic, prognostic, predictive, and response (FDA-NIH Biomarker Working Group, 2016). While a ***diagnostic biomarker*** detects or confirms the presence of a disease or condition of interest or can be used to identify individuals with a subtype of the disease, prognostic ***biomarkers*** identify likelihood of a clinical event, disease recurrence or progression in patients who have the disease or medical condition of interest. A ***predictive biomarker***, on the other hand, can be used to identify individuals who are more likely than similar individuals without the biomarker to experience a favourable or unfavourable effect from exposure to a medical product or an environmental agent. A ***response biomarker*** indicates if a biological response has occurred in an individual who has been exposed to a medical product or an environmental agent. Additionally, a therapeutic biomarker could be a protein, for instance, that could be used as target for a therapy.

As of 2019, biomarkers have expanded into digital measures (Coravos *et al.*, 2019), with wearables and smartphones being used to detect anomalies like atrial fibrillation (such as the Apple Watch with an ECG measuring component), irregular sleep patterns (using accelerometers), autism spectrum disorder using Electroencephalogram (EEG) (Bosl *et al.*, 2018) or tracking mental health, mood , movement and even asthma using smartphone apps.

In the past few years, a number of studies have worked towards identifying and validating neurodegenerative disease biomarkers too (Jeromin and Bowser, 2017). These biomarkers can include measurements of the blood, cerebrospinal fluid or brain imaging, for instance. Digital biomarkers are also being implemented in clinical trials for stratification of patients as well as monitoring the effects of drugs.

1.2 Applications of machine learning in neurodegeneration

With the increase in data generation and usage of new imaging as well as genetic techniques, the number of studies applying machine learning to investigate the brain further have also increased. The common goal of most of these studies is the early diagnosis of a neurological disorder or making prediction models for risk-assessment. The dimension of data varies depending on the equipment or the types of tests used and the data collection process. So, depending on the research question, sample size and type of data, suitable statistical tests and machine learning algorithms need to be applied or altered accordingly. In a very recent study (Álvarez *et al.*, 2019), researchers applied machine learning with feature selection for diagnosis and classification of neurodegenerative disorders, using Primary Progressive Aphasia (PPA) as the disease model. The main features used here were from positron emission tomography (PET) imaging, as identified from patient records via data mining, and the goal was to facilitate automatic diagnosis of this disease as well as identifying disease subtypes that correlated with the brain anatomy.

Feature selection and data mining are two of the many utilisations of big data that can facilitate knowledge discovery (Özyurt and Brown, 2009) and prediction of disease onset/worsening. This can ultimately lead to personalised health solutions. In one recent study, researchers applied deep learning techniques to investigate the neuropathology of tauopathy using digital images obtained from 22 brains after autopsy (Signaevsky *et al.*, 2019) and in another, deep learning was applied on MRI data of Alzheimer's disease patients from a longitudinal study to predict disease progression better (Pena *et al.*, 2019). Such applications and more (Singh *et al.*, 2019) of machine learning and artificial intelligence are consistently contributing to expanding our knowledge about neurodegeneration and also paving the way to learn more about related diseases.

Interpretability is crucial for the end user and for reliably using predictive models. Bias and problems can arise from either the model or the dataset itself. Sometimes, a model could also discover patterns unknown by experts, helping in generating new hypothesis. According to one research (Doshi-Velez and Kim, 2017), some of the factors to consider while evaluating the interpretability of a model, are:

- Application grounded (real tasks): Letting the end user or field experts evaluate it. E.g.: radiologists testing a fracture detection software to evaluate the model.
- Human grounded (simplified tasks): Having non-expert evaluators. E.g.: deciding which explanations seem more understandable or try to simulate the model.
- Functionally grounded (proxy) – Does not require humans. Experimentally shown to be correlated to human assessment. E.g.: decision tree depth

It is also important to consider the runtime complexity, usability, stability, reliability, knowledge needed to understand the model and how understandable a method is.

1.3 Synchronization in the brain

> *"Irrespective of whether it's neural activity, the clapping of a crowd or the rumbling of an earthquake, all of these phenomena occur because of a synchronization of oscillation patterns."*

With 120 billion neurons interacting amongst themselves, the brain indeed is a complex machinery. However, this complexity has a beautiful rhythm to it, a rhythm brought on by synchronization of brain waves. **But what are brain waves and what does synchronization really mean?**

Neurons or brain cells communicate via electrical impulses (Lovinger, 2008) and each of the neurons may oscillate in a rhythmic or wave-like pattern. In some instances, large groups of neurons oriented in the same direction may be oscillating together in harmony, creating synchronized electrical activity. This cumulative electrical activity is known as a brain wave. Due to the magnitude of these large-scale brain waves, it is possible to detect the electrical activity in different regions on the scalp with a medical device known as EEG which records the brain signals using electrodes attached to the scalp. Waves can vary in amplitudes and frequency, and there are five main kinds of brain waves of interest.

However, no single brainwave alone is considered more important than the other is. The different waves coexist; just that the dominance of a brain wave frequency can influence performance in specific functions and the synchronized ensembles may be linked to specific states of mind, like relaxation, sleep, etc.

The five brain waves in order of lowest frequency to highest are as follows:

Delta (1-4 Hz) - Delta is the slowest brain wave and is optimally associated with deep sleep. An excessive reduction in delta could lead to sleep problems.

Theta (4-8 Hz) - Theta is a slow wave, with 4 to 7 cycles per second. This could be associated with light sleep or drowsiness but also with meditation or relaxed state of mind. An increase in theta is linked to depression or problems in attention, for instance.

Alpha (8-13 Hz) – Alpha waves are dominant when an individual is calm, relaxed but alert, even with eyes closed.

Beta (13-30 Hz) – Beta are fast waves that optimally help people perform tasks requiring focus, like problem-solving, critical thinking etc. Caffeine or other energy drinks can stimulate these. Reduction in beta is linked to problems in cognition or attention.

Gamma (30-60 Hz) – Gamma waves are the fastest and said to be associated with information processing. A depiction of the different kinds of waves, as seen with an EEG recording, is shown in Figure 2.

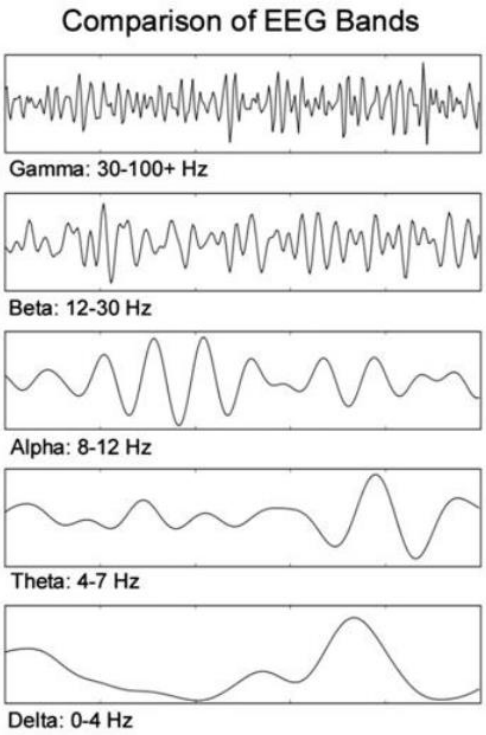

Figure 1.2: Depiction of different EEG bands

Apart from just visualizing the brain waves, we can now quantify and process the electrical signals with Quantitative EEG (qEEG). Applications of qEEG have been researched continuously in the past few years. Since EEG is a fast and non-invasive method to monitor the electrical activity of the brain, can provide a resolution of few milliseconds, and the equipment is not too expensive, it makes it a viable option to assess the changes in the electrical activity of the brain. The other neuroimaging techniques, like functional MRI (fMRI) or PET scans do not offer such high temporal resolution (they are limited to seconds), are more expensive, need more time for recording and are not mobile. Thus, EEG has some advantages over them.

EEG is used in clinics to investigate sleep disorders, monitor alertness, detecting and investigating brain regions affected by epileptic seizures (Rosenow *et al.*, 2015), drug effects and has also been used to investigate learning and cognition. In fact, EEG recordings of patients with neurodegenerative diseases like Alzheimer's disease, Parkinson's disease, Schizophrenia, Multiple Sclerosis have shown changes in patterns of the brain signals. This has opened up a very interesting field of research, one that we have explored further in our studies, focusing on Parkinson's disease and dementia.

However, it is difficult to accurately detect very low amplitude waves like gamma with an EEG on the surface of the head and distinguish them from muscle activity. Hence, for the scope of our work, we only focus on the role of the first four brain waves: delta, theta, alpha and beta.

1.4 Motivation and aim of the thesis

Dementia is a general term for a decline in mental ability severe enough to interfere with daily life. It is characterized by the loss of cognitive functioning—thinking, remembering, and reasoning—and behavioural abilities to such an extent that it interferes with a person's daily life and activities. It is not a specific disease, but several different diseases may cause dementia, Parkinson's and Alzheimer's disease being two of the leading causes (Emre, 2003*b*; Walker *et al.*, 2015). Parkinson's disease Dementia (PD-D) is associated with lower quality of life, caregiver dependency, and a higher rate of mortality. Neurological disorders are the leading cause of disability and the second leading cause of death worldwide(Carroll, 2019). Dementia is an emergent problem for ageing populations. It is also one of the non-motor symptoms of PD, which worsens outcomes and life expectancy of the patients (Emre, 2003*a*)(Levy *et al.*, 2002). Some studies have shown that patients with PD have an almost six-fold increased risk of developing dementia compared with age-matched individuals without PD (Aarsland *et al.*, 2001).

In a study carried out investigating the global burden of neurological disorders from 1990 to 2016 (Feigin *et al.*, 2019), various neurological diseases were investigated based on global deaths, disability-adjusted life years (DALYS) and prevalence. This global burden, for Alzheimer's and Parkinson's diseases, is shown in Table 1.1. About 50 million people are said to be living with dementia worldwide currently(Nichols *et al.*, 2019), and this number is predicted to increase to 152 million by 2050. Dementia is now ranked as the fifth leading cause of death, and the global economic burden comes close to a trillion dollars every year (World Health Organization.; Xu *et al.*, 2017).

Cognitive changes occur gradually in patients, with an intermediate condition between the normal cognition and dementia known as mild cognitive impairment (MCI) (Wood *et al.*, 2016). The progression rate from PD-MCI to PD dementia varies depending on factors like age, disease duration, etc., but one study found it to be 45–60% while following up patients for 4–12 years (Buter *et al.*, 2008) and a 49.28% prevalence rate was reported for dementia over 7 years (Sanyal *et al.*, 2014). Hence, methods of cognitive assessment and early identification of PD patients with a risk of dementia are of significant importance for clinicians to improve the quality of life of PD patients.

In this respect, QEEG has proved to be a useful approach for early prognosis of cognitive decline leading up to dementia. QEEG is an inexpensive, non-invasive and fast technique to assess the electrical activity of the brain. It is employed clinically as a measure of brain function in the hope of determining and differentiating certain functional conditions of the brain. QEEG is used in patients with cognitive dysfunction involving either a general decline of overall brain function or a localised or lateralized deficit.

	Absolute numbers (thousands)		Age-standardised rate (per 100 000 people)				
	2016	**Percentage change, 1990–2016**	**2016**	**Percentage change, 1990–2016**	**Males**	**Females**	**Male-to-female ratio**
Parkinson's disease							
Deaths	211 (168 to 265)	161% (152 to 171)	3 (3 to 4)	19% (16 to 23)	5 (4 to 6)	3 (2 to 3)	1·81 (1·74 to 1·89)
DALYs	3235 (2564 to 4013)	148% (140 to 156)	51 (41 to 63)	22% (18 to 26)	67 (53 to 83)	39 (31 to 49)	1·70 (1·63 to 1·76)
Prevalence	6063 (4971 to 7325)	145% (138 to 152)	94 (77 to 114)	22% (18 to 25)	112 (92 to 135)	80 (65 to 97)	1·40 (1·36 to 1·43)
Alzheimer's disease and other dementias							
Deaths	2382 (2060 to 2778)	148% (140 to 157)	41 (35 to 48)	4% (1 to 6)	37 (32 to 44)	43 (37 to 49)	0·88 (0·86 to 0·91)
DALYs	28 764 (24 511 to 33 952)	121% (115 to 127)	471 (401 to 556)	2% (0 to 4)	439 (373 to 523)	490 (417 to 576)	0·90 (0·88 to 0·92)
Prevalence	43 836 (37 756 to 51 028)	117% (114 to 121)	712 (614 to 828)	2% (1 to 2)	645 (555 to 752)	757 (652 to 879)	0·85 (0·85 to 0·86)

Table 1.1: Global deaths, DALYs, incidence, and prevalence per 100 000 people and age-standardised rates by neurological disorder category, 1990–2016 (Feigin *et al.*, 2019). Numbers in brackets are 95% uncertainty intervals. DALYs for traumatic brain injuries and spinal cord injuries include years lived with disability only (not years of life lost), because International Classification of Disease rules for cause of death reporting require that injury deaths are assigned to causes rather than consequences.

This project aims to explore the differences in high-resolution QEEG data between patients at different stages of Parkinson's disease and detect electrophysiological biomarkers for the risk of future Parkinson's disease dementia. The studies focussed on finding EEG patterns

associated with cognitive decline in PD patients using their clinical, neuropsychological and electroencephalographic data extensively at baseline and eventually, over 3 and 5 years.

The vision of this project is to detect prospective biomarkers of cognitive decline in PD that will contribute to providing a more comprehensive picture and assessment of the health status of a PD patient. Long-term assessment of Parkinson's disease patients is crucial for understanding the gradual cognitive decline and this study will analyse data recorded at three and five-year follow-ups. Using high-density EEG instead of conventional low-resolution EEG recording systems enables us to obtain more detailed information regarding the functioning of the brain. Combining QEEG and clinical features into a prognostic biomarker will allow clinicians to better assess the risk for cognitive decline.

1.5 Outline

In the following chapters, we will be going through the disease mechanisms, investigate EEG in detail and then look at applications of EEG in early diagnosis of Parkinson's disease and in using EEG as a potential marker for cognitive decline in Parkinson's disease. Chapter 2 describes the onset, progression of Parkinson's disease and describes the different diagnostic methods for cognitive decline and dementia. Chapter 3 focusses on EEG; how the signals are measured and how it has been applied so far in neurology, particularly the EEG features characteristic of Parkinson's disease and dementia. We then move on to the methodological section in Chapter 4 where we deep dive into brain signal analysis and look at machine learning methods that can be applied for analysing and interpreting the EEG data. Chapter 5 is an amalgamation of two published papers regarding EEG and early Parkinson's disease along with additional unpublished work using EEG and neuropsychological measures in classifying PD patients from healthy individuals. Going one-step further, Chapter 6 applies the findings of Chapter 5 and investigates a group of prodromal PD patients, or patients identified to be at risk of PD but not diagnosed clearly. Chapter 7 includes a publication investigating Mild Cognitive Impairment in Parkinson's disease, applying machine-learning methods to connectivity and spectral measures. Chapter 8 builds up on our knowledge and presents some results from following up the cohort at 3 and 5 years, establishing theta as a potential prognostic biomarker. Finally, Chapter 9 gathers the findings and learnings from all the described work and presents an integrated discussion.

1.6 List of Publications

- **Chaturvedi M**, Guy Bogaarts J, Kozak (Cozac) VV, Hatz F, Gschwandtner U, Meyer A, et al. Phase Lag Index and Spectral power as QEEG features for identification of patients with Mild Cognitive Impairment in Parkinson's disease. Clin Neurophysiol . (2019) DOI: 10.1016/j.clinph.2019.07.017
- **Chaturvedi M,** Hatz F, Gschwandtner U, Bogaarts JG, Meyer A, Fuhr P and Roth V (2017). Quantitative EEG (QEEG) measures differentiate Parkinson's disease (PD) patients from healthy controls (HC). Front. Aging Neurosci. 9:3. doi: 10.3389/fnagi.2017.00003
- **Chaturvedi M**, Yilmaz R, Gschwandtner U, Greulich K, Reimold M, Fuhr P, Roth V, Timmers M, Streffer J, Berg D, Liepelt-Scarfone I (2019) Quantitative EEG as a potential prodromal marker for Parkinson's disease. (Submitted)
- Cozac VV, **Chaturvedi M**, Hatz F, Meyer A, Gschwandtner U, Roth V, Fuhr P (2019) EEG slowing and axial motor impairment are independent predictors of cognitive worsening in a three-year cohort of patients with Parkinson's (Submitted)
- Cozac VV, **Chaturvedi M**, Hatz F, Meyer A, Fuhr P and Gschwandtner U (2016) Increase of EEG Spectral Theta Power Indicates Higher Risk of the Development of Severe Cognitive Decline in Parkinson's Disease after 3 Years. Front. Aging Neurosci. 8:284. doi: 10.3389/fnagi.2016.00284
- Cozac VV, Auschra B, **Chaturvedi M**, Gschwandtner U, Hatz F, Meyer A, Welge-Lüssen A and Fuhr P (2017) Among Early Appearing Non-Motor Signs of Parkinson's Disease, Alteration of Olfaction but Not Electroencephalographic Spectrum Correlates with Motor Function. *Front. Neurol.* 8:545. doi: 10.3389/fneur.2017.00545
- Eichelberger D, Calabrese P, Meyer A, **Chaturvedi M** et al., "Correlation of Visuospatial Ability and EEG Slowing in Patients with Parkinson's Disease," Parkinson's Disease, vol. 2017, Article ID 3659784, 11 pages, 2017. doi:10.1155/2017/3659784
- Dahdal P, Meyer A, **Chaturvedi M**, Nowak K, Roesch A, D, Fuhr P, Gschwandtner U, Fine Motor Function Skills in Patients with Parkinson Disease with and without Mild Cognitive Impairment. Dement Geriatr Cogn Disord 2016;42:127-134
- Cozac, V. V., Schwarz, N., Bousleiman, H., **Chaturvedi, M**., Ehrensperger, M. M., Gschwandtner, U., Hatz, F., Meyer, A., Monsch, A. U., Taub, E. and Fuhr, P. (2015), The Verbal Fluency Decline After Deep Brain Stimulation in Parkinson's Disease: Is There an Influence of Age? Movmnt Disords Clncl Practice. doi: 10.1002/mdc3.12231

2. Parkinson’s disease

Parkinson's disease (PD) is a progressive neurodegenerative disorder that affects 1–2 per 1000 of the population at any time. It’s prevalence increases with age (de Lau *et al.*, 2004; Barbosa *et al.*, 2006), to 1-2% of persons older than 60 years (Poewe *et al.*, 2008; Sveinbjornsdottir, 2016; Tysnes and Storstein, 2017). As of 2016, 6.1 million people worldwide were estimated to be affected (Dorsey *et al.*, 2018).

It is caused by the gradual loss of the dopamine-producing brain cells of the substantia nigra — located just above where the spinal cord meets the midbrain. The dopamine release facilitates the communication between the substantia nigra and parts like the basal ganglia, frontal lobe which are responsible for coordinating movements. The loss of dopamine obstructs this communication, resulting in movement disorders where people start losing control and start experiencing tremors, stumbling etc. Parkinson’s disease is one such movement disorder.

2.1 Disease progression

Parkinson's disease-related functional changes in basal ganglia

The basal ganglia is a group of nuclei embedded deep in the brain hemispheres(Lanciego *et al.*, 2012). This includes the striatum, globus pallidus, substantia nigra, and subthalamic nucleus (STN) which closely interact with the cerebral cortex and thalamus(DeLong and Wichmann, 2010) and the balance of signals facilitates movement control. In the basal ganglia, the striatum is the main input nucleus, and the dopamine receptors facilitate the modulatory effect of dopamine released from nigrostriatal terminal (Gerfen, 1992; Gerfen *et al.*, 1995). In PD, the loss of dopaminergic neurons in the substantia nigra results in the striatal dopamine depletion leading to an imbalance and thus, enhanced activity of the basal ganglia output nuclei, affecting the output to the motor cortex. At first, this may translate to symptoms like rigidity, slow movements, freezing but can gradually lead to tremors.

This collective basal ganglia unit is not only responsible for motor control but is also now found to be involved in other functions like attention, working memory, planning, learning, emotions and more.

Motor and non-motor symptoms

Parkinson's disease is characterised by some cardinal motor features such as bradykinesia, rest tremor, and rigidity. The motor symptoms can also include tremor, gait, speech or handwriting impairment (Moustafa *et al.*, 2016). They start appearing in the early stages of the disease and depend mainly on the dopamine reduction (Hughes *et al.*, 1992; Magrinelli *et al.*, 2016). Non-motor symptoms such as cognitive impairment, olfactory impairment, autonomic dysfunction, sleep alterations, behavioural abnormalities and cognitive deficits are also common in Parkinson’s disease patients (Pfeiffer, 2016; Aarsland *et al.*, 2017; Bago Rožanković *et al.*,

2017; Cozac *et al.*, 2017). These have a major impact on quality of life (Schrag *et al.*, 2000; Erro *et al.*, 2016).

Prodromal Parkinson's disease

When subtle signs of PD are present in a patient but do not fulfil the diagnostic criteria of the disease, it is referred to as, prodromal Parkinson's disease (Hughes et al., 1993, Berg et al., 2015a; Heinzel et al., 2016). By the time the full clinical picture allows the clinical PD diagnosis defining individuals in the prodromal PD period, at least 30-60% of dopaminergic cells (Dauer and Przedborski, 2003; Greffard et al., 2006; Cheng et al., 2010; Grosch et al., 2016) are likely to have been lost in the process of neurodegeneration of the substantia nigra. Several features characteristic of the prodromal stage, when combined, can denote an increased risk for onset of PD in the future (Ross *et al.*, 2012; Berg *et al.*, 2013; Noyce *et al.*, 2014) and may even correspond to the neuropathological staging of PD-associated pathology. A better understanding of the prodromal period is essential for the identification of individuals who could potentially convert to Parkinson's disease within a short time frame as a potential target group for upcoming neuroprotective trials.

An expert group of the International Parkinson's disease and Movement Disorder Society (MDS) has proposed research diagnostic criteria for the prodromal phase of Parkinson's disease, as a first attempt to quantify the risk of a single person to be in the prodromal stage of the disease (Berg *et al.*, 2015*a*). By use of a data-driven probabilistic approach, considering age to influence the incidence of disease onset, the occurrence of specific Parkinson's disease related risk and prodromal marker were combined into a prodromal risk score, based on the positive or negative likelihood ratio of each marker to predict future Parkinson's disease onset. So far, this approach is validated in several cohorts, confirming a higher prodromal risk score increasing the risk for Parkinson's disease conversion and higher prognostic values for conversion within longer follow-up periods. The prodromal risk scores have positive and negative predictive values between 19% to 77.8% and 52.9% to 99% (Mahlknecht *et al.*, 2016, 2018; Fereshtehnejad *et al.*, 2017; Pilotto *et al.*, 2017; Mirelman *et al.*, 2018). The time course of Parkinson's disease progression is illustrated in Figure 2.1. As seen, the prodromal period can start up to 10 or even 20 years before the disease can be diagnosed in its early stages.

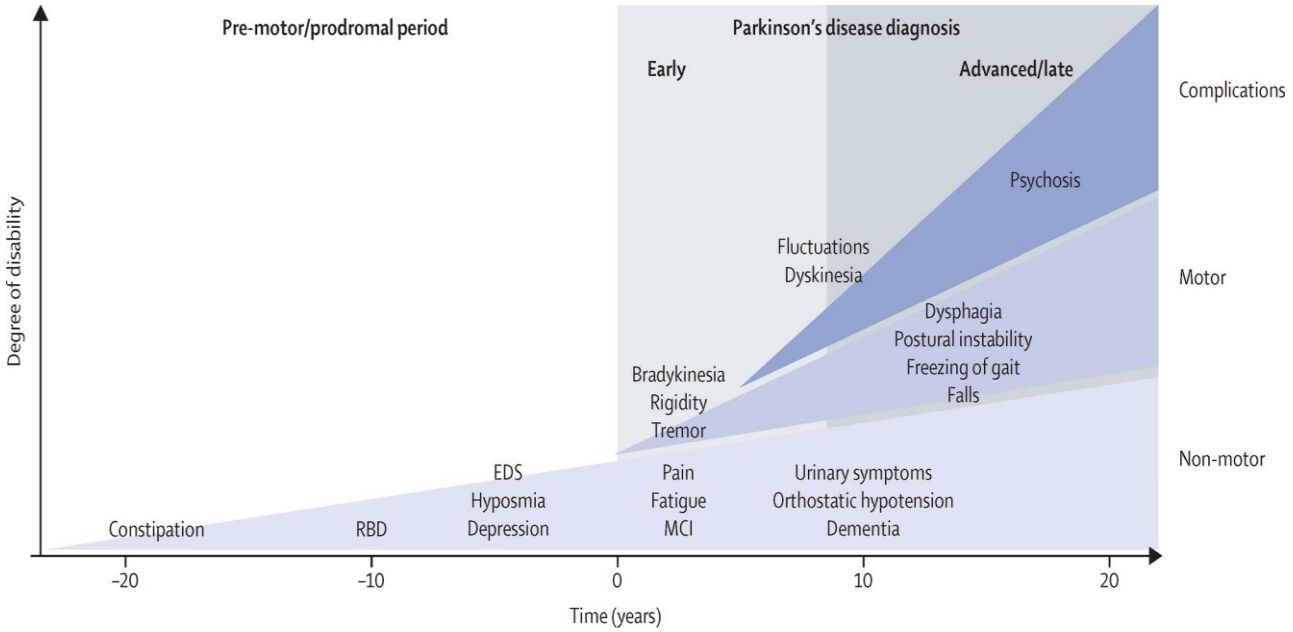

Figure 2.1: Clinical symptoms and time course of Parkinson's disease progression (Kalia and Lang, 2015)

Pathophysiology of disease progression

PD can have two forms: familial and sporadic. While the familial form is caused by genetic irregularities, among others in the gene for alpha-synuclein, the sporadic form may be caused by genetic and environmental factors and has been researched continuously(Rietdijk *et al.*, 2017). Some elements of sporadic PD are said to include neuroinflammation, oxidative stress, and alpha-Synuclein misfolding and aggregation (Drouin-Ouellet and Cicchetti, 2012; Zaltieri *et al.*, 2015).

The origin of sporadic Parkinson's disease and the spread of the disease through the different regions of the brain is not fully confirmed yet. But, several studies have been carried out to investigate this course further, and one popular hypothesis was put forth by Braak (Braak *et al.*, 2003; Braak and Del Tredici, 2017). According to his theory, the progression in Parkinson's disease goes through several stages, although it has been argued that this only describes a specific subset of patients with young-onset and long duration of the disease (Rietdijk *et al.*, 2017). It is said to begin when a pathogen comes into contact with and affects the neurons in the gut as well as in the olfactory system. The different stages are illustrated in Figure 2.2.

In the first two stages, some unknown pathogens or microbial products are said to come into contact with olfactory and/or enteric neurons, which trigger the aggregation of α-Synuclein. The earliest effects in the brainstem and olfactory system, as a result, could be seen as symptoms like constipation and losing the sense of smell.

The aggregated α-Synuclein spreads toward the central nervous system via the olfactory bulb and the vagus nerve during Stages 3 and 4. By this time, the olfactory system is likely to have been significantly damaged, and the disease spreads in the limbic system, which is linked to

emotion, long-term memory. Eventually, in Stage 5, the aggregated α-Synuclein arrives at the substantia nigra. Genetic factors are likely to contribute to PD, but the exact mechanism remains to be clarified.

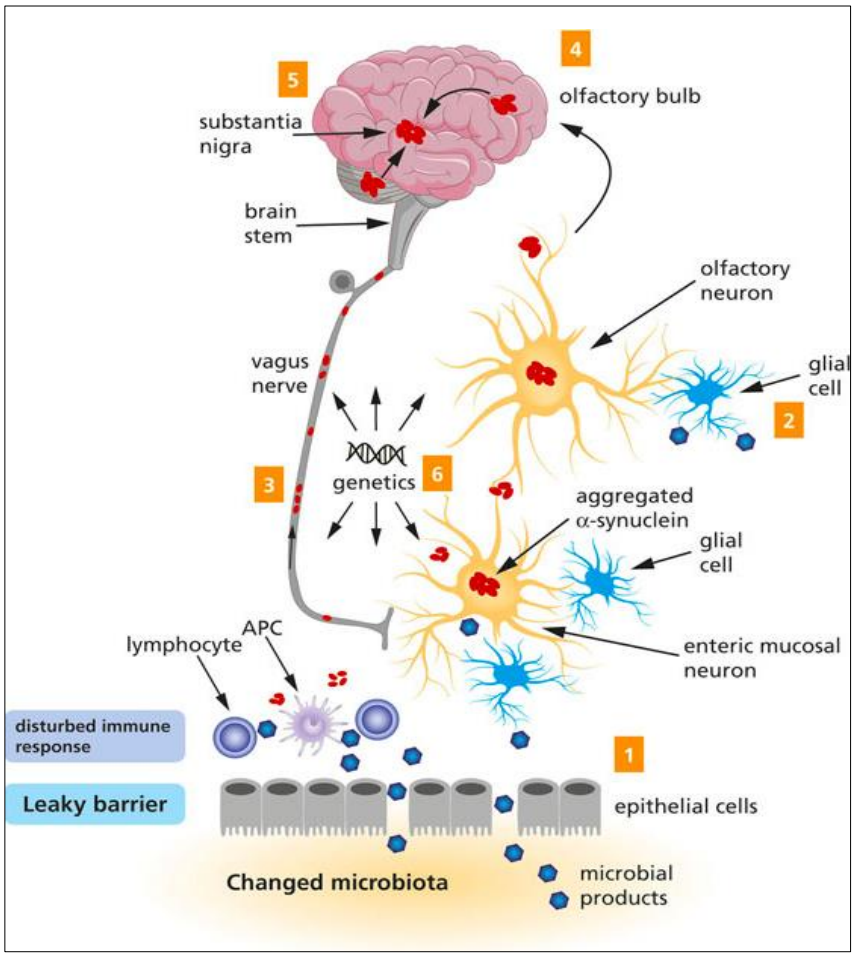

Figure 2.2: A schematic representation of Braak's hypothesis of Parkinson's disease(Rietdijk *et al.*, 2017)

Other studies state that the pathophysiology of PD is not limited to dopaminergic neurons of the substantia nigra, but implicates a *distributed brain network*: putamen, striatum, thalamus, brainstem, and cortex (Galvan and Wichmann, 2008).

2.2 Cognitive decline and dementia

Cognitive impairments in Parkinson's disease patients are a major non-motor symptom and may be present since the earliest stages. These symptoms significantly affect the daily life of patients and prevent them from carrying out several routine tasks requiring cognitive functioning. Cognitive decline due to neurodegeneration occurs gradually, with an intermediate condition between normal cognition and dementia known as mild cognitive impairment (MCI) (Petersen *et al.*, 2014). In many cases, PD patients with MCI eventually progress to dementia in the long term.

A study showed the prevalence of MCI in about 40% of newly diagnosed PD patients (Monastero *et al.*, 2018). The prevalence of dementia in PD patients also depends on age, disease duration, motor severity (Emre, 2003*a*; Poewe *et al.*, 2008; Goldman and Litvan, 2011) and other factors like sleep disorders, depression(Jozwiak *et al.*, 2017; Goldman *et al.*, 2018).

Some studies have reported a 45-60% progression rate from PD-MCI to PD dementia (PD-D) while following up patients for 4–12 years (Janvin *et al.*, 2006; Buter *et al.*, 2008; Williams-Gray *et al.*, 2013; Wood *et al.*, 2016; Pedersen *et al.*, 2017; Weil *et al.*, 2018) and a 49.28% prevalence rate for dementia over 7 years (Sanyal *et al.*, 2014). MCI can also be a stable stage for many patients, as is demonstrated in a longitudinal study over three years (Lawson *et al.*, 2017)

Understanding the neural basis of cognitive dysfunctions in PD is essential because mild cognitive impairment (MCI) in PD is considered as a precursor of dementia (Caviness et al., 2007). Any methods to detect the process of cognitive impairment would be highly beneficial to identify patients at risk of significant decline leading to dementia.

2.3 Current diagnostic methods for Parkinson's disease

Molecular diagnosis has emerged as a powerful technique for the early detection of various neurodegenerative disorders (Agrawal and Biswas, 2015). Earlier, the diagnosis of Parkinson's disease was based on clinical examination and eventually, based on the response to dopamine agents and the development of motor fluctuations (Suchowersky *et al.*, 2006). Researchers have been working to develop biomarkers such as blood tests or imaging scans that could be sensitive and specific for Parkinson's disease (Berg *et al.*, 2012; Chahine *et al.*, 2014; He *et al.*, 2018).

Having reliable, non-invasive ways to detect Parkinson's disease is particularly vital, as the traditional standard for the confirmed diagnosis of PD is post-mortem neuropathological examination, which does not help in any clinical interventions for the patient. As the clinical symptoms of the disease only appear years after the onset of neurodegeneration (Dauer and Przedborski, 2003; Grosch *et al.*, 2016), identifying people who might be at risk of PD would be very useful for neuroprotective trials and therapies. Neuroimaging markers may visualize the process of neurodegeneration until symptomatic treatment can be applied. Figure 2.3 illustrates some disease progression markers through different phases of PD.

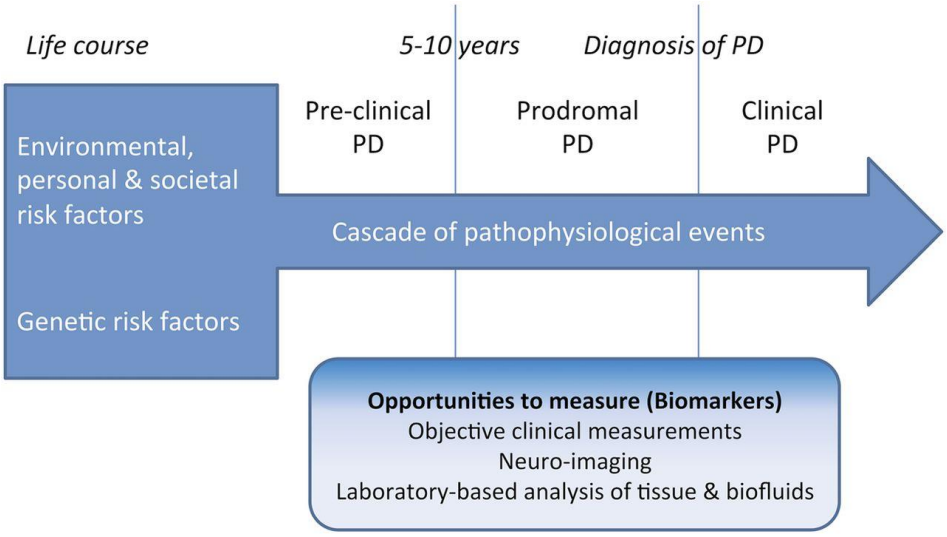

Figure 2.3: A schematic showing determinants of risk, the prediagnostic phase (preclinical and prodromal phases) and clinical phase of Parkinson's disease, along with the parallel application of risk and disease progression markers to measure disease activity across phases (Noyce *et al.*, 2016)

Here are some of the regular and some of the more recent methods used for diagnosing and investigating Parkinson's disease patients:

1. Unified Parkinson's Disease Rating Scale (UPDRS)

The Unified Parkinson's Disease Rating Scale (UPDRS) is the most used clinical rating scale for Parkinson's disease (PD)(Goetz, 2010). It was originally developed in the 1980's but then revised in 2001 by the Movement Disorder Society (Movement Disorder Society Task Force on Rating Scales for Parkinson's D, 2003). Primarily, it consists of 50 questions to assess the motor and non-motor impairments in an individual. Some parts need to be completed by the patient and their caregivers, while some others by doctors themselves. The questions spanning four parts investigate:

- non-motor experiences of daily living
- motor experiences of daily living
- motor examination
- motor complications

2. Smell test

Since the loss of smell is an early sign of PD, testing the olfactory function is an integral part of the diagnosis. We use the Sniffin Sticks Screening 12 Test ('Sniffin' Sticks & Taste Strips - Tobacco industry, Medical devices & Prototype construction'.; Kobal *et al.*, 1996), which consists of 12 felt-tip pens filled with an odorant, e.g., orange, coffee, and fish (Cozac *et al.*, 2017). Removal of the cap releases the odour. The type of the odorant is coded and is not known to the examinee. The pen is held approximately 2 cm in front of the examinee's nostrils, and the examinee receives a verbal command to inhale the odour with both nostrils for 2 s. Then, the examinee is given a card with four variants of odour (including the correct one), and—in a forced-choice paradigm—is asked to select the correct odour. The number of correctly identified odorants is summed up to calculate the "SnSc" ranging from 0 to 12.

3. Neuropsychological tests

A series of neuropsychological tests are carried out to assess the cognitive profile of an individual. Two of the commonly used scales are the Mini Mental State Examination (MMSE) and the Montreal Cognitive Assessment (MoCA) (Biundo *et al.*, 2016). Individuals scoring less than 24 points out of 30 points in the MMSE ratings are likely to have severe cognitive impairment or dementia. For a detailed assessment and for diagnosing MCI, we carry out a set of 23 neuropsychological tests; resulting in aggregate five cognitive scores (domains): Memory, Attention + Working Memory, Executive Function, Language and Visual-Spatial Function. The tests falling under each domain are shown in Table 2.1 (Chaturvedi *et al.*, 2019). Besides, we calculate an aggregate overall test score and diagnose MCI based on the Litvan 2012 level II criteria (Litvan *et al.*, 2012). As per this established criterion, an individual can be diagnosed as having MCI if either two tests in one cognitive domain are impaired or one test is impaired in two different cognitive domains, demonstrated by performance approximately 1 to 2 Standard Deviations below appropriate norms.

Domain	**Neuropsychological tests**
Memory	California Verbal Learning Test (Delis *et al.*, 1987): (1) trial 1; (2) trial 5; (3) savings; (4) discriminability
	Rey-Osterrieth Complex Figure (Spreen and Strauss, 1998): savings (immediate recall divided by copy)
Executive Function	Five-Point Test (Regard *et al.*, 1982): correct answers
	Semantic verbal fluency test (Isaacs and Kennie, 1973): correct answers
	Phonemic verbal fluency (Thurstone, 1948): correct answers
	Trail-Making Test (Reitan, 1955): time for part B divided by time for part A
Attention and Working Memory	Test of Attentional Performance (TAP) – Alertness (Zimmermann and Fimm, 2007): (1) reaction time with alerting sound; (2) reaction time without alerting sound.
	TAP – Divided Attention: (1) reaction time to auditive stimuli (2) reaction time to visual stimuli (3) number of omissions
	Trail-Making Test: time for part A
	Digit span from the German version of the Revised Wechsler Memory Scale (Härtig *et al.*, 2000): (1) correct forwards (2) correct backwards
	Corsi blocks from the German version of the Revised Wechsler Memory Scale (Härtig *et al.*, 2000): (1) correct forwards; (2) correct backwards
Visuo-Spatial Function	Rey-Osterrieth Complex Figure: copy
	Block Design Test (Härtig *et al.*, 2000): sum score
Language	Boston Naming Test (Morris *et al.*, 1989): correct answers
	Similarities from the German version of the Revised Wechsler Memory Scale (Härtig *et al.*, 2000): correct answers

Table 2.1: Psychological tests grouped into five cognitive domains. Table adapted from (Chaturvedi *et al.*, 2019)

The detailed clinical diagnostic criteria for Parkinson's disease dementia **(**Emre et al., 2007) is shown below:

1. **Core features**

    1. Diagnosis of Parkinson's disease according to UK Brain Bank criteria
    2. A dementia syndrome with insidious onset and slow progression, developing within the context of established Parkinson's disease and diagnosed by history, clinical, and mental examination, defined as:
        - Impairment in more than one cognitive domain
        - Representing a decline from premorbid level
        - Deficits severe enough to impair daily life (social, occupational, or personal care), independent of the impairment ascribable to motor or autonomic symptoms

2. **Associated clinical features**

    1. Cognitive features:

        - Attention: Impaired. Impairment in spontaneous and focused attention, poor performance in attentional tasks; performance may fluctuate during the day and from day to day
        - Executive functions: Impaired. Impairment in tasks requiring initiation, planning, concept formation, rule finding, set shifting or set maintenance; impaired mental speed (bradyphrenia)
        - Visuo-spatial functions: Impaired. Impairment in tasks requiring visual-spatial orientation, perception, or construction
        - Memory: Impaired. Impairment in free recall of recent events or in tasks requiring learning new material, memory usually improves with cueing, recognition is usually better than free recall
        - Language: Core functions largely preserved. Word finding difficulties and impaired comprehension of complex sentences may be present

    2. Behavioral features:

        - Apathy: decreased spontaneity; loss of motivation, interest, and effortful behaviour
        - Changes in personality and mood including depressive features and anxiety
        - Hallucinations: mostly visual, usually complex, formed visions of people, animals or objects
        - Delusions: usually paranoid, such as infidelity, or phantom boarder (unwelcome guests living in the home) delusions
        - Excessive daytime sleepiness

3. **Features which do not exclude PD-D, but make the diagnosis uncertain**
    1. Co-existence of any other abnormality which may by itself cause cognitive impairment, but judged not to be the cause of dementia, e.g. presence of relevant vascular disease in imaging
    2. Time interval between the development of motor and cognitive symptoms not known

4. **Features suggesting other conditions or diseases as cause of mental impairment, which, when present make it impossible to reliably diagnose PD-D**
    1. Cognitive and behavioural symptoms appearing solely in the context of other conditions such as:
        i. Acute confusion due to
            1. Systemic diseases or abnormalities
            2. Drug intoxication
        ii. Major Depression according to DSM IV
    2. Features compatible with "Probable Vascular dementia" criteria according to NINDS-AIREN (dementia in the context of cerebrovascular disease as indicated by focal signs in neurological exam such as hemiparesis, sensory deficits, and evidence of relevant cerebrovascular disease by brain imaging AND a relationship between the two as indicated by the presence of one or more of the following: onset of dementia within 3 months after a recognized stroke, abrupt deterioration in cognitive functions, and fluctuating, stepwise progression of cognitive deficits)

Apart from the above-mentioned clinical tests, we now also have some more recent imaging methods that aim to diagnose early Parkinson's disease.

4. **DaTscan**

The DaTscan (GE) is a dopamine transporter (DAT) single photon emission computerised tomography (SPECT) imaging technique (Seifert and Wiener, 2013). It uses small amounts of a radioactive drug (Ioflupane l 123 Injection) and brain imaging to detect how much dopamine is available in the brain. The detection of loss of functional dopaminergic neurons in the striatum helps identifying patients with clinically uncertain Parkinsonian Syndromes(European Medicines Agency, 2018). Ioflupane (123I) INN, the active substance (otherwise referred to as 123I-FP-CIT or 123I-CIT-FP) is an iodinated cocaine analogue that has high affinity to the dopamine transporter (DaT) located on presynaptic nerve endings (axon terminals) in the striatum. This binding of DaTscan is claimed to reflect the number of dopaminergic neurons in the substantia nigra. A single photon emission computed tomography (SPECT) scanner is used to measure this amount and location of the drug in the brain. This technique can differentiate between changes in the nigrostriatal

dopaminergic system in patients with Parkinsonism and healthy controls (Cummings *et al.*, 2014). It helps in differentiating Essential Tremor from Parkinsonian Syndromes related to idiopathic Parkinson's disease, Multiple System Atrophy and Progressive Supranuclear Palsy (Bajaj *et al.*, 2013; Ogawa *et al.*, 2018). However, DaTscan is unable to discriminate between Parkinson's Disease, Multiple System Atrophy and Progressive Supranuclear Palsy. To patients, DaTscan is presented as a sterile 5% (v/v) ethanolic solution for intravenous injection without dilution. The recommended dose for adults and the elderly by the European Medicines Agency is 111-185 MBq. Further, the patients must undergo appropriate thyroid blocking treatment before the injection to minimise thyroid uptake of radioactive iodine. SPECT imaging should take place between three to six hours post-injection.

5. **Transcranial ultrasound**

Transcranial sonography (TCS) is another relatively new method which displays echogenicity of human brain tissue through the intact skull (Li *et al.*, 2016; Smajlovic and Ibrahimagic, 2017). TCS of brain parenchyma is used as a diagnostic tool in movement disorders, particularly idiopathic PD and in the differentiation of idiopathic Parkinson's disease (PD) from other parkinsonian disorders. TCS through the preauricular bone window allows the depiction of characteristic abnormalities in the echogenicity of SN and basal ganglia. Compared to other neuroimaging methods, TCS permits different visualisations of brain structures and has high-resolution imaging capacity for echogenic brain structures.

6. EEG

Electroencephalography (EEG) has been used extensively as a non-invasive and cost-effective tool to study brain activity since it was first developed in 1924 by Hans Berger. It records the electrical activity of the brain (Rana *et al.*, 2017) and provides quantitative information on brain functions. The apparatus is easy to use, takes only a few minutes, is inexpensive and now can also be transported easily. EEG has been used to detect changes in brain signals in Parkinson's patients, as they progress from having normal cognition to MCI to dementia. This is elaborated on further in Chapter 3.

The polysomnography verified rapid eye movement (REM) sleep behaviour disorder (RBD) is a known risk marker for Parkinson's disease (Galbiati *et al.*, 2019). Besides, reduced dopamine transporter (DAT) binding on single-photon emission computed tomography (SPECT), occurrence of Parkinson's disease-related mild parkinsonian signs indicating subthreshold parkinsonism and hyperechogenicity of SN (SN+) assessed by transcranial sonography (TCS) are anticipated to constitute the highest likelihood for future Parkinson's disease (Berg *et al.*, 2015*a*). Though it is an ongoing discussion, we know little about neurophysiological methods outside the frame of RBD that contribute to the prediction of future onset of Parkinson's disease.

3. QEEG features as biomarkers for cognitive decline in Parkinson's disease

3.1 Neurophysiology underlying generation of EEG signals

EEG records the electrical fields generated in the brain. **But how do these fields even get generated?** The source of this activity is the brain cells or neurons. Each neuron consists of a cell body, dendrites, axon and an enclosing membrane. Figure 3.1. shows a simplified structure.

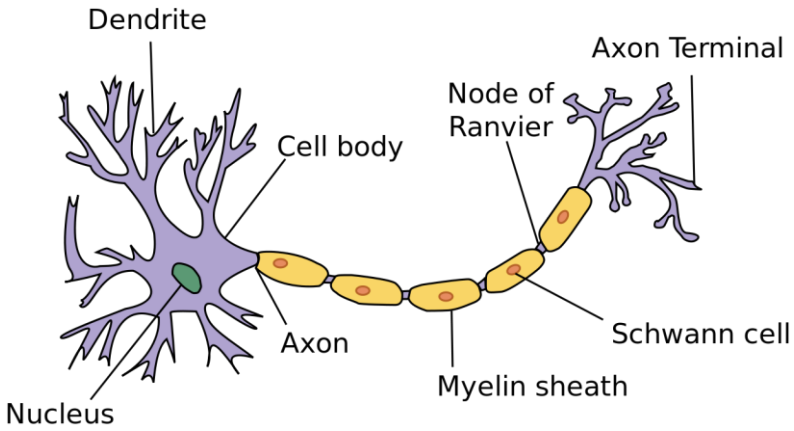

Figure 3.1: Structure of a neuron. Credit: Dhp1080 [CC BY-SA 3.0]

The surface membrane contains proteins known as ion channels that allow small positive or negative charged atoms to pass through. The inside of the membrane is said to be more negative than the outside; around -70 mV, although it keeps fluctuating depending on the ions coming in from other neurons.

When the voltage across the membrane changes, some of these ion channels allow production of a fast signal known as a nerve impulse or action potential (Lovinger, 2008). Basically, an axonal potential leads to the generation of excitatory postsynaptic potentials (ESPs) (Purves *et al.*, 2001) which causes the apical dendrite to release ions through its membrane. The resulting depolarisation of the membrane establishes an electrical potential difference between the apical dendrite and the cell body. This depolarisation is what causes the action potential.
The dendrite typically carries signals or chemical inputs towards the cell body, and the axon carries them away from the cell body towards the junction known as synapse. The action potential is depicted in Figure 3.2.

Neurons can be of different types; pyramidal cortical neurons are the ones located in the cerebral cortex; they are close to the cortical surface and aligned perpendicular. Since the EEG picks up electric signals from the surface, most signals likely come from these pyramidal neurons.

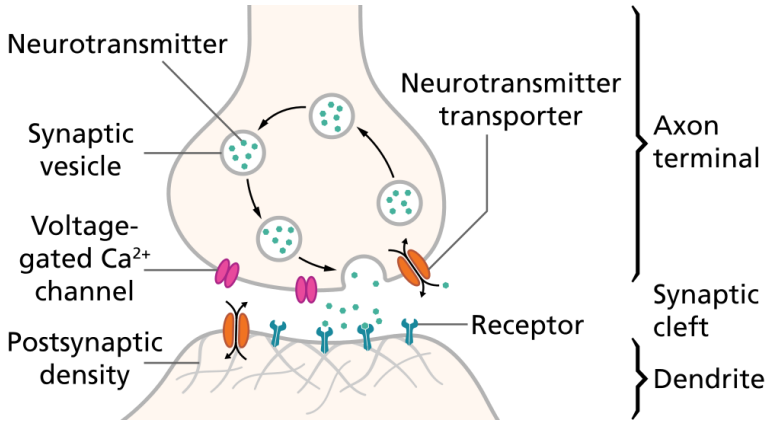

Figure 3.2: An action potential, or spike, causes neurotransmitters to be released across the synaptic cleft, causing an electrical signal in the postsynaptic neuron. (Image: By *Thomas Splettstoesser* / CC BY-SA 4.0)

3.2 Slowing of EEG in Parkinson's disease

EEG is a fast and non-invasive method to monitor the electrical activity of the brain. One of the consistent findings with Parkinson's disease, especially related to cognitive decline, has been the slowing of EEG (Bočková and Rektor, 2019). Slowing of EEG waves has been related to non-motor symptom manifestation (Bonanni *et al.*, 2008; Serizawa *et al.*, 2008; Morita *et al.*, 2009), primarily cognitive dysfunction recently discussed as a potential PD prodromal marker (Postuma and Berg, 2016).
In other words, spectral powers in ranges above 8 Hz (such as alpha, beta) are lower, and those below 8 Hz (theta, delta) are higher in Parkinson's disease patients, in those with and without cognitive decline. (Stoffers *et al.*, 2007; Babiloni *et al.*, 2011; Klassen *et al.*, 2011, Benz *et al.*, 2014*b*; Dubbelink *et al.*, 2014; Caviness *et al.*, 2016).

Increased theta, delta powers and reduced alpha, beta powers, are shown to be associated with severity of cognitive impairment in PD (Benz *et al.*, 2014*b*, Cozac *et al.*, 2016*b*, Geraedts *et al.*, 2018*a*). It is also characteristic in classification of mild cognitive impairment (PD-MCI) (Fonseca *et al.*, 2009; Bousleiman *et al.*, 2015; Mostile *et al.*, 2019) and diagnosis of Parkinson's disease dementia (Klassen *et al.*, 2011; Al-Qazzaz *et al.*, 2014; Caviness *et al.*, 2015; Babiloni *et al.*, 2017).

In de novo Parkinson's disease patients, an increase in theta and a decrease in alpha spectral powers has been reported compared to healthy controls, along with decreased beta measures which were associated with the severity of motor impairment (Stoffers *et al.*, 2007, 2008; Gongora *et al.*, 2019). Beta frequency in the right posterior temporal region has been reported to be negatively associated with disease severity, (He *et al.*, 2017) though other studies were not able to verify the association of a specific EEG pattern and motor impairment in Parkinson's disease (Geraedts *et al.*, 2018*a*). Slowing of EEG waves has also been related to non-motor symptom manifestation (Bonanni *et al.*, 2008; Serizawa *et al.*, 2008; Morita *et al.*, 2009), primarily cognitive dysfunction which was recently defined as a Parkinson's disease prodromal marker (Heinzel *et al.*, 2019). For instance, increased theta, delta and reduced alpha, beta spectral powers, are associated with severity of cognitive impairment in Parkinson's disease

(Benz *et al.*, 2014*b*, Cozac *et al.*, 2016*b*, Geraedts *et al.*, 2018*a*). In patients diagnosed with depression, which is also a risk factor for Parkinson's disease (Ishihara and Brayne, 2006), absolute theta power was seen to be associated with the condition (Cai *et al.*, 2018). Overall, there is evidence that alteration in EEG might occur in non-RBD individuals suspected to be in the prodromal stage of Parkinson's disease.

It is interesting to note that slowing, in general, is also observed in Alzheimer's disease patients. In the case of Alzheimer's disease, alpha/theta spectral ratio was used to distinguish patients from healthy individuals (Schmidt *et al.*, 2013). In one case(Morita *et al.*, 2009), a spectral ratio (sum of alpha and beta powers divided by the sum of delta and theta powers) was found associated with a decline in the MMSE score, which is an indicator of cognitive decline.
Based on our research and general evidence, we included the alpha/theta ratio in some of our studies to investigate the effect in Parkinson's disease patients.

But researchers have observed differences while comparing both of these diseases. In one such study (Benz *et al.*, 2014*b*), slowing of EEG was more pronounced in Parkinson's patients, in comparison to Alzheimer's disease patients.

3.3 EEG connectivity in Parkinson's disease patients

Apart from spectral powers, another group of features of interest in learning about brain functions is connectivity. The brain, as we know, is highly complex and contains several interconnected elements. This connection matrix or the collective network in the brain is referred to as the 'connectome'(Sporns *et al.*, 2005; Abbott, 2016; Vecchio *et al.*, 2017).

While the connectome can be explored at different scales, a lot of recent research focusses on the functional aspect instead of structural, thus referring to it as the 'functional connectome'(Biswal *et al.*, 2010). Typically, functional MRI (fMRI) was used to investigate the functional connectivity. However, owing to its lack of temporal resolution, EEG is also now used to explore better.

Brain network connectivity has been increasingly studied in the past few years. The extensive study of the normal brain organization has led to an understanding of different types of networks, hubs. Healthy brain networks are seen to be associated with cognitive functions. So, the disruption of these networks could potentially lead to neurological disorders.

Network analysis has been applied to disorders like frontotemporal dementia and PD. For AD and PD, it is suggested that the changes in networks are increased. Network changes could also suggest changes in the structural pathology. Certain brain regions might be affected more in this regard in the case of AD, PD, dementia patients.

Different measures can quantify connectivity. Some standard measures include graph measures, coherence and phase lag index. A decrease in alpha coherence is reported to be strongly associated with Alzheimer's disease dementia(Musaeus *et al.*, 2019).

In the case of Parkinson's disease, brain connectivity alterations are found associated with cognitive deterioration (Bertrand *et al.*, 2016; Gao and Wu, 2016; Hassan *et al.*, 2017). Studies

investigating PD patients have reported early changes in frontal inter-hemispheric coupling (Carmona *et al.*, 2017) and indicate network decentralisation to progress over time in these patients.

In the earliest clinical stages of PD, delta and alpha1 band resting-state functional connectivity was seen altered in temporal cortical regions (Olde Dubbelink *et al.*, 2013). As the disease progressed, connectivity in the alpha2 band decreased. EEG slowing and reduced functional connectivity in the alpha2 band has also been found to be associated with non-dopaminergic disease severity in PD (Geraedts *et al.*, 2018*b*).

Another study investigating procedural memory in Parkinson's disease found strong delta functional connectivity in patients and it was associated with weak offline memory consolidation after learning a visuo-motor skill (Manuel *et al.*, 2018). Coherence measures, as seen in a separate study, indicate distinct cortical activity in PD with and without MCI (Carmona Arroyave *et al.*, 2019). Such changes could potentially be a marker for disease progression.

In patients with RBD, which is a risk factor for PD, studies observed decreased delta-band functional connectivity in the frontal regions (Sunwoo *et al.*, 2017). Alterations in the form of bursts in alpha, theta spectral bands, in comparison to healthy individuals, derived from a few minutes of eyes-closed resting EEG (Ruffini *et al.*, 2019) were associated with prognosis for development of Parkinson's disease or dementia with Lewy-bodies. This further supports the assumption that EEG might help to characterise individuals at risk for Parkinson's disease progression.

3.4 EEG features in Parkinson's disease dementia patients

Since QEEG is useful for identifying PD patients at early stages of cognitive impairment, it can also be helpful for the early prognosis of dementia (Fonseca *et al.*, 2009; Klassen *et al.*, 2011; Dubbelink *et al.*, 2014, Gu *et al.*, 2014*a*). In two such studies comparing Parkinson's disease patients with and without dementia(Olde Dubbelink *et al.*, 2013; Ponsen *et al.*, 2013), demented patients showed weaker Phase lag Index (PLI) in the alpha band, especially in the frontal and temporal regions. General region-to-region connectivity was stronger in theta band and weaker in delta, alpha, and beta bands in PD patients with dementia.
A graph theory analysis performed to follow up over four years on connectivity changes in PD patients without dementia also saw alterations in the alpha and theta bands(Olde Dubbelink *et al.*, 2014).

Concerning spectral power, increase in theta, delta with a decrease in alpha, beta was the common trend (Bonanni *et al.*, 2008; Kamei *et al.*, 2010). There is a lot we still do not know about the brain and its functioning, and every study is one-step forward to confirming theories and making new hypotheses to investigate further. In our case, we focussed on a few of the features mentioned above and conducted extensive studies to investigate Parkinson's disease patients at baseline and then at different cognitive stages, in line with our aim (Section 1.3).

4.Computational methods for Brain Signal Analysis

The data for the studies described in Chapters 5, 7, 8 were collected at the University Hospital Basel and the Memory Clinic, Basel, starting in 2011. The brain signal analysis in this context refers to analysing the quantified data obtained from a high-density EEG system (system with 256 electrodes) at the University Hospital Basel. The patients were recruited on the following criteria: PD according to UK PD Brain Bank (UPDRS, 2003), Mini-Mental Score Examination (MMSE) above 24/30, no history of vascular and/or demyelinating brain pathology, sufficient knowledge of German language. The local ethics committees (Ethikkommission beider Basel, Basel; Switzerland; EK 74/09) approved the study, and all participants gave written informed consent before study inclusion. The clinical and EEG data used in Chapter 6 were collected at the outpatient clinic of the Department of Neurodegeneration, University of Tübingen. Diagnosis of PD was made according to the UK Brain Bank criteria (Liepelt-Scarfone *et al.*, 2015) at baseline and follow-up visits. Inclusion criteria were, Hoehn & Yahr stage ≤ 2.5, age >50 years, no deep brain stimulation, no verified genetic mutation known to cause PD, and neither history of drug or alcohol abuse, nor delirium or diagnosis of Parkinson's Disease dementia were included. The High-Risk PD and control individuals were investigated in the PMPP study (Liepelt-Scarfone *et al.*, 2013*a*). The EEG data for these patients were recorded using a standard 10-20 system (21 electrodes). Further details of the EEG systems, data recording and processing, are described in Section 4.1. In Section 4.2, we go one step ahead to see what suitable machine learning methods were applied to analyse and interpret all of the EEG data.

4.1 EEG Recording and processing

EEG systems record the electric potentials generated by the brain using electrodes placed on the scalp. The recording system mainly consists of:

- electrodes with conductive media, which record the signals from the surface of the scalp
- amplifiers with filters, which transform the signals recorded in microvolt to an optimal range for accurate digitalization
- A/D converter which changes the signals into the digital form,
- recording device like a computer that stores and displays the recorded signals.

EEG lets us measure potential changes over time by measuring the voltage difference between each electrode and the chosen reference electrode. EEG recording systems can be of different types. The most common form is the 10-20 system, where the ‘10' and ‘20' refer to the electrodes being placed 10% or 20% of the distance away from each other. Each electrode is named with one or two letters denoting the brain region (such as Fp = frontopolar; F = frontal; C = central; P = parietal; O = occipital; T = temporal), followed by a number to denote whether it is placed on the left or the right hemisphere. While odd numbers refer to the left hemisphere, even numbers refer to the right one. Electrodes on the midline are denoted using a ‘Z' instead of a number. This is also illustrated in Figure 6 below. For reference, Nasion refers to the point between the forehead and nose, and inion refers to the bump at the back of the skull.

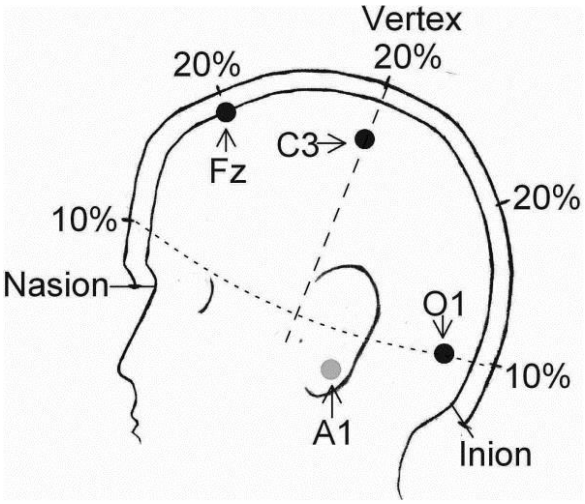

Figure 4.1: Head measurements and electrode placement according to the 10-20 electrode placement system (Jasper, 1958). The longitudinal line from the nasion to inion is divided into 10% and 20% segments. Distances along the transverse line (dashed) and the circumference (dotted) are not to scale because the 3-dimensional head is drawn in 2-dimensional profile. Approximate locations of Fz, C3, O1, and A1 (behind the ear) are indicated.

The other system can be a high-density one with 256 electrodes. The high-density recording system enables us to aggregate nearby signals, thus potentially reducing noise. Grouping the electrodes into regions is a way to get initial insights into connectivity between different anatomical parts of the brain, building upon our previous knowledge. In our case, we recorded 20 min of EEG in resting-state eyes-closed condition, using such a 256-channel EEG System (Netstation 300, EGI, Inc., Eugene, OR). EEG recordings were done in the afternoons, and patients were seated comfortably in a relaxing chair, instructed to close their eyes. A technician present in the recording room controlled for vigilance of the patients. Before the EEG recording, patients were also asked to self- rate their sleepiness level from 1 to 9 using the Karolinska Sleepiness Scale (Åkerstedt and Gillberg, 1990; Kaida *et al.*, 2006; Miley *et al.*, 2016). The placement of electrodes using a high-density system is shown in Figure 4.2 below. We see electrodes grouped into 10 regions of interest for simplifying the interpretation: frontal left/right, central left/right, parietal left/right, temporal left/right, and occipital left/right, but it is possible to change this mapping and group them into 22 specified regions, or not group them at all. While grouping, we do not consider the electrodes placed at the mid-line of the scalp or on areas outside the scalp such as the neck, cheeks and electrodes to exclude spurious signals. Depending on the EEG feature calculated, not grouping the 214 electrodes into any region can result in a massive amount of data.

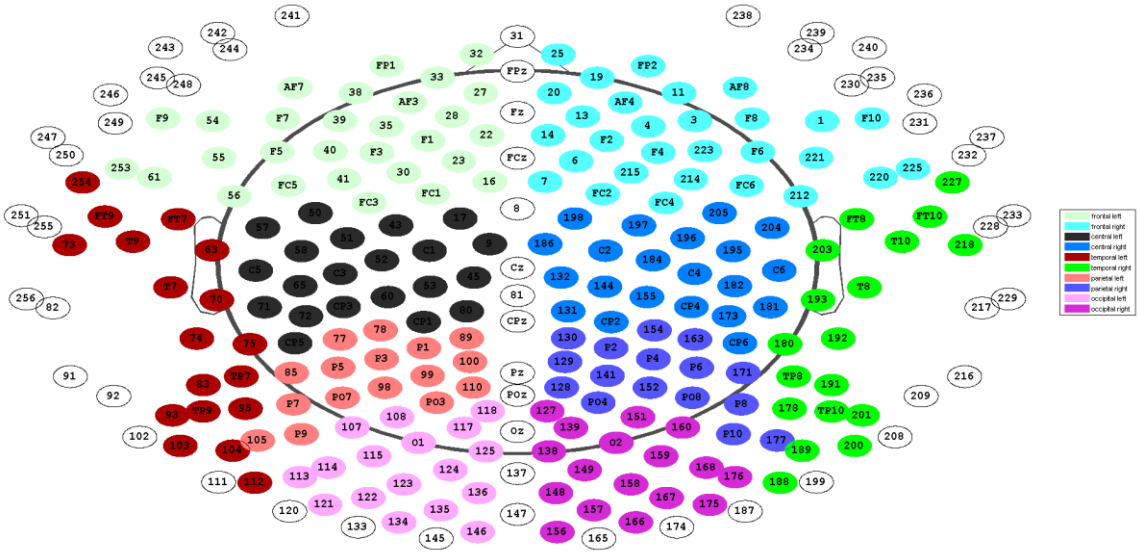

Figure 4.2: Placement of 256 electrodes on the scalp, grouped into 10 regions of interest.

For the data acquired in Tübingen, EEG data were recorded using a standard IS 10-20 system (5 minutes resting condition with eyes open and closed, each for 30 seconds, five times in a row). We obtained relative spectral powers for 18 electrodes in six power bands. Moreover, global spectral measures and median frequencies were obtained.

All data were segmented and processed in an automated way using a MATLAB based in-house software (TAPEEG, https://sites.google.com/site/tapeeg/)(Hatz *et al.*, 2015), as described in our publications (Chaturvedi *et al.*, 2017, 2019). EEG's were filtered (Firls:0.5–70 Hz, 50 Hz notch) at a sampling rate of 1000 Hz and an inverse Hanning window was used to stitch together shorter segments, to have at least 3 minutes of cleaned EEG data. Artefacts like eye movements, traces of sleep, blinking, ECG, etc. were detected and removed. After performing automated bad-channel detection (Hatz *et al.*, 2015), the average of all ‘good' channels was used to re-reference the EEG to a common average montage.

The independent component analysis implementation of EEGLAB (Delorme and Makeig, 2004) ("runica" with default settings) was used to remove further artefacts.
Artefact removal, referencing channel, and ensuring that uniform settings in terms of amplifier, filters. ICA is applied consistently and is crucial for maintaining the quality of the data and facilitating the data analysis. A variation in the processing can be semi-automated, where a visual control step is incorporated after the EEG segment selection step.

Post-processing with Inverse Solution

While EEG continues to be an exciting tool for investigating neural activity, it has certain limitations as the recordings occur only at the surface of the head, which prohibits direct access to the neural source domain and recording the actual neural activity. To overcome this challenge, source analysis techniques try to estimate the location and dynamics of the

underlying neural generators of EEG. Low-Resolution Electromagnetic Tomography (LORETA) is one possible approach that computes an instantaneous, three-dimensional, discrete linear solution consisting of the smoothest of all possible neural current density distributions (Pascual-Marqui, 2002). LORETA has gained widespread popularity and has been used on hundreds of scientific publications

Inverse solution is a method of localizing deep brain activity based on recordings from the scalp. sLORETA computes electric neuronal activity based on images of standardized current density, obtained from the digital MRI information recorded in the Montreal Neurological Institute Brain Atlas (Aubert-Broche *et al.*, 2006). The source space or the cortical grey matter and hippocampus were divided into 5011 solution points with subsequent reduction to 76 regions of interest (ROIs) based on the Anatomical Automatic Labeling (AAL) atlas (Tzourio-Mazoyer *et al.*, 2002). The ROIs can be calculated by either selecting the 'maxpower' or the voxel with maximal power in different frequency bands for every region, or 'center' referring to the centre voxel for every region. To ensure uniformity and to reduce variability, we considered the centre voxel for the calculation. The software package Sloreta (Key Institute) was used to calculate the inverse solution matrices and source activity was calculated for all 5011 solution points.

4.1.1 EEG Features

Frequency - spectral power

Spectral analysis is a process used for quantifying EEG. It is used to decompose a complex EEG signal into its component frequencies by applying Fourier Transformation (Walczak and Chokroverty, 2009, p. 12). A power spectrum reflects "the amount of activity" in frequency bands(Cozac, 2017). Relative power is used to assess the relative contribution of a particular frequency to the EEG signal (Heisz and McIntosh, 2013) and is calculated by dividing the absolute power in a given frequency band by the total power. We calculated median relative spectral powers in the following frequency ranges (Hz): 1–4 (delta), 4–8 (theta), 8–10 (alpha1), 10–13 (alpha2), 8–13 (alpha), and 13–30 (beta).
Spectral power can be assessed globally (over the whole scalp) and over definite scalp regions. Using a high-density electrode system enables us to aggregate nearby signals, thus potentially reducing noise.

Connectivity – Phase Lag Index

We used Phase Lag Index (PLI) as a measure of functional connectivity. PLI is calculated from the asymmetry of the distribution of instantaneous signal phase differences between two brain regions. (Cozac, 2017). It is based on the idea that a consistent phase lag translates to a time lag between two time series (Bastos and Schoffelen, 2016). In other words, PLI reflects the degree of synchronization between couples of signals; it denotes functional connection between regions of the brain, mentioned above (for instance, PLI in theta frequency range for connection

between temporal left and temporal right regions reflects the level of synchronization of oscillations in 4 – 8 Hz in these 2 regions, from "chaotic" (lower PLI) to synchronized (higher PLI)). The main approach is to disregard phase differences which centre around 0 mod π (Stam *et al.*, 2007). It is calculated as:

$$PLI = |<sign\ [sin\ (\Delta\Phi\ (t_k))]> |$$

where $\Delta\Phi$ is the phase difference at time point t_k between two time series, calculated for all time-points per epoch (4096 in our case), *sign* stands for signum function, < > denotes the mean value and || indicates the absolute value. The instantaneous phases were estimated with the Hilbert transform using a 50% overlapping sliding window approach.

PLI values range between 0 and 1, where 0 can indicate possibly no coupling and 1 refers to perfect phase locking. We mapped the 214 electrodes to the ten anatomically defined regions. For each region, the average connectivity of all its electrodes to all other regional groups of electrodes was determined (Hardmeier *et al.*, 2014). The connectivity between all pairs of regions was calculated, including the connectivity within a region.

4.2 Machine learning and statistical methods for analysing EEG data

For computing frequency and connectivity measures using QEEG, all calculations were first done for all electrodes and then averaged to corresponding anatomical regions of the brain. Extracting and analysing features from each electrode is manageable when using a low-density electrode system, such as the 10-20 EEG. But, when using 256 electrodes, even after excluding electrodes placed at neck, cheek, ears to avoid artefacts, we still get a huge number of connections between the remaining 214 electrodes, which makes it computationally expensive as well as confusing for the correct interpretations.

For this purpose, we map signals from the usable 214 electrodes to Frontal left/right, central left/right, temporal left/right, parietal left/right, occipital left/right regions of the brain. Relative power was obtained for five frequency bands: delta (1–4Hz), theta (4–8Hz), alpha1 (8– 10Hz), alpha2 (10–13Hz), and beta (13–30Hz), by calculating the ratio of the signal power within a frequency band to the total signal power (1–30Hz). Electrodes placed on the mid-auricular line were also excluded while mapping and were not a part of the 214 electrodes used.

A total of 68 different frequency measures can be extracted and used for further analysis and feature selection. These included global and regional powers, as described previously, and the median, peak frequency measures. Additionally, if we calculate any power ratios like alpha1/theta, it would result in a total of 79 features.

While calculating PLI for each region, the average connectivity of all its electrodes to all other regional groups of electrodes was determined, including PLI for within a region. This resulted in 55 PLI measures for each band. This number would vary of course depending on how many

regions we use for grouping, or if we would consider not grouping into regions at all. But essentially, what this means is that in our context of data from in-house patients, the number of features to be analysed are far too many than the number of patients we have. This makes it challenging to apply quite a few of the statistical methods effectively. Data of this kind where p>> n, or the number of observations is far less than the number of variables, are especially common in medical or genetic projects. In such cases, applying classical methods may seem to yield effective results on the training set but not necessarily for predicting new data. The risk of overfitting is quite high. One way to deal with this challenge is by using sparse models and working with the lowest possible number of input variables to achieve good prediction accuracy. This is known as sparse data modelling.

Our dataset had highly correlated features, and the goal was to find out which features were important for classification. Machine learning has been applied in several medical studies for prediction and diagnostic classification (Khodayari-Rostamabad *et al.*, 2013; Singal *et al.*, 2013; Johannesen *et al.*, 2016). Differences can be noted in the way each method works and, in the results, obtained.

In this section, we will review some of the machine learning and statistical methods suited to handle data like ours.

4.2.1 The importance of sample size

One of the most frequent and critical questions in statistical analysis is determining the appropriate sample size (Greenland, 1988; Gupta *et al.*, 2016). An in-appropriate sample size leads to questionable results. There is no absolute rule of thumb to determine the sample size; however, in regression analysis, it is often believed that there should be at least ten observations per variable. For example: If we are using three independent variables, then a clear rule would be to have a minimum sample size of 30. It is also possible to follow a statistical formula to calculate the sample size. This requires making multiple models on the dataset. Some studies provide detailed guidance on calculating the appropriate sample size for different kinds of study designs (Charan and Biswas, 2013; Gupta *et al.*, 2016; Hanley, 2016).

4.2.2 Supervised learning methods

Supervised learning refers to methods that first learn from a training dataset and then make predictions on an unseen test set (Baştanlar and Ozuysal, 2014; Raymond and Medina, 2018). This process continues until an optimal level of performance.
Such algorithms take a known set of input datasets (input variables (x)) and their known responses to the data (output variable (Y)) to learn the regression/classification model. A learning algorithm then trains a model to generate a prediction for the response to new data or the test dataset (Raymond and Medina, 2018).

$$Y = f(X) + b$$

The goal is to approximate the mapping function so well that when we have new input data (x) that we can predict the output variables (Y) for that data. Supervised learning uses classification and regression algorithms to develop predictive models (Talabis *et al.*, 2015). These algorithms include linear regression, logistic regression, decision trees, neural networks, Support Vector Machine (SVM), and others.

The classification task predicts discrete responses, which classify the data. The primary application of classification includes prediction of actives and in-actives from high throughput screening results in the drug discovery process, medical imaging, and speech recognition, to name a few. Also, handwriting recognition uses classification to recognise letters and numbers, to check whether an email is genuine or spam (Shobha and Rangaswamy, 2018), or even to detect whether a tumour is benign or cancerous. Regression techniques predict continuous responses. A linear regression attempts to model the relationship between two variables by fitting a linear equation to observed data (Schneider *et al.*, 2010). For example, say, data is collected about how happy people are after getting so many hours of sleep. In this dataset, sleep and happy people are the variables. By regression analysis, one can relate them and start making predictions.

In this thesis, we applied both regression and classification models on Parkinson's disease data. Some of the widely used techniques are:

- Linear regression for regression problems.
- Logistic regression for classification
- Penalized regression for classification of sparse data
- Random forest for classification and regression problems.
- Support vector machines for classification problems.

Linear regression for regression problems

Regression algorithms deal with modelling the relationship between variables that are refined iteratively using a measure of error in the predictions made by the model (Alexopoulos, 2010; Shobha and Rangaswamy, 2018). Linear regression is an approach to model the relationship between a scalar-dependent variable y and one or more explanatory variables (or independent variables) denoted x (Schneider *et al.*, 2010). It is a popular way of analysing data described in a linear model. For example, we may relate the weights of individuals to their heights using a linear regression model. This method is mostly used for forecasting and finding out the cause and effect relationship between variables.

A simple linear regression relates two variables (x and y) with a straight-line equation, while a nonlinear regression generates a line as if every value of y is a random variable. The line can be modelled based on the linear equation shown below and is depicted in Figure 4.3.

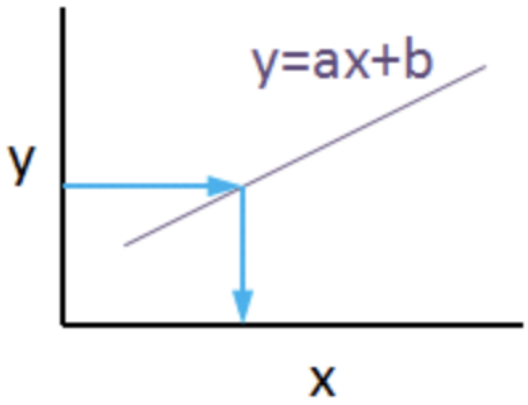

Figure 4.3: Plotting a linear equation

y= ax + b

In the equation above, "y" is the scalar dependent variable on "x". a is the slope of the line and b is the y-intercept.

The motive of the linear regression algorithm is to find the best values for a and b.
Linear regression is easier to use and interpret. However, if a good fit with linear regression is not possible, then nonlinear regression is used. Logarithmic functions, exponential functions, and trigonometric functions are among the other fitting methods in nonlinear regression.
When we deal with more than one explanatory variable, we apply multiple linear regression.
Here multiple correlated dependent variables are predicted, rather than a single scalar variable (dependent variable).

Logistic Regression

Logistic regression is another type of regression analysis, used for prediction when the dependent variable is binary (Nick and Campbell, 2007). To understand which independent variables have the most effect on the model, we look at the log-odds ratios. This shows us how the log-odds or probability of success changes with a change in one unit of the independent variable, whether positive or negative. A negative coefficient or an odds ratio of less than 1 signifies that the outcome or success would be less likely with its increase (Sperandei, 2014; Ranganathan *et al.*, 2017). The logistic function is depicted in Figure 4.4.
The logistic regression equation, in terms of the odds ratio, can be written as shown below:

$$\frac{p}{1-p} = \exp\left(b_0 + b_1 x\right)$$

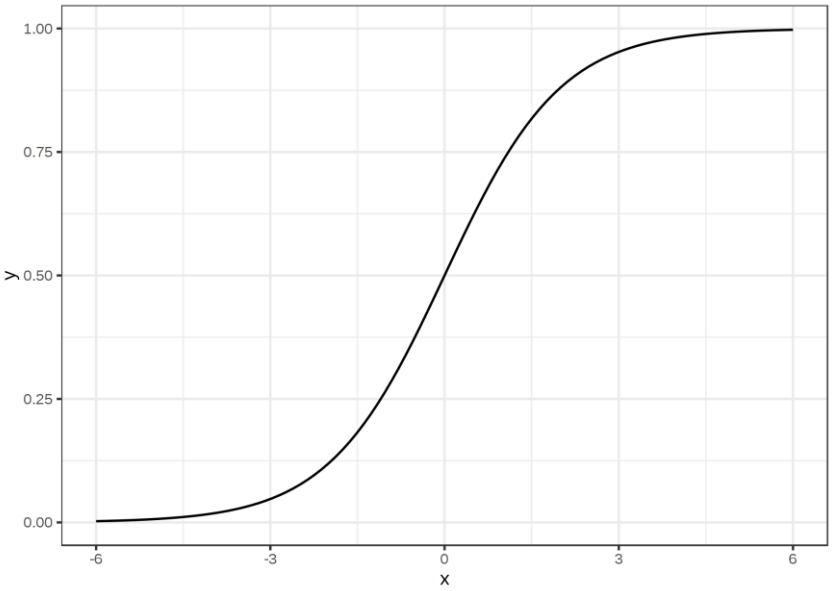

Figure 4.4: The logistic function

Taking the natural log of both sides, we can write the equation in terms of the log-odds (logit) which is a linear function of the predictors. The coefficient (b1) is the amount the logit (log-odds) changes with a one unit change in x.

$$ln\left(\frac{p}{1-p}\right) = b_0 + b_1 x$$

So, the probability of a sample being in a particular class (y=1, for instance), would be:

$$P(y^{(i)} = 1) = \frac{1}{1 + exp(-(\beta_0 + \beta_1 x_1^{(i)} + \ldots + \beta_p x_p^{(i)}))}$$

Here too, the rule of thumb applies while planning out an experiment and deciding upon the number of independent variables to include in the model. However, since we typically have a lot more variables than the number of observations, we face the risk of overfitting, poor prediction accuracy and a poorly designed experiment. Besides, multicollinearity is a big issue to tackle when dealing with data like ours.

Therefore, this might lead us to think if logistic regression might not be ideal for the classification of groups using EEG data.

Penalized regression for classification of sparse data

To combat the problems of sparse data and multicollinearity, we can apply a penalty to the logistic regression model and use a regularized regression model instead. The least absolute shrinkage and selection operator (LASSO) method has been used in different studies for feature selection and computing risk predictive models (Wu *et al.*, 2009; Fontanarosa and Dai, 2011). By penalizing (or equivalently constraining the sum of the absolute values of the estimates), some of the parameter estimates may turn out to be exactly zero. The larger the penalty, the further estimates are shrunk towards zero. So, the non-zero coefficients can denote the influential variables and help us in feature selection.

The lasso estimate $(\hat{\alpha}, \hat{\beta})$ was defined by Tibshirani(Tibshirani, 1996*a*) as:

$$(\hat{\alpha}, \hat{\beta}) = \arg min \left\{ \sum_{i=1}^{N} \left(y_i - \alpha - \sum_j \beta_j x_{ij} \right)^2 \right\}$$

$$\text{Subject to } \sum_j |\beta_j| \leq t$$

The $t \geq 0$ is a tuning parameter, where for all *t*, the solution for α is $\hat{\alpha} = \bar{y}$. We can assume without loss of generality that $\bar{y} = 0$ and omit α. The tuning parameter controls the amount of shrinkage that is applied to the estimates. Values below $t < t_0$ will cause a shrinkage of the coefficients, so that some coefficients will become zero.

In many cases, lasso-penalised models have shown improved prediction accuracy while selecting only a limited number of covariates that are included in the model. The penalized (Goeman, 2010) (Goeman, 2010) package in R(version 3.2.1) (R Core Team, 2018) was used to create a logistic regression model and apply the L1-LASSO penalty. Tenfold cross-validation and optimisation was carried out to find the optimal lambda value.

Decision Trees

Decision tree algorithm recursively, at the same time greedily, classifies a dataset following depth-first or breadth-first strategy until all the instances are assigned to a class (Mitchell, 1997). Directed edges characterize decision trees and start with a single node that has no incoming edges and every other node with only one incoming edge. Nodes with an outgoing edge are described as test nodes while those that terminate the tree, without further outgoing edges, are termed leaf nodes or the actual decision nodes. The leaf nodes are assigned with class labels (Quinlan, 1986).

The general algorithmic framework for constructing a decision tree on a training set of instances, described by the vector of descriptors and a class label, involves the following steps:

1. Analyse the dataset for border-line cases (e.g., "all instances of the training set contain the same class label," or "all the descriptors of the dataset contain the same value"). Create a single-node tree with the most common class label, if necessary.

2. If the dataset is valid, proceed with the tree construction. From all the descriptors select one or several, that split the original training set into subsets according to a split criterion of choice. The split criterion can involve only one descriptor (univariate splitting criterion) or several descriptors (multivariate splitting criterion) (Rokach and Maimon, 2005). The criterion may vary depending on the tree type. The criteria used in different decision trees include impurity based criterion (Rokach and Maimon, 2005) like information gain (Quinlan, 1987), Gini index (Breiman *et al.*, 1984; Gelfand *et al.*, 1989) etc.

3. Based on the criterion selected in the previous step, construct child nodes for each of the subsets, into which the criterion splits the set assigned to the parent node. Connect the new nodes with the parent node with edges that represent the thresholds or ranges for the descriptors chosen on step 2. For example, the univariate criterion based on information gain may select one descriptor and identify several ranges of values of this descriptor, that maximize the information gain for training set instances belonging to each particular range. As a result, a descriptor is placed in the current test node, and child nodes are created for each of the identified ranges.

4. The optional step of bottom-up pruning may be performed. Pruning is referred to either deleting some of the existing branches of the tree or to merging several nodes to one. Pruning approaches differ depending on the particular implementation of the decision tree.

5. The steps 2 - 4 are repeated recursively for all nodes until the whole dataset is partitioned to subsets that contain only instances of one class, or if a predefined misclassification tolerance criterion is fulfilled.

The process of applying a decision tree is generally very straightforward - the decision tree is traversed from root to leaf following the edges that are applicable for the current classified instance descriptors. The class assigned to the instance is taken from the leaf node of the tree.

A sample decision tree from an article on blood-brain permeability (Suenderhauf *et al.*, 2012) is displayed in Figure 4.5. In this figure, the tree was constructed based on a univariate criterion, which split the original set into subset based on threshold values for the descriptors (aLogP, BCUTS and tPSA).

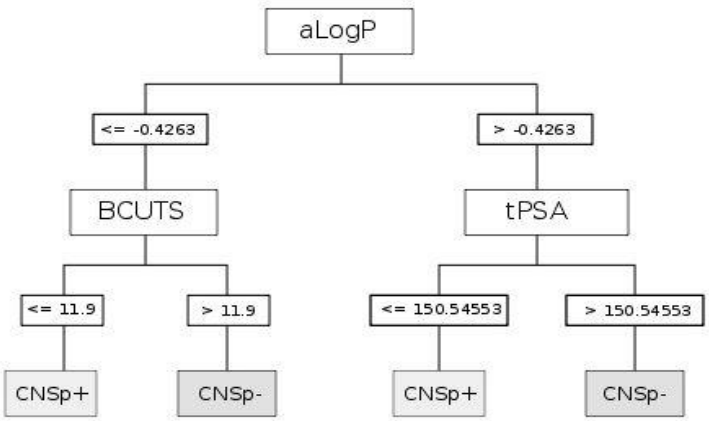

Figure 4.5: Example of decision Tree for blood-brain permeability data (Suenderhauf *et al.*, 2012).

Random Forest

Random forest is a bagging technique for both classification and regression. The general concept is to divide the data into several portions, use a relatively weak classifier/regressor to process, and then combine them. Random forest is flexible and can enhance the accuracy/performance of the weak algorithm to a better extent, at the expense of heavier computational resources required. The solution quality (in terms of accuracy for classification or MSE for regression) in each bag should be relatively high in order for bagging to perform promisingly.

Random forest (RF) is an ensemble of unpruned classification trees that performs classification through a majority vote approach, taking all the decisions of the trees into consideration to perform the final prediction (Breiman, 2001*a*). RF frequently performs better than single tree classifiers and, sometimes, has a better accuracy than many other ML algorithms. Also, it is relatively robust against noise. The RF learner exploits both bagging (Breiman, 1996) and the random subspace method (Tin Kam Ho, 1998) to construct randomised decision trees.

RF can be said to be a special case of bagging as it combines results from several unstable classifiers through bootstrapping, similar to C4.5 (J48 in WEKA). In bootstrapping, random sampling is performed with replacement from the training dataset. Because of the random selection, around 2/3 of the instances from the initial training set are used in each sample. Further, the randomness is introduced by the random selection of a subset of attributes to be considered at each node of every decision tree. The algorithm for RF is mentioned below (Breiman, 2001*a*):

1. Bootstrapped sample is generated from the original dataset, where the size of the sample equals the size of the original dataset, and random examples are chosen with replacement from the original dataset.
2. A tree is constructed using the bootstrapped sample as the training dataset, using the modified standard decision tree algorithm:

i. At each node, the set of candidate attributes are restricted to a randomly selected subset.

ii. The decision tree is not pruned.

3. Steps 1 and 2 are repeated for all the trees, creating a forest of trees, derived from different bootstrap samples.

4. On classifying an example, combine decisions of all trees in the forest. The majority of votes takes the decision.

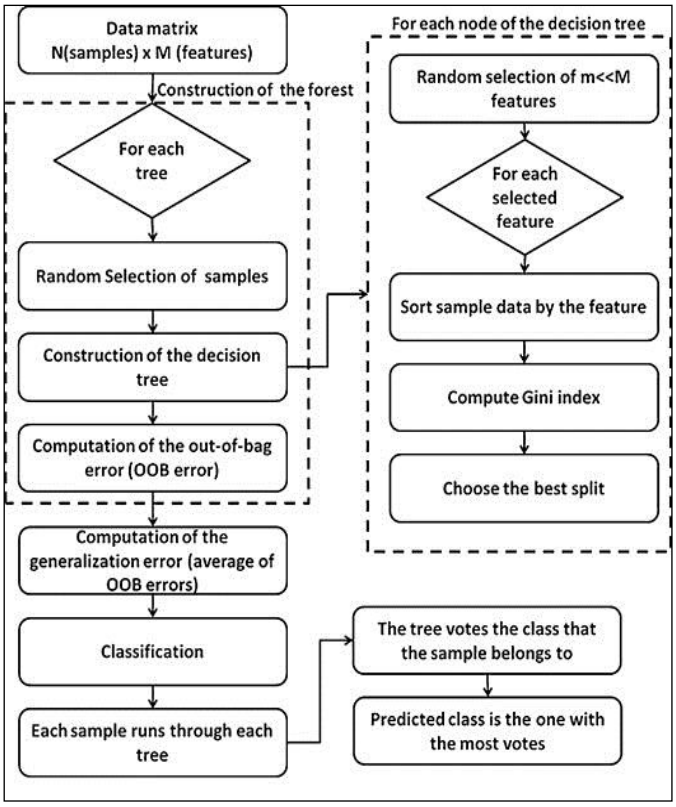

Figure 4.6: Schematic representation of Random forest algorithm (Tripoliti *et al.*, 2011)

The error rate of RF for classification depends on the correlation and the strength between each tree classifier. Its robustness depends on the randomness in each generated tree. If all the trees are identical in the ensemble, then it will perform the same as any single tree. So, bootstrapping and random attribute selection is crucial in reducing the correlation between each tree in the RF. Its strength also depends upon the strength of each single tree as robust performance of trees strengthens the forest. The diverse number of robust trees lowers the overall error rate and enhances the accuracy and strength of the RF learner.

Support Vector Machines

SVM is a classification algorithm, whereas its regression counterpart is SVR (support vector regression). Formulated as a quadratic programming problem, SVM is a linear classifier because its decision boundary for classification is linear. You can turn SVM into a non-linear classifier by employing the concept of kernel, at the expense of heavier computational resources required. The above applies analogously to SVR as a matter of course.

Support Vector Machines (SVM) is a very well-known machine learning technique used in data mining field, which is used in various domains for real-world classification problems. Due to its high generalization capabilities and ability to identify global and non-linear solutions, it has become a very popular choice of technique among the data mining researchers and scientists. Vapnik and colleagues (Cortes and Vapnik, 1995) first introduced the SVM and successfully applied in various areas ranging from handwritten character recognition, text classification to image retrieval (Cortes and Vapnik, 1995; Joachims, 1998; Tong and Chang, 2001). Briefly, it is based on drawing a hyper-plane or simply a decision plane that defines the decision boundaries (Figure 4.7).

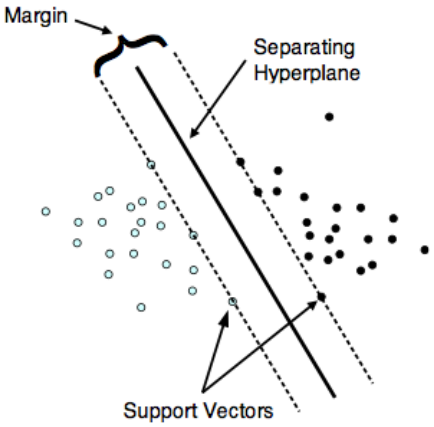

Figure 4.7: A linear SVM (Meyer and Wien, 2001)

It separates a set of objects having different class memberships. Let's say there is a simple classification example problem (Boser *et al.*, 1992; Cortes and Vapnik, 1995) represented by dataset

$$\{(\mathbf{x}(J_1), y_1), (\mathbf{x}(J_2), y_2), ..., (\mathbf{x}(J_N), y_N)\}$$

where,

$$\mathbf{x}(J_i) = (x_1(J_1), x_2(J_i), ..., x_M(J_i)) \in \Re^N$$

represents an N-dimensional data point and

$$y_i \hat{I} \{-1, 1\}$$

represents the label of class of that data point. The SVM algorithm is applied to find the best separating hyperplane that provides maximum margin and therefore the maximum separation of classes. Frequently, such separation cannot be achieved in the initial descriptor space. Therefore, to achieve it, the data points are first transformed into a higher dimension feature

space by a non-linear mapping function, say Φ . The possible separating hyperplane is defined as

$$\mathbf{w} \times \Phi(\mathbf{x}) + b = 0 \qquad (1)$$

where, ω is the weight vector normal to the hyperplane. If the dataset is completely linearly separable, the hyperplane can be found by solving the following optimization problem:

$$\text{minimize}: \frac{1}{2}\|\mathbf{w}\|^2 \quad (2)$$

$$s.t: y_i\left(\mathbf{w} \times \Phi(\mathbf{x}(J_i)) + b\right) \geq 1, i = 1..N$$

However, the real-world problems are not linearly separable despite being transformed into a higher dimensional space due to the presence of noise. So, the optimisation problem in Eqn. 2 is modified by the introduction of slack variables, $\chi_i \geq 0$ and the optimization problem is rewritten as

$$\text{minimize}: \frac{1}{2}\|\mathbf{w}\|^2 + C\sum_{i=1}^{N} \chi_i \quad (3)$$

$$s.t: y_i\left(\mathbf{w} \times \Phi(\mathbf{x}(J_i)) + b\right) \geq 1 - \chi_i, i = 1..N, \chi_i > 0$$

The slack variables $\chi_i \geq 0$ hold for misclassification, and therefore the penalty term $C\sum_{i=1}^{N} \xi_i$ is used to account for total misclassifications (training errors of the model). This new optimised function in Eq. (3) is to maximise the margin and to minimise the number of misclassifications (the penalty term). The parameter *C* is usually selected using grid optimisation of the SVM algorithm.

Although SVM produces very accurate results for balanced datasets, it is sensitive towards imbalanced datasets and may fail to produce optimal solutions. There are several studies which analysed this problem (Veropoulos *et al.*, 1999; Wu and Chang, 2003; Akbani *et al.*, 2004). It is possible to apply weights to the minority class in order to overcome the imbalanced data problem.

While linear and logistic regression generally require linearly separable data, SVMs can handle data that is not linearly separable, using non-linear kernel functions like Radial Basis Function kernels (Pochet and Suykens, 2006).

4.2.3 Cross- Validation

In order to have stable and reliable predictive models and avoid over-fitting of the data, it is important to validate them. In particular, when the data is limited and no external data set is available for validation, one way to deal with this issue is splitting the data in order to use only

one part for training the model and having an unseen dataset for testing. This is the basis for cross-validation, a technique for evaluating models (Berrar, 2019).

Cross-validation can be implemented in several ways. One technique is simply based on the method described above, in which the data is split into two parts (can be 70-80% training, and the remaining test) and predictions are made on the test set after the model is trained on the first part. The errors are averaged and can be seen as a measure to evaluate the performance of the model on the test set. However, this holdout method can have a high variance, based on which data points get selected into the training set and which ones go into the test set.

To improve over this method, we can apply k-fold cross validation, in which the data set is divided into k subsets, and the holdout method is repeated k times. The most common implementations are 5 or 10 fold cross-validation, again depending on the size of the data. In a 10-fold cross-validation, the data would be split into 10 parts. In each run, one part would be used as the test set and the remaining 9 merged to form the training set. Since the average error is obtained at the end, each data point gets placed in the test set once and the splitting of data into the two groups has less effect on the overall performance. However, this can turn out to be computationally expensive. One alternate method is to randomly split the data k different times and repeat the process as many times as desired, averaging the errors from all the runs (Kim, 2009; Refaeilzadeh *et al.*, 2009) . In Chapter 7, we implement repeated k-fold cross validation, repeating 5-fold cross validation 20 times.

Yet another technique of implementing this method is Leave-one-out cross validation. In this case, k- fold cross validation is applied in a way that k equals the total number of data points. So, the model would run as many times as the number of data points, with only one sample being used as the test set in each run.

5.Diagnostic value of EEG in early Parkinson's disease

As the process of neurodegeneration starts years before the clinical symptoms manifest, our goal was to detect differences in brain patterns in early stage Parkinson's disease patients as compared to healthy individuals and use these findings for monitoring the disease progression. In Section 5.1, we apply machine learning to identify a subset of six QEEG spectral power features that can distinguish between the two groups effectively. Theta power, especially in the temporal left region, as well as the alpha1/theta ratio in the central region of the brain come up as two of the most important differentiating features. The text in this section is based on a published study (Chaturvedi *et al.*, 2017). A major strength of the overall study was the availability of an extensive neuropsychological test battery, evaluating the attention, long-term memory, short term or working memory, visuo-spatial function and executive functions of the patients. This led to questions about whether these tests contained additional information that could complement the EEG patterns and increase the classification accuracy of early stage PD patients and healthy individuals. Section 5.2 investigates this additive value of neuropsychological scores to EEG measures. We see that combining EEG and 24 neuropsychological scores does increase the overall prediction accuracy by a maximum of 10% and the importance of the attention domain as well as the overall cognition score is reflected in the ranking of important features. Investigating the relationship between EEG and neuropsychological scores in early stage PD patients further, we focused on the visuospatial impairments. This published study (Eichelberger *et al.*, 2017) follows in Section 5.3 and shows the reduction of the alpha1/theta ratio in the parietal regions to be related with visuo spatial impairments in non-demented PD patients.

5.1 Machine learning in high-density QEEG feature selection for classification

5.1.1 Introduction

Neurodegenerative disorders may begin at any point during the lifetime of an individual and progress for years or decades before becoming clinically manifest(Savica *et al.*, 2010; Reiman *et al.*, 2012). This poses a major obstacle for research into prevention and delays treatment.
A few studies have shown that quantitative EEG (QEEG) could be useful for early prognosis of dementia(Fonseca *et al.*, 2009; Klassen *et al.*, 2011; Dubbelink *et al.*, 2014, Gu *et al.*, 2014*b*). Some alterations in the electrical activity of the brain have also been found to be prevalent in Parkinson's disease patients without dementia (Berendse and Stam, 2007; Stoffers *et al.*, 2007) Benz et al.(Benz *et al.*, 2014*a*) reported significant QEEG differences between patients with AD and PD, observing more pronounced slowing of EEG in patients with PD as compared to the AD group. Having a set of QEEG features that could detect patients in the early stages of Parkinson's disease would be useful in providing treatment and care to the individuals. Schmid et al.(Schmidt *et al.*, 2013) carried out such a study for AD and investigated alpha/theta spectral ratio as a measure to distinguish healthy individuals from patients with AD. Han et al. (Han *et al.*, 2013) recorded EEG's in Parkinson's disease patients and healthy controls and found an increase of relative powers in the delta, theta bands, while observing a decrease of relative powers in the alpha, beta bands. We have investigated the regional powers in Parkinson's disease patients and healthy controls in order to see if a subset of QEEG features obtained from high-density EEG recordings could accurately distinguish between the two groups. Based on previous studies, we speculated that alpha/theta spectral ratio could be a good feature for discriminating between the diseased and healthy individuals. Our aim was also to find an optimal method for feature selection that could deal with high dimensionality, multicollinearity and avoid the risk of overfitting of the data.

The current study explores the differences in high-resolution QEEG data between PD patients (with and without MCI) and healthy controls (HC) at baseline, using regression and machine learning meth

5.1.2 Methods

Subjects

68 patients with Parkinson's disease were recruited from the Movement Disorders Clinic of University Hospital of Basel from 2011 to 2015 by advertising in the magazine of the Swiss Parkinson's Disease Association. The patients were diagnosed according to the United Kingdom Parkinson's Disease Brain Bank criteria (Gibb and Lees, 1988). A neuropsychological examination was carried out in all individuals during the recruitment process. Knowledge of the German language was a requirement to be included in the study. 9 patients had to be excluded due to presence of other medical conditions and 1 patient dropped out due to an accident. After processing and visually inspecting the EEG data, 8 patients had to be excluded either due to artifacts present or low voltage signals. A group of 50 PD patients (33 males and 17 females) was selected and compared with an age and education matched group of 41 healthy controls (21 males and 20 females), who were recruited from the Memory Clinic, University Center for Medicine and Aging of Basel and from the University Hospital of Basel. The sample size can detect an effect size of 0.59 with a statistical power of 80% at a 5% significance level.

Mean age of the PD group was 68.8 (+/-7) years, with an average disease duration of 5.3 (+/-5.1) years, while that of the healthy group was 71.1 (+/-7) years. The studies were approved by the local ethics committee (Ethikkommission beider Basel, ref. no.: 135/11, 294/13, 260/09). All participants gave their written consent.

Neuropsychological assessment

A comprehensive battery of neuropsychological tests was applied to test for the following cognitive domains: attention, working memory, executive functions, memory and visuo-spatial functions. The raw scores of the tests were normalized and transformed into adjusted z-scores (Berres *et al.*, 2000) based on the data collected for 604 age-, sex- and education-matched healthy individuals. The tests were used for thorough examination of patients and diagnosis of Mild Cognitive Impairment (MCI) according to the criteria published by Litvan et al(Litvan *et al.*, 2012). Patients with dementia were excluded for this study and only those with MCI or with normal cognition were included.

EEG recording and processing

A 256-channel EEG System (Netstation 300, EGI, Inc., Eugene, OR) was used to record 12 minutes of continuous EEG (eyes closed) for all individuals. The participants were seated on reclining chairs, asked to relax while staying awake and to have minimum of eye as well as body movements. Three minutes of EEG data, with single segments of at least 30 seconds without artifacts (e.g. eye movements, signs of drowsiness), were selected and down sampled

(500 Hz). Data from 214 electrodes (excluding cheeks, neck electrodes) were filtered (0.5–70 Hz) and an inverse Hanning window was used to stitch together shorter segments. Resulting EEG data were re-referenced to average reference and bad channels were interpolated with the spherical spline method. Additionally, the independent component analysis implementation of EEGLAB (Delorme and Makeig, 2004) ("runica" with default settings) was used to remove further artifacts. To obtain the power spectra, Welch's method (Welch, 1967) was applied. Relative power was obtained for five frequency bands: delta (1–4 Hz), theta (4–8 Hz), alpha1 (8–10 Hz), alpha2 (10–13 Hz), and beta (13–30 Hz), by calculating the ratio of the signal power within a frequency band to the total signal power (1-30 Hz). The electrodes were mapped to ten regions of interest on the scalp, corresponding to the left and right frontal, central, parietal, temporal and occipital. Median and peak frequencies were also calculated from the occipital region. Compared to classical electrode designs (with typically 21 channels), high density electrode systems allow us to aggregate the signals from nearby locations, which in many cases, leads to significant noise reduction.

A total of 79 different measures were extracted and used for further analysis and feature selection. These included global power for each band, power in every region in all five frequency bands, alpha1/theta ratios for all regions and the median as well as peak frequency measures.

Statistical analysis

Potential confounding by factors, such as age, sex, and education of the patients was accounted for by calculating linear regression models. The dataset had highly correlated features and the goal was to find out which features were important for classification. For this purpose, a comparison was done between Logistic regression and three machine learning methods including Random Forest(Breiman, 2001*b*; Liaw, A. & Wiener, M., 2002), Support Vector Machine (SVM) (Chang and Lin, 2011) and J48 Decision Trees(Salzberg, 1994) using the Weka software(Hall *et al.*, 2009), version 3.7. Ten-fold cross-validation was applied to all the methods. A ranking of variables was obtained from Random Forest on the basis of mean decrease in accuracy and Gini coefficients. Machine learning methods have been used in quite a few medical studies for prediction and diagnostic classification(Khodayari-Rostamabad *et al.*, 2013; Singal *et al.*, 2013; Johannesen *et al.*, 2016). Differences can be noted in the way each method works and, in the results, obtained.

While linear and logistic regression generally require linearly separable data, SVMs can handle data that is not linearly separable, using non-linear kernel functions like Radial Basis Function kernels (Pochet and Suykens, 2006). Decision Trees work by creating a flowchart which consists of "leaf" nodes (representing a classification) and decision nodes (which can have several "branches"). Their hierarchical tree structure makes them easy to understand and interpret. A random forest algorithm makes use of several decision trees that are combined in a "bootstrap aggregation" scheme. Based on random subsets of the data, random forests grow a series of individual trees, and the whole forest of such trees can then be used to identify a set of

vital features. Random Forests do not require real-valued features and can handle high dimensional data. However, some bias can be introduced with any of the methods, including Random Forest (Strobl *et al.*, 2007).

Additionally, penalized logistic regression was applied to the data to obtain a subset of features that would not be highly correlated to each other. The least absolute shrinkage and selection operator (LASSO) method has been used in different studies for feature selection and computing risk predictive models (Wu *et al.*, 2009; Fontanarosa and Dai, 2011). In many cases, lasso-penalized models have shown improved prediction accuracy while selecting only a limited number of covariates that are included in the model.

The penalized (Goeman, 2010) package in R(R Core Team, 2018)(version 3.2.1) was used to create a logistic regression model and apply the L1-LASSO (Tibshirani, 1996*b*, 1997) penalty. Tenfold cross validation and optimization was carried out to select the tuning parameter. Cross-validated ROC curves were obtained with the ROCR (Sing *et al.*, 2005) package in R.

5.1.3 Results

Table 5.1.1 shows the characteristics of the PD and HC groups. No significant differences were found in the age, education, sex distribution of the patients in the two groups.

Parameters	HC(N=41)	PD(N=50)	p value (Wilcoxon)
Age(years)	70 [53,83]	69 [55,84]	0.08
Education(years)	12 [8,19]	14 [9,20]	0.052
Males	21	33	
Females	20	17	

Table 5.1.1: Demographic characteristics of PD patients and healthy controls (HC). The data shown here are the median values and range for each parameter.

The average grand spectra for the ten regions in both groups of individuals can be seen in Figure 5.1.1.

On comparing Logistic Regression, SVM, Random Forest and J48 decision trees, Random Forest was seen to perform better overall with an area under the curve of 0.8 and accuracy of 0.78. The accuracies and AUC values of all methods can be seen in Table 5.1.2.

Method	Accuracy	AUC
Random Forest	0.78	0.8
SVM	0.747	0.73
J48	0.68	0.67
Logistic Regression	0.56	0.63

Table 5.1.2: Performance measures evaluated by logistic regression and machine learning methods

As Random Forest and LASSO are two methods that give a ranked list for feature selection, we focused on these two methods and investigated the subset of features selected by the methods.

The penalized logistic regression model obtained from using LASSO revealed the most influential variables in classifying individuals into two groups. Table 5.1.3 shows the list of names of the most influential variables.

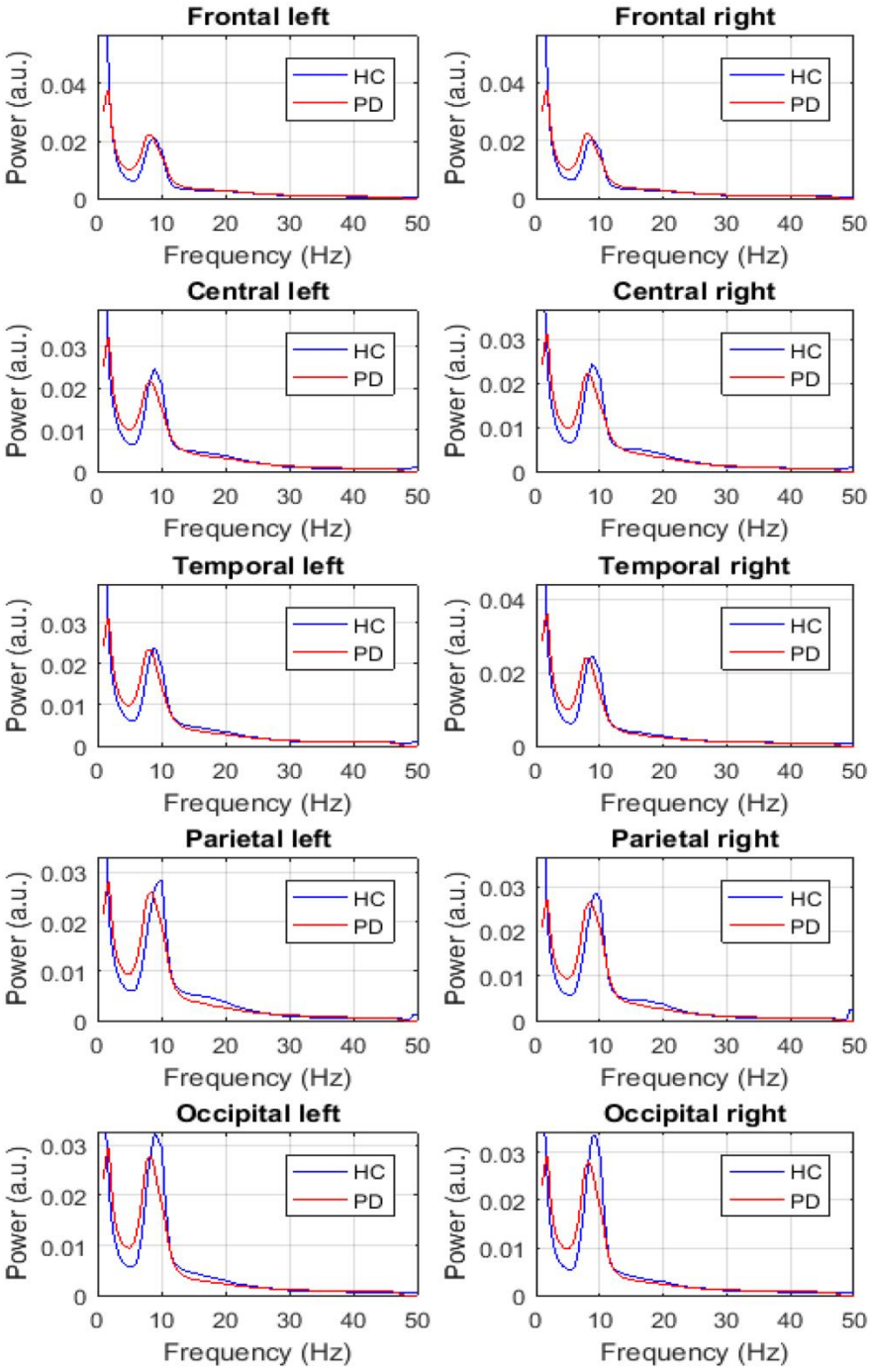

Figure 5.1.1: Comparison of average grand spectra of 10 brain regions in Parkinson's disease patients and healthy controls

Variables	Coefficients (Median)
F4.8_TL	0.531
F10.13_FL	0.243
F10.13_CR	0.069
A1.T_CL	-0.586
F13.30_PL	-0.156
A1.T_TL	-0.045

Table 5.1.3: Variables found to be influential in the logistic regression model with LASSO penalty. They are coded as F(Frequency) [Power band in Hertz]_[Brain Region]. E.g.: F4.8_TL refers to the theta band power in the temporal left region of the brain. A1.T refers to the alpha1/theta ratio. The median coefficient values depicted correspond to the box plot in Figure 5.1.2.

A boxplot depicting the non-zero coefficients of penalized logistic regression model can be seen in Figure 5.1.2. The figure shows the coefficients of penalized logistic regression model in which cross-validations were carried out. The median values of the coefficients are seen in the box plot. The different frequency bands are represented as 4.8 (theta), 8.10 (alpha1), 10.13(alpha2), 8.13(total alpha),13.30(beta).The alpha1/theta ratio is represented as A1.T and the different brain regions are abbreviated as TL/TR(temporal left/right), CL/CR(central left/right), FL/FR(frontal left/right), PL/PR(parietal left/right), CL/CR(central left/right). GP refers to the Global Power in each band. A cross-validated ROC curve was plotted after logistic regression is shown in Figure 5.1.3. It showed an area under the curve of 0.76.

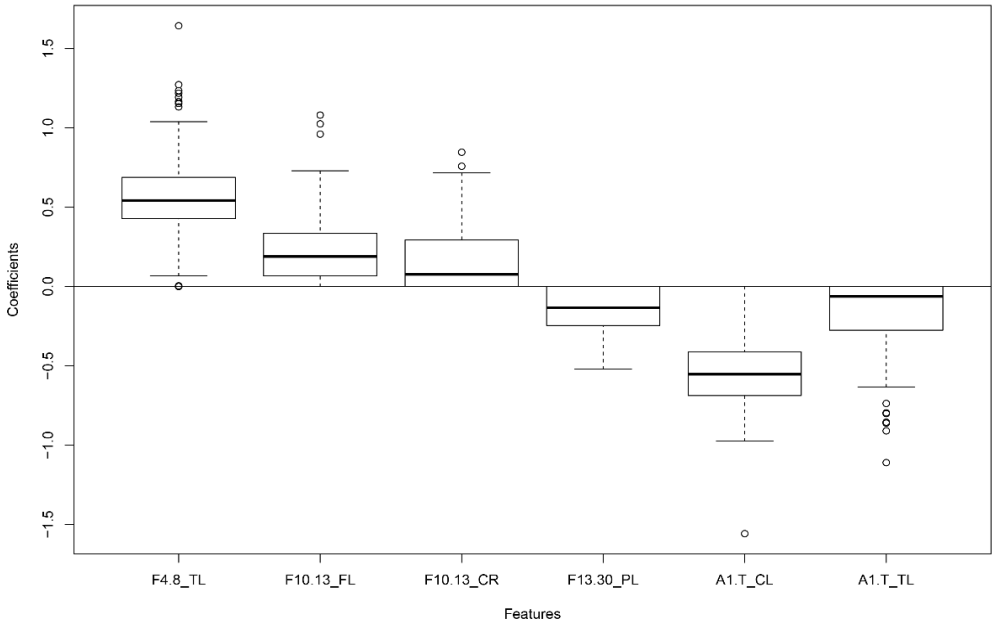

Figure 5.1.2: Box plot showing non-zero coefficients of the penalized logistic regression model obtained after 200 cross validations.

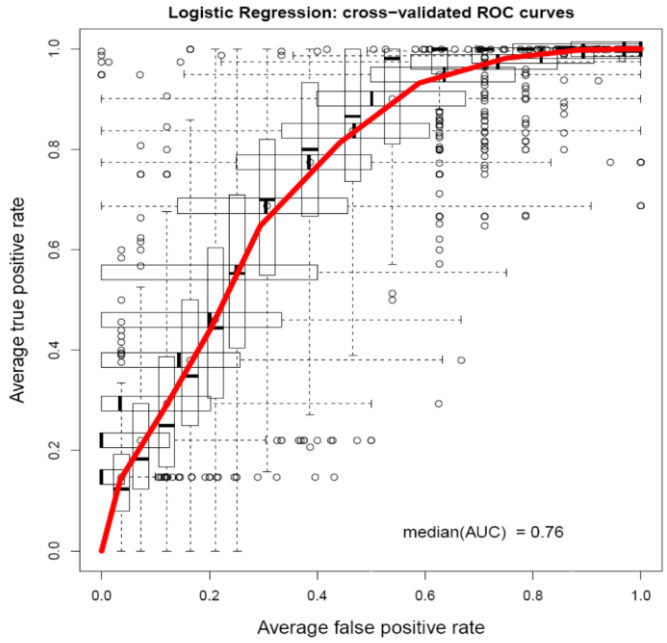

Figure 5.1.3: Cross-validated ROC curve obtained from the logistic regression model shows an AUC value of 0.76

Alpha1/theta ratio in the central left region and theta power in temporal left were found to be two of the most important features for classification.

Random Forest ranked the QEEG measures on the basis of a decrease in accuracy of classification and also in decreasing order of the Gini coefficients. A variable is deemed to be more important for the classification of data if its exclusion results in a decrease in the accuracy of the random forest model. This is determined during the out of bag error calculation phase. Hence, the higher the *MeanDecreaseAccuracy* measure for a variable, the greater is its importance. *MeanDecreaseGini* shows how each variable contributes to the homogeneity of nodes in the random forest model. A higher decrease in Gini implies that the variable plays a greater role in the classification process. The top thirty measures obtained from both rankings can be seen in Figure 5.1.4.

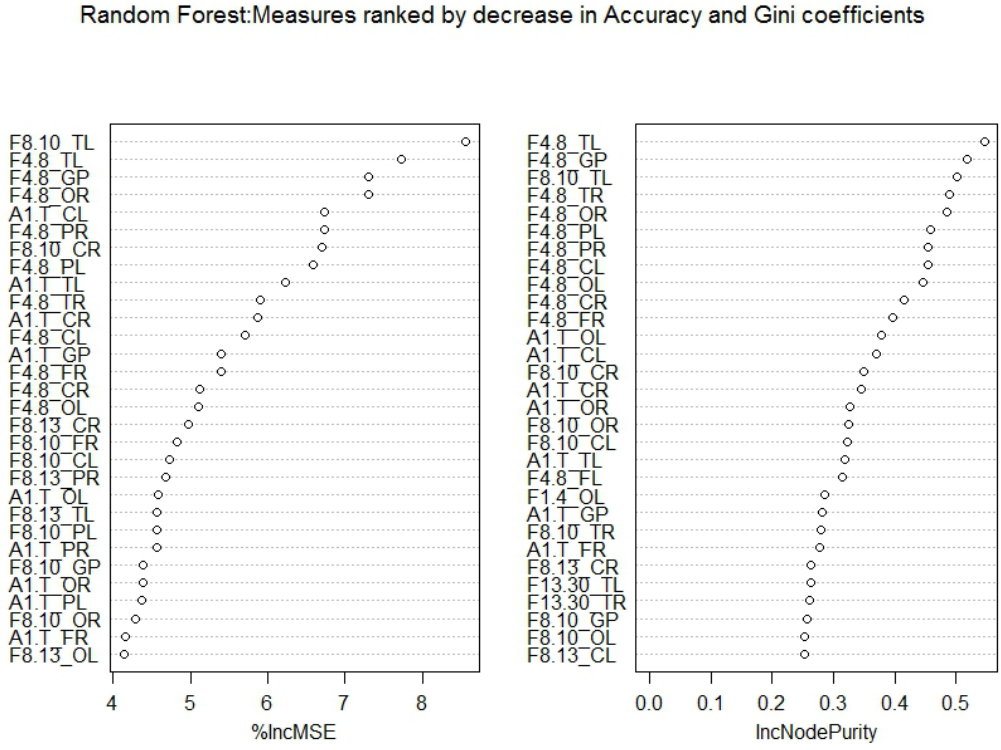

Figure 5.1.4: Variable Importance plots obtained from Random Forest in R show the top QEEG measures ranked on the basis of Mean Decrease in Accuracy and Mean Decrease in Gini coefficients.

Both methods selected a few common top features, including theta power in the temporal left region, alpha1/theta ratios in the central left and temporal left regions. The main difference was that LASSO focusses on selecting an optimal set of variables that are not highly correlated to each other but have high accuracy in the prediction model. Random Forest takes the accuracy into account but does not exclude variables that are highly correlated to each other. In this way, a small subset of features for distinguishing the two groups can be obtained using LASSO but a detailed list of influential features can be obtained using Random Forest.

5.1.4 Discussion

In this study, we investigated seventy-nine frequency measures from ten regions of interest in groups of PD patients and healthy controls. Our goals were to look for a feature selection method that would solve the problem of multicollinearity, high dimensionality and reduce the risk of overfitting of data. We also wanted to see if alpha/theta spectra ratio would come up as an important feature in distinguishing between diseased and healthy individuals. The penalized logistic regression method (LASSO) applied for classification between the groups resulted in a subset of six measures, reflecting differences in theta, alpha2, beta power and alpha1/theta ratio in certain regions. Two of the most influential features included theta power in the temporal left region and alpha1/theta ratio in central left region, and were detected by both methods focused on, Random forest and LASSO. As speculated, alpha/theta spectral ratio was seen to be one of the influential features in discriminating between Parkinson's disease patients and healthy individuals.

The regression method with the LASSO penalty has been useful in selecting a group of six features out of seventy-nine. It is good for handling large number of data points and predictors at a time but can pose a problem if the variables are not relatively scaled. It can be used for different types of data, such as continuous, binomial, etc. However, on carrying out classification with Random Forest, we found that the variables were not ranked in the same way as with LASSO. This could be possibly explained by the fact that a lot of frequency measures, especially in the neighbouring regions of the brain, are highly correlated and the LASSO penalty integrated in Logistic Regression only selects one measure out of every group of highly correlated measures.

The final choice of method for feature selection would depend on the question at hand. For obtaining a model that could include a detailed list of the most important variables, Random Forest would be a good choice. If, on the other hand, the goal would be to select a small set of uncorrelated features that could result in comparable prediction accuracy, LASSO would be the preferred method. LASSO selects one set of optimal features for classification but might not reflect all the features important for clinical diagnosis.

5.2 Feature selection combining QEEG and neuropsychological measures

5.2.1 Introduction

Parkinson's disease can affect both, motor and non-motor functions of the patients. Amongst non-motor functions, cognitive impairments and behavioural disturbances can have a big impact on the quality of life (Watson and Leverenz, 2010; Watson *et al.*, 2013), and can also be an early indicator of the disease.

Neuropsychological parameters are known to be effective in diagnosing and monitoring Parkinson's disease (PD) apart from other neurodegenerative disorders like Alzheimer's disease. A battery of neuropsychological tests is used to evaluate different cognitive domains of the patients, such as Attention, Working Memory, Executive Function, Visuo-Spatial Function, and Memory (Berres *et al.*, 2000; Ph.D, 2007; Zimmermann and Fimm, 2007, Benz *et al.*, 2014*a*).

Since we investigated the effectiveness of EEG data in distinguishing PD patients from healthy controls (HC) in section 3.1, we wanted to extend this study further. Our aims were to: a) check for the correlation between EEG and neuropsychological measures, b) see if the classification performance could be improved by adding on the neuropsychological test measures and c) identify the most important features from both groups for achieving high accuracy overall.

5.2.2 Methods

This study was carried out in two iterations. The first was an extension of the research shown in Section 5.1 (Chaturvedi *et al.*, 2017) and used the exact patient cohort as published. Neuropsychological assessment of the patients was done using 18 tests that covered five cognitive domains: attention, working memory, executive functions, memory and visuo-spatial functions. An average score for each domain was calculated along with an overall cognitive score, resulting in 6 additional scores. EEG data processed with a semi-automated pipeline were used to obtain the relative power in alpha, theta, delta, beta frequency bands across 10 regions of the brain. The 5 cognitive domains as well as the overall cognitive score were correlated with EEG data of the 41 healthy individuals and 50 PD patients. LASSO was re-applied with all EEG measures together with all cognitive scores. Additionally, Random Forest algorithm was applied to the data to check for prediction accuracy and to obtain variable importance plots.

To increase the patient cohort and have a standardised processing pipeline, all EEG data were processed using an automated pipeline and this was used in the second iteration of the study. Any patients who dropped out later, had doubtful EEG data or also had another disease were excluded. Patients whose neuropsychological data were not available were also left out of this cohort. This resulted in a cohort of 66 PD patients and 59 healthy controls.

5.2.3 Results

Following up on the subset of measures selected in Section 5.1, we found attention domain to be correlated with theta power in temporal left, beta power in parietal left regions. Theta in temporal left was particularly highly correlated with memory and overall cognition scores. This was also reflected in the alpha1/theta power in the temporal left region. Table 5.2.1 shows the correlation coefficients between the shortlisted EEG features and cognitive domains.

Cognitive domains	**F13.30_PL**	**F4.8_TL**	**A1.T_CL**	**F10.13_CR**	**F10.13_FL**	**A1.T_TL**
Attention	0.307	-0.405	0.152	0.01	-0.138	0.2
Working Memory	0.114	-0.111	0.019	0.0832	-0.0006	0.089
Executive function	-0.074	-0.138	0.14	-0.06	0.023	0.176
Memory	0.198	-0.29	0.237	-0.016	-0.065	0.238
Visuo	0.131	-0.101	0.113	-0.02	-0.116	0.098
Overall Cog	0.211	-0.315	0.21	-0.004	-0.11	0.248

Table 5.2.1: Correlation between EEG features selected by LASSO and cognitive domains

Lasso was re-run on the dataset consisting of both, neuropsychological and EEG scores, to check for important features in the classification. This new subset, along with the beta coefficients, is seen in Table 5.2.2. The median AUC was 0.75 and comparable to the performance using EEG measures alone and included 5 of the EEG variables also selected by Lasso using EEG. The largest coefficients still corresponded to EEG features.

Measures	Coefficients
Intercept	0.138232898
F10.13_FL	0.096637113
F4.8_TL	0.009764126
Working Memory	-0.010300006
A1.T_TL	-0.033160499
Memory	-0.062768028
Attention	-0.115259682
Overall Cog	-0.167384416
F13.30_PL	-0.481784339
A1.T_CL	-0.622159769

Table 5.2.2: Penalized regression coefficients for EEG and neuropsychological measures in classifying PD patients from healthy individuals

In the second iteration of this study, an increased patient pool was considered and the EEG data of all 125 patients were processed uniformly using an automated pipeline. Lasso was first applied only to the 18 neuropsychological scores of all patients to assess the discriminative power between the two groups. The Rey Copy Test, associated with the visuo constructive domain, was seen to have the largest coefficient, followed by tests in the Attention and Memory domain. This is depicted in Table 5.2.3. The median AUC obtained was 0.88.

Tests	Coefficients	Domain
Rey_copy	-0.509507445	Visuo Constructive
Trail_Making_A	-0.48891941	Attention
(Intercept)	-0.441420291	
Simple_RT_no_Warning	-0.40371739	Attention
CVLT_t1	-0.401967906	Memory
Five_Point_Test	-0.345707686	Executive function
Div_Att_vis_RT	-0.290275666	Attention
Div_Att_aud_RT	-0.002014186	Attention
CVLT_sav	0.027343262	Memory
Digitspan_bw	0.224255256	Working Memory

Table 5.2.3: Coefficients of penalized logistic regression for distinguishing PD from HC using neuropsychological measures

As a next step, the EEG measures were also added to the 18 neuropsychological scores, and the classification process was run to identify influential features. The non-zero coefficients are seen in Table 5.2.4. The median AUC increased to 0.9. EEG variables had the biggest influence on the classification.

Measures	Coefficients
(Intercept)	0.1407114
F13.30_OR	2.13364294
F4.8_CR	1.02777218
CVLT_sav	0.81022275
F10.13_OL	0.70306598
F1.4_OL	0.40665649
F10.13_OR	0.37905272
Digitspan_bw	0.26727335
Rey_sav_IR_copy	0.0764899
F1.4_OR	0.03483677
A1T_TR	-0.00209984

Trail_Making_A	-0.01279106
A1T_TL	-0.10709
F8.10_PL	-0.113549
F13.30_CL	-0.27277
Block_Tapping_bw	-0.307411
A1T_CR	-0.31502294
F13.30_FL	-0.31654541
Semantic_Fluency	-0.41663774
Div_Att_aud_RT	-0.43593
Simple_RT_no_Warning	-0.47415921
Five_Point_Test	-0.51077041
Div_Att_Omissions	-0.78091621
F13.30_TR	-0.7914092
Rey_copy	-0.98296989
A1T_PR	-1.10237651

Table 5.2.4: Coefficients of penalized logistic regression for distinguishing PD from HC using neuropsychological and EEG measures

To get a ranked list of important features, Random Forest was applied on different combinations of the data set. On using the QEEG measures alone for classification, Area-under-the-Curve (AUC) value of 0.819 was obtained along with Positive and Negative predictive values (PPV, NPV) of 0.736 and 0.754 respectively. The 6 neuropsychological domain scores, when used alone, resulted in an AUC of 0.82, PPV of 0.71 and NPV of 0.8. On combining the QEEG measures and the 6 neuropsychological scores, an AUC value of 0.859 was obtained along with a PPV of 0.729 and NPV of 0.76. A slight increase in the AUC was observed on combining the QEEG and 6 neuropsychological measures, in comparison to using them alone while the PPV and NPV values did not have much difference.

However, on combining the QEEG measures with all 24 available neuropsychological scores instead of using the average domain scores and overall cognitive scores alone, the AUC value increased to 0.88 while the PPV and NPV values increased to 0.785 and 0.8.

Measures that were ranked higher in the list included the attention domain, overall cognitive score, beta frequency measures, followed by individual tests from the executive function and

attention domain. Results from the Random Forest can be seen in Table 5.2.5 and the ranked list of EEG and neuropsychological variables can be seen in Figure 5.2.1.

Parameters included	**Precision PD**	**Precision HC**	**AUC**	**FP Rate**	**Recall**
EEG	0.765	0.827	0.819	0.26	0.744
EEG+6 NP domains	0.73	0.765	0.859	0.265	0.744
EEG+24 NP scores and domains	0.78	0.8	0.88	0.213	0.792
EEG+18 NP scores	0.76	0.792	0.85	0.23	0.776
6 NP domains	0.735	0.719	0.82	0.27	0.744
18 NP scores	0.8	0.81	0.88	0.197	0.8
24 NP scores	0.78	0.727	0.866	0.217	0.78

Table 5.2.5: Random Forest classification performance using different combinations of EEG and neuropsychological scores

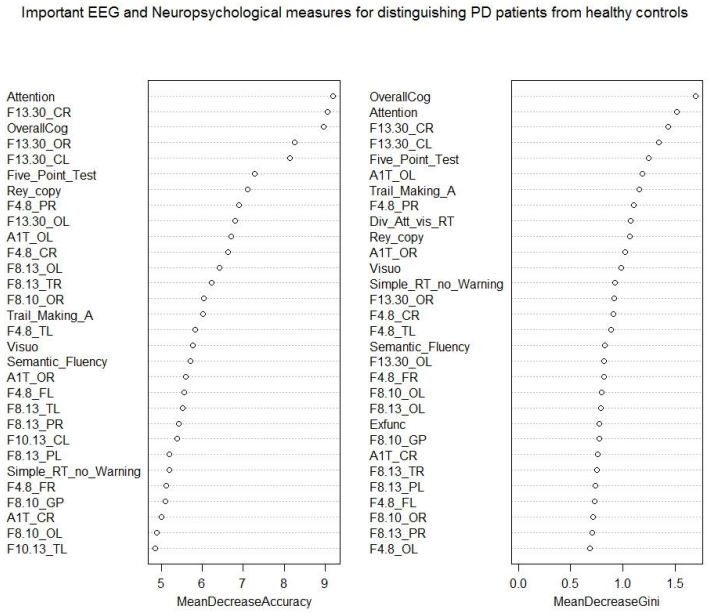

Figure 5.2.1: EEG and neuropsychological measures differentiating Parkinson's disease patients from healthy individuals

5.2.4 Conclusion

Overall, we see that EEG and neuropsychological scores have comparable performances and when combined, the accuracy increases slightly. However, what is interesting to see is that tests from the visuo-constructive domain, attention and memory are influential amongst the set of neuropsychological measures. Amongst the EEG measures, beta and theta measures were consistently ranked at the top, even when combined with neuropsychological measures.

QEEG measures and neuropsychological measures, when combined together, are useful in distinguishing Parkinson's disease patients from healthy controls with a considerable accuracy.

5.3 Visuospatial Ability and EEG Slowing in Patients with Parkinson ’s disease

As visuo-constructive domain was one of the important neuropsychological domains detected in identifying PD patients, and it is one of the first domains that start getting affected in cognitive decline, the following manuscript by Echelberger et al. (Eichelberger *et al.*, 2017) investigates the relationship between visuo spatial ability and EEG measures in PD patients.

5.3.1 Introduction

Cognitive impairment in PD has mainly been characterised by executive dysfunction, attentional, memory, and visuospatial deficits (Emre, 2003*a*; Gratwicke *et al.*, 2015). The cognitive impairment generates far-reaching individual and health economic implications. In previous studies, it has been shown that visuospatial disturbances are among the first symptoms of cognitive decline to appear in PD (Girotti *et al.*, 1988; Antal *et al.*, 1998). These deficits become more pronounced as the disease progresses (Levin *et al.*, 1991) and they are independent of the severity of motor dysfunction and of the overall intellectual status. Interestingly, studies have shown that PD-patients with visuospatial deficits or memory impairment show a higher conversion rate to Parkinson’s disease dementia (PDD) than individuals with executive deficits (Muslimović *et al.*, 2005; Williams-Gray *et al.*, 2007).

The cause of the visuospatial deficits, however, remains unclear (Laatu *et al.*, 2004). A study (Pereira *et al.*, 2009) showed that patients with Parkinson’s disease and mild cognitive impairment (PD-MCI) have a greater grey matter atrophy in both occipitotemporal and dorsoparietal cortices compared to healthy controls. Furthermore, previous research showed that these patterns correlate with visuoperceptual and visuospatial abilities. These results are in line with the dual-stream hypothesis of visual processing which differentiates between two linked visual projection systems (Ungerleider and Haxby, 1994). The first system expands from the area 17 (primary visual cortex) over the dorsal visual route towards the areas of the upper temporal lobe and the parietal lobe (occipitoparietal projection system). These areas participate in the analysis of visuospatial information such as movement, depth, position, orientation, and 3D characteristics of objects. The second projection system, the ventral visual stream, is responsible for pattern recognition (analysis of shapes, colours, objects and faces). It extends beyond area 17 to the lower temporal lobe.

Biomarker-based detection might lead to a better understanding of the cause of the visuospatial decline in PD-patients. Research (Kamei *et al.*, 2010) verified a positive correlation between deficient executive functions in PD and frontal EEG slowing. This relationship indicates that the deficits in executive tasks in PD could be due to a frontal dysfunction. Based on these findings, it would be interesting to investigate whether visuospatial abilities are related to parietal and occipital EEG activity in PD-patients.

More precisely, it is hypothesized that PD-patients with a visuospatial deficit manifest an EEG slowing which should be particularly pronounced in the parietal and the occipital lobe, compared to frontal, central and temporal areas. To avoid confounding with overall cognitive performance the EEG slowing is matched with a test of memory span measures (short term memory). This association, in turn, is expected to be stronger in the frontal lobe compared to central, temporal, parietal and occipital areas.

5.3.2 Materials and Methods

Subjects and clinical Assessments

Participants were recruited between 2011 and 2015 from the outpatient clinic for movement disorders of the University Hospital Basel or through announcements in the Journal of the Swiss Parkinson's Disease Association. Altogether 72 patients with PD participated in the study. The data used in this study were baseline data collected from two studies. The first study was a computer-based, multi-dimensional and disease-specific training of cognition in patients with PD that has already been published (Zimmermann *et al.*, 2015*a*). The second study was an ongoing group-based stress management training in patients with PD. Clinical assessment was performed with optimally medicated patients by means of the sum score of the motor section of the Unified Parkinson's Disease Rating Scale (UPDRS) subscale III. Depression was assessed by Beck`s Depression Inventory (BDI) (Schrag *et al.*, 2007). The levodopa-equivalent (LED) was estimated (Tomlinson *et al.*, 2010). Inclusion criteria for the study were idiopathic PD according to UK Parkinson's disease Brain Bank Criteria (Gibb and Lees, 1988) and signed informed consent. Patients were excluded if they had other severe brain disorders, insufficient knowledge of the German language or if the EEG and the neuropsychology measurement were set apart more than 60 days. For this study, the data of 57 patients with PD were included. Fifteen patients were excluded due to a Mini-Mental State Examination (MMSE) score of <24 (n = 3), because of undergoing a deep brain stimulation (n = 6) or due to insufficient EEG quality (n = 6).

Neuropsychological Assessments

Patients were assessed with a comprehensive neuropsychological test battery. The following tests of this battery were used for this study: Clock Drawing Test, Rey-Osterrieth Complex Figure Test (ROCF) copy task (Duley *et al.*, 1993), Block Design Test (Tewes, 1991) and verbal Digit Span forward.

The *Clock Drawing Test*(Thalmann *et al.*, 2002) is a reliable measure of cognitive dysfunction (Cahn-Weiner *et al.*, 1999; Riedel *et al.*, 2013) and correlates with visuospatial tests like the ROCF and the Block Design (Hochrein *et al.*, 1996; Pinto and Peters, 2009).

The *ROCF* is a common neuropsychological screening method for visuospatial abilities (Karádi *et al.*, 2015). Particularly, the copy variant of the task measures visuospatial construction while the delayed variant indicates visuospatial memory performance(Aebi and Mistridis, 2009). In the ROCF, the patients had to copy a complex figure. Afterwards, they had to reproduce it as complete as possible after a delay of 30 minutes. The ROCF was evaluated according to Aebi and Mistridis [34] based on Spreen and Strauss. The sum score ranges from 0 to 36 points. The data were transformed into education and age-controlled z-scores.

Block Design is a subtest of the revised Hamburg Wechsler Intelligence Scale for Adults. The patients received at the beginning 4 and later 9 blocks, with different colour patterns on each side. With the blocks the patients had to build a predetermined pattern within a restricted period. The sum score ranges from 0 to 51 points; lower values are indicating more severe visuospatial disabilities.

Verbal Digit Span was applied to measure short-term memory. This test is a subtest of the Wechsler Memory Scale German adaption. The examiner reads a series of digits aloud which have to be repeated by the subject afterwards. Each correctly repeated series granted a point, adding up to a sum score ranging from 0 to 12 points, where higher values indicate better short-term memory performance.

EEG Data

During 15 min an eyes-closed, resting-state, 256-channel EEG was recorded (Netstation 300; EGI Inc., Eugene, Oreg., USA). Semi-automatic processing of the data was applied in order to calculate the relative power in alpha (8-18Hz) and theta (4-8Hz) frequency bands across the 10 brain regions. The processing was done in the same way as described in Section 4.1. Relative alpha/theta ratios were calculated from the frequency results.

Statistical Procedure

The R software version 3.2.3 was used for statistical analysis. The level of statistical significance was set at p=.05.

A linear mixed effect model (LME) with the alpha/theta ratio as the dependent variable was used to test the association between EEG slowing and visuospatial test scores. The test performance was used as fixed factor and the patients as random factor. Consequently, a b-value below zero indicates that the worse the alpha/theta ratio, the deeper the test-performance. The LME is a linear model that allows repeated measurement. This model was adopted due to the repeated measurements, caused by EEG electrode subdivision into the five brain areas. An exhaustive search, with age, gender, years of education, motor symptoms (UPDRS III), disease duration, depression scale (BDI), MMSE and LED showed that gender and age were confounding factors for alpha/theta ratio. The assumptions for LME are homoscedasticity (homogeneous variance), linearity, no influential data points, and independence (collinearity).

The plot of the standardized residuals showed a heterogeneous variance relating to the fitted values. A logarithmic transformation was performed in order to achieve a normal distribution. After the logarithmic transformation the residuals in the used LME models were normally distributed around zero and therefore the requested homogeneous variance was achieved. Plots of the random effects showed an unsystematic arrangement around zero. This confirmed a normal distribution of the errors (linearity). Influential data points were not found. Furthermore, there was no correlation between the predictor variables.

In a first step, the LME calculations showed no correlation between alpha/theta ratio and the task performance. Because of this finding, a median split was used to separate potentially clinically conspicuous from inconspicuous patients in regard to the visuospatial ability. The median split was calculated separately for each neuropsychological test. Group A included patients from the lowest task's performance up to the median and group B included patients from the median up to the best task's performance. Clinical and demographic variables between the median split groups were analysed by means of X^2-test or Mann–Whitney U-test as appropriate. The difference in relative alpha/theta ratio between the left and the right cerebral hemisphere was calculated by a Wilcoxon's matched pairs signed rank test. There were no significant differences in the relative alpha/theta ratio between the right- and left-sided electrode in the PD-patients (p=.316). Therefore, the analyses were based on combined data of the alpha/theta ratio for the right- and left-sided electrode locations. Furthermore, to compare the results, the LME were calculated with z-scaled Block Design and the Digit Span scores.

5.3.3 Results

The visuospatial decrease which would be expected in PD-patients, was weak in this population (see table 5.3.1). The descriptive statistics of the clinical performance split in the two median groups A and B, are shown in table 5.3.2. Significant differences between group A and B had been obtained in the Clock Drawing Test with regards to the MMSE and the BDI and in the Digit Span with regards to the disease duration. Otherwise there were no significant differences between the groups. The exhaustive search had shown that gender and age were confounding factors for all used neuropsychological tests. The EEG alpha/theta ratio was different between males and females in all areas [parietal $U(57/57) = 211$, $p = 0.024$, frontal $U(57/57) = 200$, $p = 0.014$, central $U(57/57) = 205$, $p = 0.018$, temporal, $U(57/57) = 210$, $p = 0.023$ and occipital $U(57/57) = 194$, $p = 0.010$].

PD patients (N=57)	**Mean**	**SD**
Sex (M/F)	40/17	
Age (years)	67.21	(6.96)
Education (years)	14.67	(3.01)
UPDRS III	14.77	(11.13)
MMSE	28.70	(1.06)
Disease duration (years)	5.25	(0.50)
Dose of L-dopa (mg/day)	597.60	(372.06)
BDI	7.22	(4.47)
Clock Drawing Test (incorrectly/correctly drawn)	16/41	
ROCF	28.83	(4.19)
Block Design Test	24.79	(7.56)
Verbal Digit Span forward	7.49	(1.72)

Table 5.3.1: Descriptive statistics and tasks performance of total group.

Note. Means and standard deviations relate to raw values. UPDRS III= Unified Parkinson's Disease Rating Scale subscale III (range 0-108); MMES= Mini-Mental State Examination (range 0-30); BDI=Beck Depression Inventory (range 0-63); ROCF= Rey-Osterrieth Complex Figure Test.

	Clock Drawing Test			**ROCF**			**Block Design Test**			**Digit Span**		
	Incorrectly drawn N= 16	Correctly drawn N=41		A N= 26	B N=29		A N= 29	B N=27		A N= 29	B N=28	
allocation	Median	Median	*p*	Median	Median	*p*	Median	Median	*p*	Median	Median	*p*
Sex (M/F)	11/5	29/12	1.000	19/9	20/7	.833	20/9	19/8	1.000	20/9	20/8	1.000
Age	67.5	67	.930	66.5	69.0	.295	67.0	69.0	.384	67.0	67.5	.994
Education	15	15	.964	14	15	.572	14	15	.092.	15	15	.413
UPDRS III	13.5	13.5	.765	17.0	10.0	.166	15.5	13.0	.511	14.0	13.5	.818
MMSE	28.5	29	**.036***	29	29	.347	29	29	.209	29	29	.322
Disease duration	5.27	3.37	.160	4.30	3.24	.508	4.12	3.37	.558	2.94	4.74	**.038***
Dose of L-dopa	666	510	.247	650	495	.206	590	550	.906	510	585	.296
BDI	4.5	8.0	**.024***	6.5	7.18	.901	6.5	7.35	.655	7	7	.941

Table 5.3.2: Descriptive statistics of median split groups.

Note. Values are expressed by median; UPDRS III= Unified Parkinson's Disease Rating Scale subscale III (range 0-108); MMSE= Mini-Mental State Examination (range 0-30); BDI=Beck Depression Inventory (range 0-63); ROCF= Rey-Osterrieth Complex Figure Test; A= group with lower tasks performance; B= group with higher tasks performance ** p < .001, * p <.050, . p < .1.

Clock Drawing

The LME results for the Clock Drawing Test are show in table 5.3.3. A significant lower alpha/theta ratio was recognised in PD-patients with an incorrectly drawn clock compared to PD-patients, who had produced a correctly drawn clock. The group difference was more distinct in parietal areas than in central, temporal and occipital areas.

	Δ incorrectly and correctly drawn		comparison b parietal/ other areas
brain area	*b*	*p*	*b*
Parietal	0.54 (0.18)	**0.003***	
Frontal	0.44 (0.18)	**0.016***	0.134
Central	0.40 (0.18)	**0.025***	**0.046***
Temporal	0.40 (0.18)	**0.027***	**0.040***
Occipital	0.36 (0.18)	**0.045***	**0.009***

Table 5.3.3: Correlation between alpha/theta ratio and Clock Drawing Test

Note. *b* = beta coefficient (standard errors); using a linear mixed effect model (LME); ** p < .001, * p<. 05. p < .1.

ROCF

As shown in table 5.3.4, in group A of the ROCF, the results revealed that the deeper the parietal alpha/theta ratio, the worse the ROCF performance. An increase of 1.0 z-score in the ROCF increased the parietal alpha/theta ratio by b = 0.59, t (24) = 2.73, p =.012. There was also a significant positive association between occipital alpha/theta ratio and the ROCF performance in the ROCF group A. An increase of 1.0 z-score in the ROCF increased the occipital alpha/theta ratio [b = 0.50, t (24) = 2.31, p =.030]. No significant association was found in the other cortical areas (see table 4). Furthermore, the association in the parietal areas were different from the frontal [b = -.19, t(104) = -2.28, p = .025], central [b = -.24, t(104) = -2.88, p = .005] and temporal [b = -.24, t(104) = -2.88, p = .005]. There was no significant difference between the association in parietal areas and the association in occipital areas [b = -.09, t (104) = -1.06, p = .290]. In the ROCF group B, there was neither an association between alpha/theta ratio and the ROCF z-score nor a significant difference between the association in parietal areas and the associations in the remaining areas.

Block Design Test

The LME results for the Block Design Test are shown in table 5.3.5. No significant correlation was found between the alpha/theta ratio and the Block Design performance. In the Block Design group A, there was simply a tendency towards a positive correlation between the parietal alpha/theta ratio and the Block Design performance. An increase of 1.0 z-score in the Block Design Test increased the alpha/theta ratio [b = 0.48, t (25) = 1.96, p = .062]. No associations

were found in the other cortical areas. The association in the parietal areas differed from the association in temporal areas [b = -.24, t (108) = -2.54, p = .013]. Furthermore, there was a trend towards a difference between the association in parietal areas and the association in frontal [b = -.16, t (108) = -1.71, p = .090] as well as central areas [b = -.16, t (108) = -1.68, p = .096].

Verbal Digit Span forward

The results in both Digit Span groups, A and B, showed no correlation between the alpha/theta ratio and the Digit Span performance (see table 6). However, in the Digit Span group A a slight tendency towards a negative correlation between the alpha/theta ratio and the Digit Span performance was observable in frontal [b = .0.35, t(25) = -2.05, p = .051], central, [b = -.29, t(25) = -1.73, p = .096] and parietal areas, [b = -.34, t(25) = -2.02, p = .054]. There were no associations in the other cortical areas. Furthermore, the association in the parietal areas was different from the occipital areas, [b = .14, t (108) = 2.21, p = .030] in group A. In group B a difference between the association in parietal areas and the association in central areas, [b = -.16, t (104) = -2.07, p = .041], was observable (see table 5.3.6).

	ROCF A			ROCF B		
brain areas	*b*	*p*	comparison *b* parietal/ other areas *p*	*b*	*p*	comparison *b* parietal/ other areas *p*
Parietal	0.59 (0.21)	**.012***		-0.06 (0.17)	.738	
Frontal	0.39 (0.21)	.079.	**.025***	-0.08 (0.17)	.653	.724
Central	0.34 (0.21)	.123	**.005***	-0.00 (0.17)	.984	.337
Temporal	0.34 (0.21)	.123	**.005***	-0.01 (0.17)	.967	.372
Occipital	0.50 (0.21)	**.030***	.290	-0.02 (0.17)	.900	.530

Table 5.2.4: Correlation between alpha/theta ratio and Rey-Osterrieth Complex Figure Test

Note. *b* = beta coefficient (standard errors); using a linear mixed effect model (LME); ** p < .001, * p <. 05. p < .1.

	Block Design A			Block Design B		
brain areas	*b*	*p*	comparison *b* parietal/ other areas *p*	*b*	*p*	comparison *b* parietal/ other areas *p*
Parietal	0.49 (0.25)	.062.		0.02 (0.15)	.886	
Frontal	0.32 (0.25)	.202	.090.	-0.01 (0.15)	.938	.588
Central	0.33 (0.25)	.198	.096.	0.05 (0.15)	.711	.578
Temporal	0.25 (0.25)	.328	**.013***	0.05 (0.15)	.735	.631
Occipital	0.40 (0.25)	.121	.353	-0.01 (0.15)	.962	.640

Table 5.2.5: Correlation between alpha/theta ratio and Block Design Test

Note. *b* = beta coefficient (standard errors); using a linear mixed effects model (LME); ** p < .001, * p <. 05. p < .1.

	Digit Span A			Digit Span B		
brain areas	*b*	*p*	comparison *b* parietal/ other areas *p*	*b*	*p*	comparison *b* parietal/ other areas *p*
Parietal	-0.34 (0.17)	.054.		0.25 (0.22)	.272	
Frontal	-0.35 (0.17)	.051.	.944	0.13 (0.22)	.548	.156
Central	-0.29 (0.17)	.096.	.469	0.08 (0.22)	.707	**.041***
Temporal	-0.28 (0.17)	.107	.381	0.15 (0.22)	.505	.218
Occipital	-0.19 (0.17)	.265	**.030***	0.13 (0.22)	.510	.210

Table 5.2.6: *Correlation between alpha/theta ratio and verbal Digit Span forward*

Note. *b* = beta coefficient (standard errors); using a linear mixed effects model (LME); ** p < .001, * p <. 05,. p < .1.

5.3.4 Discussion

The aim of this study was to investigate possible relationships between parietal and occipital EEG slowing and visuospatial deficit in non-demented PD-patients. The EEG slowing was measured by determining the alpha/theta ratio in the frontal, central, temporal, parietal, and occipital lobe. The visuospatial ability was assessed by three different neuropsychological tests: Clock Drawing Test, ROCF and Block Design Test. An LME was used to explore the association between visuospatial performances and alpha/theta ratio.

Inconsistent with previous findings, the PD-patients in our study showed only slight deficits in visuospatial ability. This might be explained by the high education level of the patients in our sample. Recent studies indicated that a high education is predictive for a slower cognitive decline (Kornhuber, 2004; Stern, 2009; Meng and D'Arcy, 2012). In order to separate potentially clinically conspicuous from inconspicuous patients with regards to the visuospatial ability, a median split was used.

The results of this study show that PD-patients with a parietal EEG slowing manifest a visuospatial deficit. This result is in line with findings from voxel-based morphometry MRI analysis, indicating correlations between visuospatial ability in PDD-patients and changes in the occipitotemporal and dorsoparietal cortices in comparison to healthy controls (Pereira *et al.*, 2009). Nombela et al. (Nombela *et al.*, 2014) also reported a correlation between parietal activity and visuospatial performance. In line with our hypothesis, the association between the EEG slowing and the visuospatial task performance is particularly pronounced in parietal areas compared to frontal, central and temporal areas (see figure 5.3.1). In addition, no differences between the association in parietal and occipital areas were detected in our sample. This finding indicates, that the association is not explained by the global EEG slowing, as has been shown in previous studies in patients with PD (Klassen *et al.*, 2011; Olde Dubbelink *et al.*, 2014). Though other previous studies also indicated that the visuospatial ability is not correlated with global EEG slowing measured by median frequency(Zimmermann *et al.*, 2015*a*), more research is needed to substantiate this point. Our present findings are also in line with the dual-stream hypothesis of the visual processing claiming the occipitoparietal projection system to be responsible for visuospatial performance(Ungerleider and Haxby, 1994).

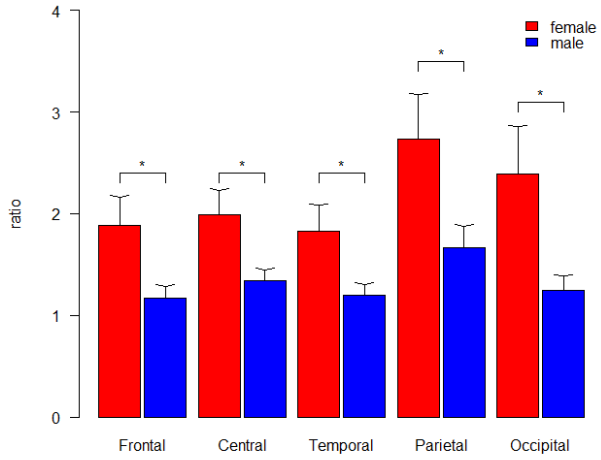

Figure 5.3.1. Difference alpha/theta ratio between gender in the different brain areas.

In all groups with test scores above the median (i.e. unimpaired visuospatial abilities), no correlations were found between the alpha/ theta ratio and the task performances, indicating that a relationship between the visuospatial ability and the EEG is only measurable if the visuospatial ability score decreases below the median.

In contrast to the results of the ROCF and the Block Design Test, the results of the Clock Drawing Test showed that PD-patients drawing an incorrect clock had lower alpha/theta ratio not only in parietal and occipital brain areas but also in all other brain areas. PD-patients with a flawless CDT-performance did not show this association (see figure 5.3.2).

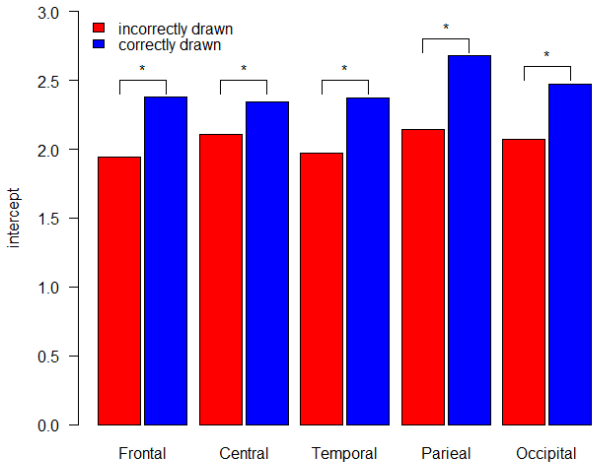

Figure 5.3.2. Comparison intercept between incorrectly and correctly drawn Clock Drawing Test groups related to the alpha/theta ratio in the different brain areas.

The neuroanatomical correlates of Clock Drawing Test performance were investigated in several studies, but the findings are inconsistent (Lee *et al.*, 2008; Matsuoka *et al.*, 2011, 2013; Shon *et al.*, 2013). This discrepancy might probably stem from the fact that the Clock Drawing Test measures also executive function, numerical and verbal memory in addition to visuospatial ability (Shulman, 2000; Karádi *et al.*, 2015). Furthermore, Matsuoka et al. explored the relationship between regional cerebral blood flow and different scoring criteria of the Clock Drawing Test in patients with Alzheimer's disease, revealing that different criteria correlate with different brain regions. Consequently, it can be concluded that for a correlative analysis between different brain areas and CDT-performance an overall classification into errorless and incorrect CDT-performance might be too simple. Hence, future studies should adopt differential scoring CDT-scoring criteria to unravel this relationship.

In our study, the results of the ROCF and the Block Design Test are consistent. In line with our findings, for both tests neuroanatomical correlation in parietal and occipital areas were also found in previous studies (Chase *et al.*, 1984; Warrington *et al.*, 1986; Wilde *et al.*, 2000; Melrose *et al.*, 2013). However, the results are more specific in ROCF than in the Block Design Test; for it we could only measure a tendency. This result could be explained as far as the in ROCF is majoritarian a visuoconstructive task; the patient merely needs to draw the figure. The Block Design Test, on the other hand, needs the abilities to perceive the figure, to analyse it and to fragment it in his components. Furthermore, the Block Design Test measures the capacity for problem-solving strategy and can provide information on how strongly the subject feels stressed by time pressure. Otherwise we did not consider the time required in ROCF performance.

The Digit Span measures working memory. Studies on healthy subjects, using either transcranial magnetic stimulation(Aleman and Van'T Wout, 2008), or functional neuroimaging(Gerton *et al.*, 2004), were able to show an involvement of the right dorsolateral prefrontal cortex in Digit Span processing. Furthermore, Gerton et al. reported that parietal and occipital areas are activated during the Digit Span forward task. In the present study no association was found between EEG slowing and the Digit Span performance. Nevertheless, a slight tendency towards a negative correlation between the alpha/theta ratio and the Digit Span performance was observed in frontal, central and parietal areas (see figure 5.3.3). The involvement of parietal areas could be explained by the use of the visual imagination strategies the subjects used during the Digit Span test. An explanation for the negative tendency could be that the Digit Span performance is not relating to EEG slowing caused by a shifting in alpha/theta ratio but by a shifting in others frequency range (e.g. theta/delta ratio or beta/alpha).

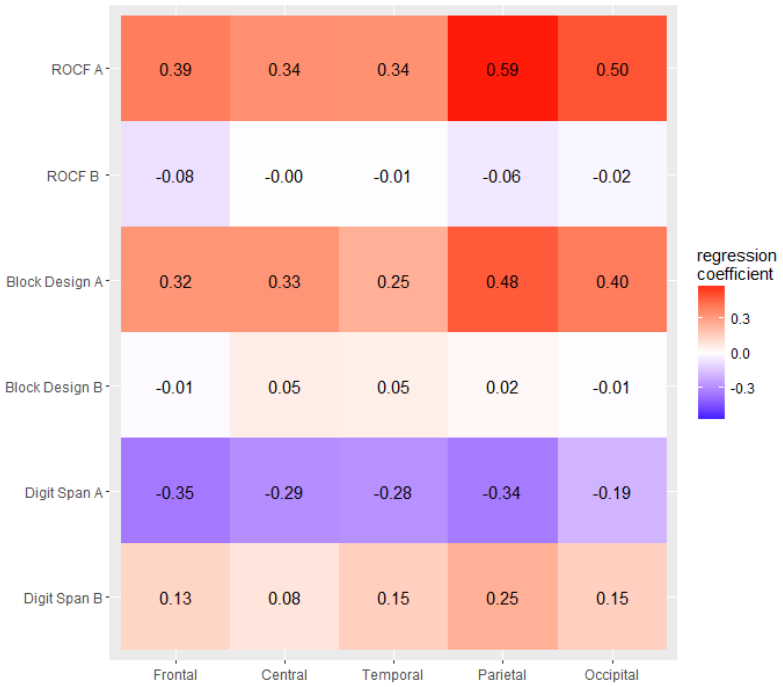

Figure 5.3.3. Correlation between alpha/theta ratio and tasks performance in different brain areas; ROCF= Rey-Osterrieth Complex Figure Test; A= group with lower tasks performance; B= group with higher tasks performance.

The results from our present study revealed no significant differences regarding confounding factors between the median split groups of the ROCF and Block Design Test. However, there were significant differences between the subgroups according to their Clock Drawing Test performance. Patients with an incorrectly drawn clock had a lower MMSE score than patients with a flawless CDT-performance. This finding is not surprising since both CDT and MMSE are also measures of global cognitive dysfunction (Ploenes *et al.*, 1994; Cahn-Weiner *et al.*, 1999; Riedel *et al.*, 2013). In addition, many studies found a correlation between these two tests (Klein, 2015; Brodaty and Moore, 1997; Shulman, 2000; Heinik *et al.*, 2004). Furthermore, PD-Patients with an incorrectly drawn clock had a lower BDI score than PD- patients with a correctly drawn clock. These findings were unexpected, as it is well-known that there is an association between depression and cognitive performance(Steffens and Potter, 2008). The results exploring the association between severity of depression and the performance in the Clock Drawing Test are inconsistent. Some authors have reported a significant negative relation (Harvey *et al.*, 2004; Sarapas *et al.*, 2012), whereas others have found minimal or no effect between the severity of depression and the Clock Drawing performance (Herrmann *et al.*, 1998; Kirby *et al.*, 2001; Elderkin-Thompson *et al.*, 2004; Quinn *et al.*, 2012). In the present study, the BDI score has no significant influence on the used LME model.

Nevertheless, the results cannot predict whether the severity of depression has an influence on cognitive performance. Another group difference is found between Digit Span performance and disease duration. Patients in the Digit Span group A have a shorter disease duration than patients in the Digit Span group B. This result contrasts some recent findings, which have shown a

reduction of working memory capacity in PD-patients as disease progresses (Johnson *et al.*, 2016; Warden *et al.*, 2016). Hence, our result might be caused by the sampling process based on a right-skewed sample and thus might represent an artefact.

While in our analyses, the exhaustive search showed that gender (see figure 5.3.1) and age were confounding factors and were consequently controlled in the LME, other authors have found only a small influence for these variables on the EEG activity (Morgan *et al.*, 2005; Klassen *et al.*, 2011). Hence, further studies are needed to determine the influence of gender and age on EEG slowing in PD-patients.

One limitation of our study is that the calculation of z-scores for the ROCF was based on a norm population whereas the calculations of z-scores for the Block Design Test and the Digit Span were based on our study population, limiting comparison of the tests. Moreover, since only 17 of 57 patients in our sample were female, the gender influence on EEG limits a generalisation. Although the unequal distribution of gender is well-known in PD (Baldereschi *et al.*, 2000; Van Den Eeden *et al.*, 2003) an equal gender distribution should be considered in future studies. Another limitation of this study is that there were no healthy controls included. Therefore, the conclusion that the findings are specific for patients with PD, cannot be drawn. A third issue is that this study did not control for multiple comparisons. Therefore, the interpretation of the results should be treated with caution, as the probability of making a false statement increases with the number of tests performed. In conclusion, in PD-patients with only slight deficits in visuospatial abilities, the visuospatial performance is related to parietal and occipital EEG slowing. The association between the EEG slowing and the visuospatial task performance is particularly pronounced in parietal areas compared to frontal, central and temporal areas.

6. Predictive value of EEG in prodromal Parkinson's disease patients

After feature selection for classification of PD patients from healthy individuals using a high density qEEG system and getting insights into the additive effect of neuropsychological tests for the classification as well as association between EEG and visuo-spatial domain, one of the goals was to test if similar qEEG features would be selected if using a low density recording system and further on, if such changes in brain signals could be detected already at a prodromal stage. For this purpose, a collaborative study was carried out with the University of Tübingen. The aims of this study were: a) to identify specific EEG patterns differentiating patients with early Parkinson's disease from healthy controls using a 10-20 EEG system, b) evaluate whether this pattern is associated with striatal dopamine active transporter binding and can be identified in persons in the prodromal stage of the disease. The text below is based on a manuscript currently in submission for peer-review.

6.1 Introduction

Neurodegeneration in the substantia nigra (SN) is already advanced with a loss of 30-60% of dopaminergic cells (Dauer and Przedborski, 2003; Greffard *et al.*, 2006; Cheng *et al.*, 2010; Grosch *et al.*, 2016) by the time Parkinson's disease (PD) can be diagnosed clinically. When subtle signs of PD are present but do not fulfil the diagnostic criteria, it is referred to as prodromal PD (pPD) (Hughes *et al.*, 1993, Berg *et al.*, 2015*a*; Heinzel *et al.*, 2016). Several features characteristic of this stage, when combined, can denote an increased risk for onset of PD in the future (Ross *et al.*, 2012; Berg *et al.*, 2013; Noyce *et al.*, 2014), and may even correspond to the neuropathological staging of PD associated pathology (Mahlknecht *et al.*, 2015; Adler and Beach, 2016; Braak and Del Tredici, 2017).

RBD(Galbiati *et al.*, 2019), reduced dopamine transporter (DAT) binding on SPECT, occurrence of PD related mild parkinsonian signs indicating subthreshold parkinsonism and hyperechogenicity of SN (SN+) assessed by transcranial sonography (TCS) are anticipated to constitute the highest likelihood for future PD (Berg *et al.*, 2015*a*). To date, the contribution of neurophysiological methods to predict pPD is unclear. Alteration in quantitative electroencephalography (qEEG) have reported in RBD as well as non-RBD individuals with depression, a potential prodromal marker of PD (Stoffers *et al.*, 2007; Sunwoo *et al.*, 2017; Bočková and Rektor, 2019; Gongora *et al.*, 2019; Ruffini *et al.*, 2019).

We present data from the "Progression Markers in the Premotor Phase of Parkinson's disease" study (Liepelt-Scarfone *et al.*, 2013*b*), designed to investigate the progression of various clinical and biological markers in pPD. Aim of this analysis was to identify a specific qEEG pattern differentiating patients with early PD from healthy individuals and evaluate whether it is identifiable in people at potentially high risk for PD, indicating that specific alterations in qEEG activity might be a prodromal marker. We also aimed to see if this pattern was related to

DAT tracer binding and explore the predictive ability of qEEG data for PD related motor and non-motor worsening after two years.

6.2 Materials and methods

Patients

Idiopathic Parkinson's disease patients were recruited consecutively at the outpatient clinic of the Department of Neurodegeneration, University of Tübingen from January 2011 to December 2012, using the UK Brain Bank criteria (Gibb and Lees, 1988; Liepelt-Scarfone *et al.*, 2015). Patients were at an early stage of the disease with Hoehn & Yahr stage ≤ 2.5 and aged over 50 years. HR-PD and controls were investigated in the PMPP study (Liepelt-Scarfone *et al.*, 2013*b*). We primarily defined the status of HR-PD by the presence of SN+ assessed by TCS, which is associated with an increased risk of developing Parkinson's disease in older aged persons (Berg *et al.*, 2013, 2015*a*). In addition to SN+, the following criteria defined group status of HR-PD:

i. one of the Parkinson's disease cardinal (bradykinesia, rigidity and resting tremor, defined by any of items 3.3-3.8, 3.14,3.17-3.18 of MDS UPDRS-III) motor signs assessed by the Unified Parkinson's Disease Rating Scale or
ii. presence of at least two of the following markers – hyposmia (Sniffin' sticks <75% correct identified odours) (Hummel *et al.*, 2001), lifetime prevalence of major depression according to the ICD-10 criteria (World Health Organization, 1992), clinical rated one-sided reduced arm swing or a positive family history of Parkinson's disease according to the criteria by Marder and co-workers (Marder *et al.*, 1996).

This combination of SN+ and prodromal markers is based on previous studies (Liepelt *et al.*, 2011). Based on these past results, the chosen marker combination of our HR-PD group was estimated to reflect around 4% of persons in the healthy population. In total, 1300 participants were pre-screened according to the protocol of the PRIPS and TREND study (Berg *et al.*, 2012). Healthy controls had normal echogenicity of the SN, no signs of current psychiatric disease and a negative family history of Parkinson's disease. Exclusion criteria for participants were: neurological diseases affecting the central nervous system, Parkinson's disease surgery, history of drug or alcohol abuse, prior use of cholinesterase inhibitors or memantine, or a Minimental State Examination (Folstein et al., 1975) <24 indicating severe cognitive deficits indicative for dementia. The local ethical committee of the University of Tübingen approved the study, and we performed it as per the 1964 Declaration of Helsinki and its later amendments (World Medical Association Declaration of Helsinki, 1997). All individuals gave written informed consent.

In total, 70 subjects were included in the PMPP study and reassessed after two years. Of those, three participants did not have an EEG recording due to technical problems. Additionally, we excluded one subject from data analysis due to the diagnosis of a meningioma near the brain stem. Therefore, the present study is based on the data of 16 Parkinson's disease patients, 37 HR-PD and 13 controls.

Assessments

EEG recording and analysis

EEG data were recorded using a standard IS 10-20 system (five minutes resting condition with eyes open and closed, each for 30 seconds, five times in a row). EEG's were processed with an automated pipeline using TAPEEG (https://sites.google.com/site/tapeeg/) (Hatz *et al.*, 2015). The data were filtered (Firls: 0.5–70 Hz, 50 Hz notch), artefacts like muscle and eye movement were removed along with bad channels. Further artefact removal was done using the independent component analysis implementation of EEGLAB (Delorme and Makeig, 2004) ("runica" with default settings). We obtained relative spectral powers for 18 electrodes in six power bands, global spectral measures and median frequencies.

Penalized logistic regression was applied to identify the most influential EEG features distinguishing Parkinson's disease patients from healthy controls (Chaturvedi *et al.*, 2017) and obtain a subset of features that would not be highly correlated to each other. We then investigated this pattern in the HR-PD disease group at baseline. The least absolute shrinkage and selection operator (LASSO) method (Tibshirani, 1996*b*, 1997) has been used in different studies for feature selection and computing risk predictive models (Wu *et al.*, 2009; Fontanarosa and Dai, 2011; Mavaddat *et al.*, 2019). In many cases, lasso-penalized models have shown improved prediction accuracy while selecting only a limited number of covariates that are included in the model.

We used the penalized (Goeman, 2010) package in R (R Core Team, 2018) to create a logistic regression model with the L1-LASSO penalty and carried out cross-validation, optimization to select the tuning parameter. Cross-validated ROC curves were obtained with the ROCR (Sing *et al.*, 2005) package in R.

123I-FP-CIT-SPECT

Due to requirements of the local ethical committee, imaging of DAT binding in nigrostriatal region was limited to the HR-PD and Parkinson's disease group and measured by ^{123}I-FP-CIT-SPECT (DaTSCAN^{TM}). Participants received a single intravenous injection of ^{123}I-FPCIT (GE Healthcare, Zeist, Netherlands) with a recommended dose of 185 MBq. Three hours post-injection, SPECT images were acquired with a dual-head gamma camera high-resolution collimator (Symbia®, Siemens, Germany, acquisition time was will be approximately 40 min). Based on the software BRASS® (Hermes Medical Solution, Inc), we defined uptake values for the right and left caudate and the putamen as regions of interest. In addition, sides were pooled to match sides with lower (more affected) and higher (less affected) tracer binding in either the right and left regions of interest as well as summed up to a total summary uptake score of caudate and putamen. The putamen/caudate ratio was also calculated.

Transcranial sonography

To define the echostatus of the SN, a TCS was conducted with a 2.5 Mhz transducer in all participants (Antares® ultrasound machine, Siemens, Germany). Resolution of this system is approximately axial=0.7 mm, lateral=3 mm. Echogenicity of the SN was measured planimetrically according to the consensus guideline (Berg *et al.*, 2006). SN+ was defined as an area of echogenicity above 0.19 cm² of either the right or left side of the SN. This cut-off is the 90th percentile of a large sample of neurodegenerative healthy individuals (Liepelt *et al.*, 2011; Berg *et al.*, 2013).

Motor assessment

Severity of parkinsonian signs was assessed by the MDS Unified Parkinson's Disease Rating Scale motor part (MDS-UPDRS-III)(Goetz, 2010) and the modified Hoehn & Yahr stage score(Goetz *et al.*, 2004). Based on their motor performance after two years, we categorized patients as having stable (no increase in MDS-UPDRS-III score) or progressive motor signs. Progressive signs referred to either ≥1 point or ≥3 points increase in the MDS-UPDRS-III.

Previous studies identified an UPDRS-III score of 2.5 points as the minimal clinically meaningful differences in Parkinson's disease (Shulman *et al.*, 2010), but changes have been reported to be below this cut-off in a non-Parkinson's disease sample over time (Liepelt-Scarfone *et al.*, 2015). For calculation of the LRs to define the probability of being in the prodromal stage of Parkinson's disease, MDS-UPDRS-III scores referring to postural and action tremor were excluded as suggested by the MDS criteria (Berg *et al.*, 2015*a*).

Non-motor assessment

We used the German version of the University of the Pennsylvania Smell Identification Test (UPSIT) to evaluate progression in olfactory dysfunction over the study period. Subjects with actual or chronic diseases that might reduce olfactory performance (e.g. chronic rhinitis) were excluded from data analysis. Age- and gender-corrected standard scores were analysed, a value below one standard deviation of published population norms (z=-1.0) were classified as hyposmia at baseline and follow-up.

Urinary and erectile dysfunction and constipation were rated on a 5 point scale to code for symptom severity ranging from no presence of symptoms (score=0) to permanent medical therapy needed (score=4) (Wenning *et al.*, 2004). Examination of orthostatic hypertension was based on a standardised blood pressure measurement (UMSARS part III) (Wenning *et al.*, 2004). According to the protocol, we manually assessed the systolic, diastolic blood pressure (S/DBP) and heart rate of the participants after 2 minutes lying in supine position and again after 2 minutes of standing. The RBD Screening Questionnaire (Stiasny-Kolster *et al.*, 2007) was used to assess the symptoms and severity of RBD. Acute state of depression was diagnosed during consensus guidelines (World Health Organization, 1992). Since we used the lifetime prevalence

of major depression for study group assignment, newly diagnosed major depression within the follow-up period was included as a prodromal marker in the follow-up.

Additionally, male sex and history of smoking expressed as pack-years were registered. We defined subjects with a pack-year value of zero as never-smokers. All subjects with a pack-year value ≥1 were classified as former smokers including current smokers.

Neuropsychological battery

A comprehensive neuropsychological test-battery assessed all major areas of potential cognitive disability, known to be disturbed in early Parkinson's disease. This included the short version of the intelligence task "Leistungsprüfsystem 50+" (LPS 50+K) (Sturm W. Willmes K. Horn W, 1993), covering for both crystalline and fluid intelligence, including the letter fluency test (subtest 6). The Tower of London (TL-D) test assessed the planning and executive function (Tucha O. Lange KW, 2004)), the Trail Making Test (TMT) part A and B (Memory Clinic NPZ, 2005) assessed psychomotor speed (A) and set-shifting (B). The Stroop Color-Word Interference test (Stroop) (Baeumler G., 1985) to screen for impairment in direct attention. Two subtests of the computerised assessment battery of attentional performance (TAP) (Zimmermann P. Fimm B., 2002), namely the value of phasic alertness from the "Alertness" and the median reaction time from the subtest "Divided Attention" part was applied to further test for attentional dysfunction. The Logical Memory I and II of the Wechsler Memory Scale Revised (WMS-R) (Wechsler and Härting, 2004) assessed complex memory function, the Digit Span forward and backward section of the WMS-R (Wechsler and Härting, 2004) assessed working memory performance. The Block design of the Wechsler Adult Intelligence Scale (Tewes, 1991), was used to test visual-spatial abilities. German norm data (percentile rank score, PR) provided in the test manual of the neuropsychological assessments, referring to an age matched population for each subject investigated were used to compare test performance. If available (TL-D, Stroop, TMT and TAP), we chose norms corrected for both age and education.

Data analysis and statistics

LR+ and LR-, for the risk mentioned above and prodromal markers, were defined according to the recommendations of the MDS guideline for prodromal Parkinson's disease (Berg *et al.*, 2015*b*). For details, we refer to supplementary Table 1. Total LR for baseline and follow-up, respectively, for every study participant, was calculated, with a higher total LR indicated a higher intra-individual number of the assessed risk or prodromal markers. Finally, we calculated the age-adapted quantitative post-test probability score (0 to 100%) for each patient in a neurodegenerative process that may lead to future Parkinson's disease after two years. The cut-off for the post-test probability score was 50 and 80% to define possible and probable prodromal Parkinson's disease (Berg *et al.*, 2015*a*; Liepelt-Scarfone *et al.*, 2017). Besides the EEG analysis described above done using R, the rest of the data were analysed using IBM SPSS Statistics 22.0 for Windows. Non-parametric test statistic was applied. Therefore, data are presented as median and range or number/percentage if not indicated otherwise. Demographics and clinical data between groups were compared by use of the Kruskal-Wallis (healthy controls vs HR-PD

vs Parkinson's disease), the Mann-Whitney U Test (e.g. between-group comparison and post hoc comparison) or Chi² test or Fisher's exact test as appropriate.

To identify the association of the tracer binding in 123I-FP-CIT-SPECT, the likelihood ratios, the post-test probability prodromal score and the identified Parkinson's disease-specific EEG profile, a linear regression analysis was done taking each feature of interest as a dependent variable and the EEG risk score as an independent variable, correcting for age and sex as potential confounders. In a second model exploring the association of DAT tracer binding, additionally the MDS-UPDRS-III score was added as an independent variable into the analysis. Spearman correlation analysis (rho) was done in the total sample.

6.3 Results

Table 6.1 gives an overview of the distribution of risk and prodromal marker in each study group. The disease duration was 31 (range: 15-56) months, patients were assigned to the following Hoehn & Yahr stages: 1=6.3%, 1.5=6.3%, 2=68.8% and 2.5=18.8%. All Parkinson's disease patients were medicated with dopaminergic medication: intake of antidepressants was recorded in 10 participants, five (31.3%) with a diagnosis of Parkinson's disease and five (13.1%) individuals classified as HR-PD. Participants of the control group took none of these drugs.

In summary, 18 subjects (Parkinson's disease=31.3%, HR-PD=35.1%) reported a first, six (Parkinson's disease=18.8%, HR-PD=8.1%) a second-degree relative, and four patients (Parkinson's disease=18.8%, HR-PD=2.7%) other family relatives with Parkinson's disease symptoms. In addition to the recruitment criteria, urinary urgency was more frequent in HR-PD compared to the control group at baseline. Around two thirds (n=28, 75.7%) of the HR-PD group had either mild bradykinesia, rigidity or resting tremor, with bradykinesia as the most frequent symptom (70.3%). However, only five patients of the HR-PD group scored more than six on the MDS-UPDRS-III scale.

	Controls	**HR-PD**	**PD**	**p-value**	**HR-PD$_{EEG-}$**	**HR-PD$_{EEG+}$**	**p-value**
Number	13	37	16		27	10	
Age	62 (54-76)	62 (54-73)	64 (50-80)	0.89	62 (54-73)	62.5 (57-70)	0.85
Years of Education	12 (10-20)	15 (11-22)	13.5 (8-24)	0.33	16 (11-22)	15 (11-22)	0.96
Risk markers							

Male gender	7 (53.8%)	26 (70.3%)	9 (56.3 %)	0.48	18 (66.7%)	8 (80.0)	0.69
Smoking	3 (23.1)	14 (38.9)	6 (37.5))	0.58	11 (40.7)	3 (33.3)	1.00
Positive family history for first degree relatives	0	12 (35..1)	5 (31.3)	**0.042**#	9 (33.3)	4 (40)	1.00
Substantia nigra hyperechogenicity	0 (0)	37 (100)	15 (93.8)	**<0.00**╫#	27 (100)	10 (100)	1.00
Prodromal markers							
One-sided reduced arm-swing*	0 (0)	13 (35.1)	14 (87.5)	**<0.001**╫#‡	9 (33.3)	4 (40)	1.00
MDS-UPDRS-III	0 (0-2)	4 (0-12)	26 (9-55)	**< 0.001**╫#‡	3 (0-12)	4 (0-6)	0.85
MDS-UPDRS-III >6	0 (0)	5 (13.5%)	16 (100)	**<0.001**╫‡	5 (18.5)	0 (0)	0.30
UPSIT	40 (14-62)	15 (4-90)	5.5 (9-54)	**< 0.001**╫‡	24 (5-90)	14 (4-26)	0.07
Hyposmia, Sniffin‘ Sticks < 75%*	1 (8.1)	18 (48.6)	12 (75)	**0.002**╫	13 (48.1)	5 (50)	1.00
Olfactory impairment	2 (15.4)	23 (62.2)	13	**0.001**╫#	15 (55.6)	8 (80)	0.26
RBD	1 (7.7)	4 (10.8)	4 (25)	0.38	3 (11.1)	1 (10)	1.00

Urinary dysfunction	0 (0)	15 (40.5)	10 (62.5)	**0.002**╫#	12 (44.4)	3 (30)	0.48
Erectile dysfunction	0 (0)	7 (18.9)	3 (18.8)	0.29	4 (14.8)	3 (30)	0.36
Constipation	0 (0)	2 (5.4)	3 (18.8)	0.18	2 (7.4)	0 (0)	1.00
Orthostatic hypotension	0 (0)	2 (5.4)	6 (37.5)	**0.003**‡	2 (7.4)	0 (0)	1.00
Lifetime depression, n (%)*	1 (15.4)	13 (35.1)	8 (50)	0.16	8 (29.6)	5 (50)	0.44
New-onset depression	1 (7.7)	11 (32.4)	5 (35.7)	0.20	8 (30.8)	3 (37.5)	1.00

Table 6.1. Overview of demographics, risk and prodromal marker of study groups

*. Markers used for recruitment and study group assignment only; post-hoc comparison p<0.017: ╫.Parkinson's disease (PD) vs. all controls; #.High risk for PD (HR-PD) group vs. controls; ‡.Parkinson's disease patients vs. HR-PD group.

6.3.1 Differentiation between controls and Parkinson's disease according to EEG pattern

By using penalized logistic regression (LASSO), we identified theta power in the right occipital lobe (O2) and alpha1 activity in the left parietal lobe (P3) as primary factors differentiating controls from Parkinson's disease. This resulted in a risk score obtained from the following equation: (1.62*Theta-O2) + (0.75*Alpha1-P3) + 3.75. The probability of each patient being diagnosed as Parkinson's disease or the predicted risk can be obtained by applying the formula: exponential (patient's risk score) ÷ (1 + exponential (patient's risk score)). Cross-validated median values for sensitivity and specificity was 71% and 75% respectively, with an area under the curve (AUC) of 0.80. Figure 6.1 shows the cross-validated ROC curves.

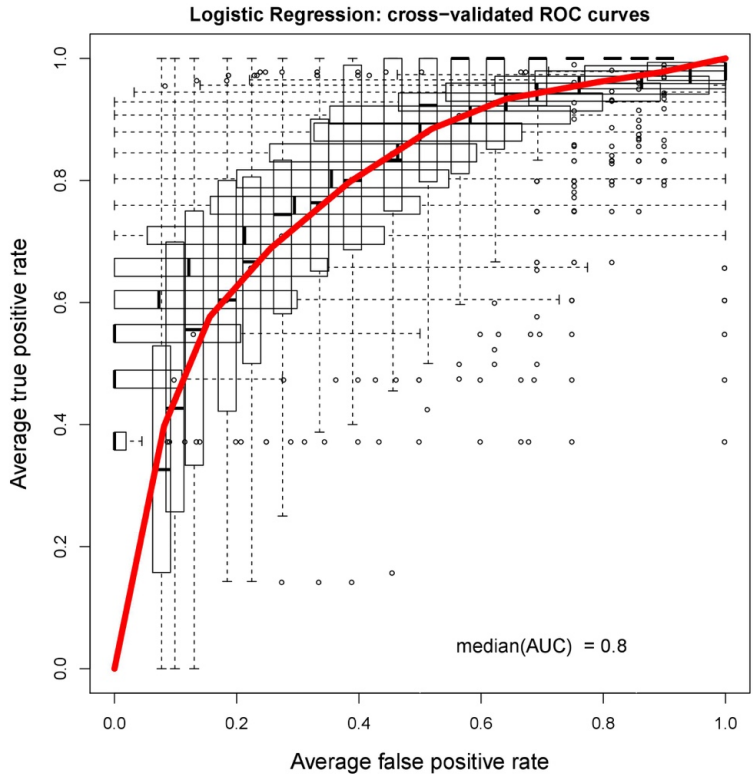

Figure 6.1: Cross-validated ROC curves from the penalized regression model differentiating PD patients from healthy individuals

According to the risk score, ten participants classified as HR-PD (27%) had a higher probability of having a Parkinson's disease-specific EEG profile. Figure 6.2 shows how the three study groups differ with regards to the two chosen features, theta power in the O2 electrode and alpha1 power at P3. On single marker level, the clinical profile of the HR-PD group with similarities in EEG to Parkinson's disease patients (HR-PD_{EEG+}) and without similarities (HR-PD_{EEG-}) did not statistically differ, except a tendency of slightly lower UPSIT total scores in the HR-PD_{EEG+} group ($p=0.07$, see Table 6.1). The HR-PD_{EEG+} group had no intake of antidepressants in contrast to 18.5% of HR-PD_{EEG-} group.

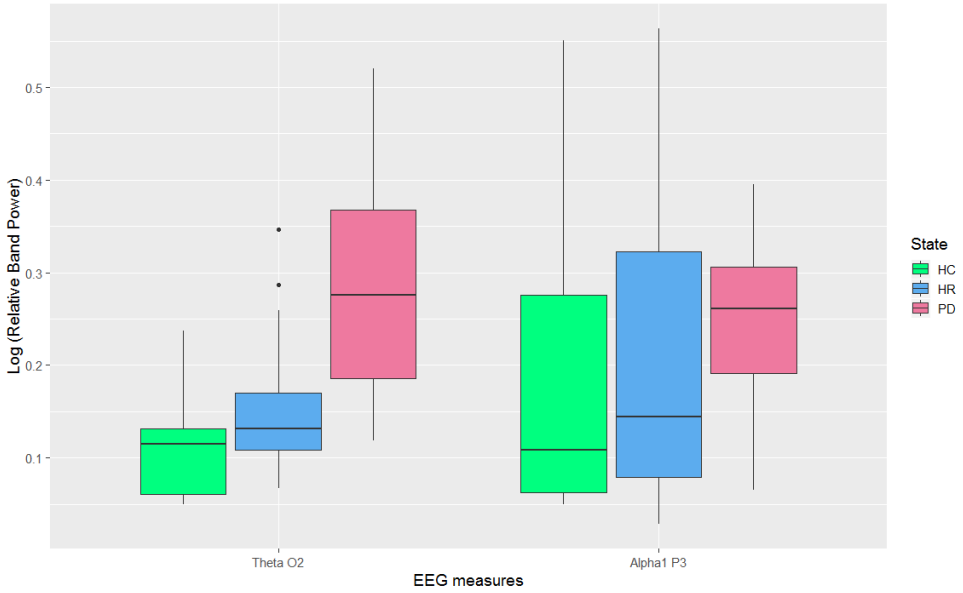

Figure 6.2: Difference in theta and alpha1 relative powers in PD, HC and high-risk groups in the right occipital and left parietal lobes respectively.

6.3.2 Association between the Parkinson's disease-specific EEG pattern and 123I-FP-CIT-SPECT

Of the total sample, we recorded 123I-FP-CIT-SPECT data of 14 Parkinson's disease patients and 18 individuals of the HR-PD group. Results of the regression analysis confirmed a significant association between the EEG risk score equation, reflecting a Parkinson's disease-specific EEG pattern with uptake values of caudate and putamen, as well as the putamen/caudate ratio independent from age and sex (see Supplementary Table 6S2). By adding the MDS-UPDRS-III score into the regression model (data not shown) the association between EEG and the tracer uptake was no longer significant for most parameters, but level of significance for association of caudate/putamen ratio and EEG was borderline (Model fit: F 17.797, $p<0.001$; $\beta=-.264$, $p=0.052$).

	$HR\text{-}PD_{EEG-}$	$HR\text{-}PD_{EEG+}$	P value
Risk LR			
Baseline	5.99 (1.45- 14.98)	5.99 (1.44-31.73)	0.39m
Non-motor prodromal LR			
Baseline	1.71 (0.18-24.33)	1.71 (0.41-8.04)	0.47m

Follow-up	0.72 (0.16-14.47)	2.49 (0.16-14.47)	**0.043m**
Motor worsening in two years			
MDS-UPDRS-III ≥1 increase, n (%)	7 (26.1%)	2 (25.0)	1.00c
UPDRS Part III ≥3 increase, n (%)	3 (11.5)	2 (25%)	0.57c
Total prodromal LR			
Baseline	9.11 (0.19-348.90)	17.97 (0.62-38.06)	0.64m
Follow-up	4.55 (0.19-71.42)	59.15 (4.16-256.75)	**0.002m**

LR, likelihood ratio; c. Fishers Exact test; m Mann-Whitney U test

Table 6.2: Comparison of risk and non-motor prodromal likelihood ratios and motor worsening between groups.

6.3.3 Association between baseline risk and prodromal marker profile and EEG

Regression analysis (Model fit: F= 3.707 p=0.016, R^2=0.15) revealed that the calculated risk marker LR was not statistically significantly associated with the EEG risk equation (β=0.180, p=0.134), independent from age (β=-0.179, p= 0.142) and sex ((β=0.276, p=0.024). In contrast, baseline LR of non-motor prodromal markers, which were not used for classification of study groups (excluding olfaction and lifetime prevalence of depression) were predicted (β=0.269, p=0.022) in addition to age (β=0.260, p=0.029) by the EEG equation (Model fit: F=5.130, p=0.003, R^2=0.19). The effect between the EEG profile and the total LR, including motor performance (Model fit: F=3.749, p=0.015, R^2=0.16) was highly significant (β =0.395, p=0.001), and not confounded by age (p=0.91) and gender (p=0.71).

Between-group comparison of the persons classified as HR-PDEEG+ and HR-PDEEG- showed that the risk and prodromal marker burden expressed as risk LRs (U=97.5, p=0.39), prodromal LRs (U=113.5, p=0.47), as well as total LRs including motor performance (U=108.5, p=0.64), did not statistically differ at baseline (see Table 6.2 for details).

6.3.4 Prediction of motor worsening after two years by EEG

We re-assessed all participants after a median follow-up interval of 23 (21 to 30) months but had to exclude five participants (3 HR-PD, 2 Parkinson's disease), who we lost to follow-up due to severe illness death or loss of contact.

Prediction of motor outcome assessed by either the total MDS-UPDRS-III score with (Model Fit: F=6.873, p<0.001, R^2=0.23) and without tremor scores (Model Fit: F= 7.236, p<0.001. R^2=0.28) according to baseline EEG data (tremor included: β=0.508. p<0.001; tremor excluded: β=0.516, p<0.001) revealed a close relationship between these variables with no impact of age (p>0.34) and sex (p>0.32) on the dependent variable.

6.3.5 Prediction of prodromal Parkinson's disease stage at the time of follow-up

At the time of follow-up, participants of the HR-PDEEG+ group had significantly higher values in non-motor prodromal (U=54, p=0.043) and total LRs (U=32.5, p=0.002) in comparison to the HR-PD_{EEG-} group. Results of regression analysis (Model fit: F=4.15, p=0.01, R^2=0.14), including the entire sample, verified that baseline EEG risk score values were associated with follow-up non-motor prodromal LRs (β=0.393, p=0.002), irrespective of person's age (p=0.36) and sex (p=0.14). The same holds for the association of post-test probability of prodromal Parkinson's disease to baseline EEG data (Model Fit: F=18.771, p<0.001, R^2= 0.50), which was highly significant (β=0.693, p<0.001), not confounded by age (p=0.30) and sex (p=0.61).

Calculations of post-test probability scores showed that 15 participants (HR-Parkinson's disease: 4/34, Parkinson's disease: 11/14) and seven participants (HR-Parkinson's disease: 1/34 -Parkinson's disease converter-, Parkinson's disease: 6/14) reached ≥50 and ≥80% post-test probability values, respectively. Of those, 13 participants (HR-Parkinson's disease: 4; Parkinson's disease; 9/11) were classified to have an EEG profile indicative of Parkinson's disease at baseline. The sensitivity of ≥50% post-test probability for the HR-PD_{EEG+} group compared to those classified as HR-PD_{EEG-} at baseline was calculated as 50%, with a specificity of 100% and a positive and negative predictive value of 100% and 87% respectively. The risk for ≥50% post-test probability, indicating state of possible prodromal Parkinson's disease, was therefore significantly higher in the HR-PD_{EEG+} group (p=0.02) with a relative risk of 27 (95% CI: 1.61 to 454.21) compared to HR-PD_{EEG-}

6.3.6 Association between EEG and cognitive function

Correlation analysis between baseline cognitive and EEG data was highest for neuropsychological tests assessing attention (TAP-Phasic Alertness, rho=-0.259, p=0.040); TAP-Divided Attention. Median, rho=-0.256, p=0.042), memory performance (Logical Memory II, rho=-0.258, p=0.037) and psychomotor speed (TMT A, rho= -0.281, p= 0.024) indicating that lower test performance in these domains was associated with higher EEG risk scores reflecting a higher probability of resembling the Parkinson's disease-specific EEG profile. By correlating follow-up cognitive data with baseline EEG values, lower performance in the Stroop test colour naming condition (directing attention, rho= -0.263, p= 0.040) and the TMT B (rho=-0.256, p=0.047) indicating attention and executive problems (set shifting) were significantly associated with the baseline EEG risk score.

6.4 Discussion

For the first time, we investigated the potential of EEG as a biomarker for Parkinson's disease in individuals potentially at high risk for Parkinson's disease primarily selected by SN+ according to TCS. TCS has been used in various studies, not only to confirm Parkinson's disease diagnosis (Li *et al.*, 2016) but also to encompass a high-risk group for future onset of Parkinson's disease (Berg *et al.*, 2011).

As the pre-clinical symptoms of Parkinson's disease are heterogenic as an expression of the underlying neurodegenerative process (Dauer and Przedborski, 2003; Grosch *et al.*, 2016), biomarkers indicating a high risk for Parkinson's disease conversion reflecting in vivo Parkinson's disease specific brain changes are needed to identify a high-risk Parkinson's disease group.

Diagnostic value of EEG for early diagnosis of Parkinson's disease

We here identified a Parkinson's disease-specific EEG pattern differentiating controls from early-stage disease patients. By using a 10-20 standard EEG system, economical in time and costs, we obtained an EEG risk score based on a subset of EEG features expressing the likelihood of Parkinson's disease-related neurophysiology alterations. The results showed that none of the individuals with a normal EEG scored higher than 50% post-test probability even if they were classified as HR-PD indicating that a normal EEG pattern predicts ones with low post-test probability perfectly. On the other hand, half of the individuals with HR-PD with a specific EEG pattern had a score higher than 50%. Theta and alpha powers, especially in the occipital, parietal and temporal regions, are reported as characteristics of Parkinson's disease patients in several studies. One study investigating 15 early-stage Parkinson's disease patients and 15 healthy individuals had found an increase in delta, theta bands in Parkinson's disease patients with a decrease in alpha, beta bands (Han *et al.*, 2013). Theta power in the left occipital region was found to be associated with disease severity in Parkinson's disease patients and also differed significantly between Parkinson's disease patients with and without mild cognitive impairment (He *et al.*, 2016). One MEG study (Bosboom *et al.*, 2006) had also reported an increase in theta power in the occipital and temporal channels to be associated with lower cognitive performance in Parkinson's disease patients without dementia.

As the penalized logistic regression method picks out features that are not highly correlated to each other, the final two features may not represent the only possible solution, but rather an optimal model resulting in a considerable classification accuracy. This could explain why some studies found power in theta temporal left region to be the most effective classifier instead of theta power in temporal right or occipital regions. Signals from electrodes placed close to each other can be more correlated than if further away, which would lead to the selection of only one amongst the cluster.

We noted that the alpha1 power was slightly increased in Parkinson's disease patients in comparison to healthy individuals, unlike our observations in other cohorts, but speculate that

it could be an effect of the dopaminergic medication on some of the patients. Some studies have found levodopa intake to result in increased spectral powers (Yaar and Shapiro, 1983), specifically in alpha and beta powers (Melgari *et al.*, 2014). A recent study reported changes in phase-amplitude coupling and coherence due to dopaminergic medication, especially in the sensorimotor cortex (Miller *et al.*, 2019). Daily intake of levodopa was also observed to affect the alpha cortical source activations in Parkinson's disease patients while in a state of quiet wakefulness (Babiloni *et al.*, 2019).

Association between EEG, TCS and 123I-FP-CIT-SPECT

Once we identified an EEG profile distinguishing Parkinson's disease from healthy controls, we wanted to investigate other clinical features, including motor and cognitive scores from their two-year follow up data, and find out how these patients progressed. A significant strength of this study was the availability of data from 123I-FP-CIT-SPECT for a subset of the patients (Benamer *et al.*, 2000; Seifert and Wiener, 2013). We found the EEG risk score associated with the caudate, putamen, as well as putamen/caudate independent from age and sex, showing that EEG reflects dopaminergic loss associated with Parkinson's disease. By controlling for motor severity in the regression model, most effects between the EEG risk score and tracer uptake were no longer significant for most parameters; however, association between the putamen/caudate and EEG was strongest. Loss of caudate uptake is found to be correlated with cognitive function in Parkinson's disease patients (Arnaldi *et al.*, 2012; Pellecchia *et al.*, 2015), especially executive function, and when combined with some other biomarkers, it has been found to potentially predict cognitive decline (Schrag *et al.*, 2017; Lanskey *et al.*, 2018).

In individuals with hyposmia, a known risk factor, and non-motor manifestation of Parkinson's disease, studies reported a higher risk of conversion in those with a 123I-FP-CIT-SPECT tracer uptake deficit (Jennings *et al.*, 2017) than in those with an intermediate DAT binding or normal 123I-FP-CIT-SPECT tracer uptake. A study investigating idiopathic RBD carried out DAT imaging at baseline and follow-ups and identified nigrostriatal changes concerning the early onset of the disease (Zou *et al.*, 2016). Such deficits, when combined with olfactory dysfunctions, have also been identified as potential predictors of Parkinson's disease (Berendse and Ponsen, 2006). Such studies verify that Parkinson's disease related dopaminergic alteration can be detected very early in the stage of neurodegeneration. In our cohort, EEG is associated with tracer binding, with lower tracer binding reflecting higher values of the EEG risk score more prominent in Parkinson's disease. Therefore, our data indicate that the identified EEG risk score might reflect dopaminergic activity, even in the prodromal stage of Parkinson's disease. A non-invasive way to detect these changes early on, such as EEG, have the potential to serve as a prodromal Parkinson's disease biomarker.

Sensitivities of 87.5% and 84.4% were reported for TCS and DAT Scan with a specificity of 96.2% for both methods (Jesus-Ribeiro *et al.*, 2016). Findings from both methods correlated with 84% of diagnosis of Parkinson's disease (Bártová *et al.*, 2014). In RBD, reduced striatal binding and SN+ in combination were also reported to predict conversion to synucleinopathy after 2-5 years, a sensitivity of 100% and specificity of 55% (Iranzo *et al.*, 2010). Comparing individuals

with a potential high and low risk for Parkinson's disease both TCS seems to have a better discriminant ability than the DAT striatal binding ratio (Noyce *et al.*, 2018), suggesting that SN+ is able to identify very early in the disease related neurodegenerative process. In our sample a combination of SN+, other risk and prodromal marker and EEG best predicted worsening of both motor and non-motor symptoms in our group.

Association between EEG and clinical marker profile

Several studies have demonstrated that non-motor markers occur early in the neurodegenerative process (Pilotto *et al.*, 2017; Postuma *et al.*, 2019). However, those markers assessed individually also frequently occur in the healthy population, dramatically lowering its positive predictive value. Therefore, a combination of different Parkinson's disease-specific clinical markers has been proposed to increase its prognostic value (Berg *et al.*, 2015*b*; Heinzel *et al.*, 2019). A higher non-motor burden is also established to be associated with a more rapid development of Parkinson's disease (Mahlknecht *et al.*, 2016, 2018; Fereshtehnejad *et al.*, 2017; Pilotto *et al.*, 2017; Mirelman *et al.*, 2018). The recent application of deep learning in distinguishing healthy individuals from patients with RBD who eventually progressed to Parkinson's disease using signals from a single electrode showed the potential of EEG in facilitating the identification of clinically relevant biomarkers (Ruffini *et al.*, 2019). Even if RBD is the prodromal marker with the highest prognostic value for alpha synucleopathies, it is prominent in only a subgroup of 16–47% of all Parkinson's disease cases, at the time of Parkinson's disease diagnosis (Högl *et al.*, 2018). Therefore, another combination of prodromal marker might also increase the risk for future Parkinson's disease accompanied by probable alteration in EEG.

Following up on the patients after two years, we found EEG to be associated with motor worsening, deficits in cognitive tests such as attention, executive function and with likelihood ratios of non-motor prodromal markers. Baseline EEG patterns of the cohort predicted ($p<0.001$) follow-up motor outcome (MDS-UPDRS-III score, excluding tremor), follow-up probability of ≥50% prodromal Parkinson's disease in HR-PD in two years and baseline prodromal marker burden. Previous work showed that beta frequency in the right posterior temporal region was related to stage of disease severity (He *et al.*, 2016). Moreover, EEG is also found to be useful in predicting motor symptoms such as freezing of gait in Parkinson's disease patients (Handojoseno *et al.*, 2018) further supporting the assumption that EEG might be a potential biomarker for disease progression in Parkinson's disease.

Similar to several studies showing the importance of theta and alpha1 power in the disease progression leading to cognitive decline (Jacobs *et al.*, 2006; Bousleiman *et al.*, 2015, Cozac *et al.*, 2016*a*; Singh *et al.*, 2018), we also found theta and alpha1 powers to be important indicators of early-stage Parkinson's disease as well as in the high-risk Parkinson's disease group. Absolute theta power was also identified to be more prominent in patients with depression compared to healthy controls (Cai *et al.*, 2018). In our study, theta was the strongest predictor and could clearly distinguish between Parkinson's disease and the healthy group, with the high-risk group falling in between. As we used the likelihood ratios including varying Parkinson's disease-related motor and non-motor symptoms to define the stage of prodromal Parkinson's

disease, our data suggests that the EEG risk scores reflect an overall symptoms burden associated to Parkinson's disease in our sample, rather than a specific clinical symptom profile. Potential limitations of this study arise from the small group of patients investigated and limited longitudinal data. The recruited HR-PD group had a marker profile measured in around 4% of the general population (Liepelt *et al.*, 2011) which needed around 1300 persons to be screened for the recruitment of HR-PD group. It needs to be considered, though, that only a subgroup of individuals of the HR-PD group will develop Parkinson's disease in their lifetime. Further longitudinal follow up of these individuals would be helpful to determine whether EEG helps to stratify those who will develop the full clinical picture of PD. The value of EEG as a potential biomarker for Parkinson's disease needs to be verified in monitoring disease progression from prodromal to the symptomatic stage in larger cohorts.

6.5 Supplementary tables

Risk markers	Assessment	Cut-off	LR+	LR-
Male gender	-	-	1.2	0.8
Smoking	Pack years	≥ 1	0.45	1.25
Positive family history for first degree relatives	Marder Questionnaire	Possible PD	2.5	1.0
Substantia nigra hyperechogenicity	TCS	*	4.7	0.45
Prodromal markers			LR+	LR-
REM sleep behaviour disorder	RBDSQ	≥5	2.3	0.76
Possible subthreshold parkinsonism	MDS-UPDRS	>6	10	0.7
Olfactory impairment	UPSIT	age and gender corrected standard score, z < -1.0	4.0	0.43
Urinary dysfunction	UMSARS item 10	≥ 1	1.9	0.9
Erectile dysfunction	UMSARS item 11	≥ 2	2.0	0.9
Constipation	UMSARS item 12	≥ 2	2.2	0.8
Orthostatic hypotension	UMSARS part-III	SBP-D > 20 or DBP-D > 10 or symptom with standing	2.1	0.87
Depression	ICD-10	-	1.8	0.85

Table 6.5.1: Assessment tools, cut-off values and likelihood ratios of risk and prodromal markers

LR, likelihood ratio; PD, Parkinson's disease; TCS, Transcranial sonography; RBDQS, REM sleep behaviour disorder screening questionnaire; UPSIT. Smell Identification Test; MDS-UPDRS, Movement Disorders Society Unified Parkinson's Disease Rating Scale; UMSARS, Unified multiple system atrophy rating scale; S/DBP-D, systolic/diastolic blood pressure drop; ICD, International statistical classification of diseases. excluding action tremor.

* Substantia nigra hyperechogenicity was defined as ≥ 90th percentile of the measurements in healthy population.

t Excluding postural and action tremor.

	Model Fit		EEG Equation		Age		Sex	
	F	p-value	ß-value	p-value	ß-value	p-value	ß-value	p-value
Nucleus caudatus								
- Right side	4.549	0.010	-0.515	0.004	-0.017	0.923	-0.192	0.257
- Left side	5.749	0.003	-0.611	0.001	0.108	0.517	-0.102	0.527
- More affected side	5.705	0.004	-0.613	0.001	0.112	0.500	-0.094	0.560
- Less affected side	4.926	0.007	-0.527	0.003	-0.019	0.913	-0.202	0.227
- Total values	5.426	0.005	-0.579	0.001	0.050	0.764	-0.148	0.367
Putamen								
- Right side	5.758	0.003	-0.634	<0.001	0.070	0.672	0.007	0.967
- Left side	5.785	0.003	-0.649	<0.001	0.156	0.350	0.048	0.764
- More affected side	5.746	0.003	-0.638	<0.001	0.095	0.568	0.013	0.936
- Less affected side	5.840	0.003	-0.649	<0.001	0.137	0.411	0.045	0.780
- Total values (both sides)	5.867	0.003	-0.646	<0.001	0.116	0.485	0.029	0.858
Putamen/Caudate Ratio	6.467	0.002	-0.669	<0.001	0.183	0.264	0.229	0.154

Table 6.5.2: Association between the PD specific EEG pattern and 123I-FP-CIT-SPECT

7.EEG Connectivity in Mild Cognitive Impairment

7.1 Introduction

Cognitive impairment, whether without dementia or dementia itself, is a critical non-motor symptom of PD, which limits treatment options, and worsens outcomes and life expectancy of the patients (Emre, 2003*a*)(Levy *et al.*, 2002)(Watson and Leverenz, 2010). As we know, cognitive course of PD is heterogeneous and clinical manifestation of dementia is preceded by subtle functional changes. Mild Cognitive Impairment (MCI) is the intermediate condition between non-altered cognition and Parkinson's disease dementia (PD-D). MCI can be a stable stage for many patients, as is demonstrated in a longitudinal study over 3 years (Lawson *et al.*, 2017) while some studies have reported the progression rate of MCI to PD-D over 4 – 12 years to be 40-60% (Williams-Gray *et al.*, 2013; Wood *et al.*, 2016; Pedersen *et al.*, 2017; Weil *et al.*, 2018). As the clinical symptoms appear much later than the onset of cognitive impairment or neurodegeneration, having methods of early identification of cognitive impairment in PD patients are of major importance for clinicians and researchers and can help improve the quality of life of patients. To add on to the previous knowledge gained from investigating spectral measures, connectivity in the form of Phase Lag Index was now evaluated as a potential qEEG marker of cognitive decline in PD. This chapter is based on a published study from 2019 (Chaturvedi *et al.*, 2019).

The aims of this study were: (a) to identify spectral and connectivity qEEG measures potentially characteristic of MCI in PD patients; (b) to compare the predictive performance of spectral and connectivity qEEG measures; (c) to check for correlation between cognitive domains and EEG features.

7.2 Methods

Subjects

We selected patients at the out-patient movement disorders clinic of the University Hospital Basel (Switzerland) on the following criteria: PD according to UK PD Brain Bank(UPDRS,2003), Mini-Mental Score Examination (MMSE) above 24/30, no history of vascular and/or demyelinating brain pathology, sufficient knowledge of German language. The study was approved by the local ethics committees (Ethikkommission beider Basel, Basel; Switzerland; EK 74/09) and all participants gave written informed consent before study inclusion.

Clinical neurological and neuropsychological assessments

Basic neurological examination was carried out in all individuals. All patients underwent comprehensive neuropsychological examinations. A series of 23 neuropsychological tests was carried out, resulting in aggregate five cognitive scores (domains): Memory, Attention+Working Memory, Executive Function, Language and Visual-Spatial Function. Overall test variables comprised an aggregate "overall cognitive score". MCI diagnosis was set on the grounds of Litvan 2012 level II criteria.(Litvan *et al.*, 2012) We identified 27 PD patients with MCI (MCI group) and 43 PD patients without MCI (non-MCI group). The individual tests grouped into domains are shown in Table 7.1. This grouping follows the same classification as used for the MCI categorization.

Domain	**Neuropsychological tests**
Memory	California Verbal Learning Test : (1) trial 1; (2) trial 5; (3) savings; (4) discriminability
	Rey-Osterrieth Complex Figure : savings (immediate recall divided by copy)
Executive Function	Five-Point Test : correct answers
	Semantic verbal fluency test : correct answers
	Phonemic verbal fluency : correct answers
	Trail-Making Test : time for part B divided by time for part A
Attention and Working Memory	Test of Attentional Performance (TAP) – Alertness: (1) reaction time with alerting sound; (2) reaction time without alerting sound.
	TAP – Divided Attention: (1) reaction time to auditive stimuli (2) reaction time to visual stimuli (3) number of omissions
	Trail-Making Test: time for part A
	Digit span from the German version of the Revised Wechsler Memory Scale : (1) correct forwards (2) correct backwards

	Corsi blocks from the German version of the Revised Wechsler Memory Scale : (1) correct forwards; (2) correct backwards
Visuo-Spatial Function	Rey-Osterrieth Complex Figure: copy
	Block Design Test : sum score
Language	Boston Naming Test : correct answers
	Similarities from the German version of the Revised Wechsler Memory Scale : correct answers

Table 7.1: Psychological tests grouped into 5 cognitive domains

EEG Recording and Processing

We recorded 12 minutes of EEG in resting-state eyes-closed condition, using a 256-channel EEG System (Netstation 300, EGI, Inc., Eugene, OR). EEG recordings were done in the afternoons and patients were seated comfortably in a relaxing chair, instructed to close their eyes. A technician present in the recording room controlled for vigilance of the patients. Before the EEG recording, patients were also asked to self- rate their sleepiness level from 1 to 9 using the Karolinska Sleepiness Scale (Åkerstedt and Gillberg, 1990; Kaida *et al.*, 2006; Miley *et al.*, 2016).

All data were segmented and processed in an automated way using TAPEEG (Hatz *et al.*, 2015). EEG's were filtered (Firls:0.5–70 Hz, 50 Hz notch) at a sampling rate of 1000 Hz and an inverse Hanning window was used to stitch together shorter segments, to have at least 3 minutes of cleaned EEG data. Artefacts like eye movements, traces of sleep, blinking, ECG etc. were detected and removed. After performing automated bad-channel detection (Hatz *et al.*, 2015), the average of all 'good' channels was used to re-reference the EEG to a common average montage.

The independent component analysis implementation of EEGLAB (Delorme and Makeig, 2004) ("runica" with default settings) was used to remove further artefacts. Electrodes placed on the neck, ears, cheeks were excluded to remove spurious signals, and 214 electrodes were mapped to ten regions of interest: frontal left/right, central left/right, parietal left/right, temporal left/right, and occipital left/right.

EEG features

Frequency - spectral power

Median relative spectral powers were calculated in the following frequency ranges (Hz): 1–4 (delta), 4–8 (theta), 8–10 (alpha1), 10–13 (alpha2), 8–13 (alpha), and 13–30 (beta) and spectral

powers for the ten regions of interest as well as global powers were obtained. Thus, we analysed features in 6 frequency ranges and 11 locations, obtaining a total of 66 spectral features.

Connectivity – Phase Lag Index

We used Phase Lag Index (PLI) as a measure of functional connectivity. PLI values range between 0 and 1, where 0 can indicate possibly no coupling and 1 refers to perfect phase locking. We mapped the 214 electrodes to the ten anatomically defined regions. For each region, the average connectivity of all its electrodes to all other regional groups of electrodes was determined (Hardmeier *et al.*, 2014). The connectivity between all pairs of regions was calculated, including the connectivity within a region. This resulted in 55 PLI measures for 6 frequency bands, totalling to 330. Both kinds of features are explained in detail in Chapter 4.

Statistical analysis

Checking for normal distribution and standardization of measures

We compared the demographic and clinical features between MCI and non-MCI groups: age, sex, total education, UPDRS III, MMSE, Hoehn and Yahr Scores, using Wilcoxon non-parametric tests to test if the groups were comparable and for any apparent biases that might be visible. We also compared the global EEG frequency and PLI measures in both groups for a first overview of differences in EEG features in PD- MCI and Non-MCI and adjusted the p-values for multiple testing.

For statistical calculations, we used R version 3.4.1 and RStudio version 1.0.143(R Core Team, 2018).

Cognitive test variables were standardized ("normalized") with reference to a normative database of 604 healthy individuals from the Memory Clinic, Felix Platter Hospital of Basel, Switzerland (Berres *et al.*, 2000).

Spearman correlation coefficients were computed to check for significant correlations between the cognitive domains and PLI measures in each power band. The p-values and confidence intervals for correlations between the cognitive domains and all PLI global measures were obtained using the Psych(Revelle, 2018) package. The probability values were adjusted using the Holm correction method implemented in the package.

The ggcorrplot(Kassambara, 2018) package was used for visualisations.

Random Forest

Random Forest is a widely used ensemble machine learning method based on decision trees. (Breiman, 2001*a*)**.** It has been successfully used in several classification and regression studies

related to neurology, such as, for predicting disease progression or classifying patients based on different features in the case of Alzheimer's disease (Sarica *et al.*, 2017; Dimitriadis and Liparas, 2018; Dimitriadis *et al.*, 2018), Parkinson's disease (Açıcı *et al.*, 2017; Chaturvedi *et al.*, 2017) and Multiple Sclerosis(Lötsch *et al.*, 2018; Zhang *et al.*, 2018).

The method works by constructing several decision trees, selecting subsets of features randomly with replacement, evaluating the best features based on majority voting and then getting predictions based on these measures. The hyperparameters can be tuned to obtain models with high predictive performance. Each variable included in the model is evaluated based on its effect on the overall accuracy of the model and a measure called 'Mean Decrease Accuracy' reflects the importance of the predictor.

It is advantageous to use Random Forest as it combines decision trees with bagging, reduces overfitting, handles large number of predictor variables and ranks variables based on their importance. This makes it more effective in feature selection.

In this analysis, Random Forest was applied with the standard implementation in R. Data were split into training (70%) and test sets (30%) and 5-fold Cross-Validation was repeated 20 times. Area-under-the-curve (AUC) measures were obtained for Receiver Operating Characteristics (ROC)-curves. Classification models were built using frequency measures, PLI measures and frequency combined with PLI measures, respectively. We then obtained a ranked list of the top features important for the accuracy of the classification model. To test whether the AUC values were significantly different while using frequency and PLI measures for classification, we carried out the Friedman test (Friedman, 1940), followed by posthoc testing to see which of the groups had significant differences (Demšar, 2006). This showed us if the AUC values significantly differed between the three groups, and if so, between which pairs. The following packages were used: Random Forest (Liaw, A. & Wiener, M., 2002), caret (Kuhn, n.d.), ROCR(Sing *et al.*, 2005), PMCMR(Pohlert, 2018).

7.3 Results

7.3.1 Participant characteristics

For the first part of the study, we wanted to check if the data set was free from any apparent bias due to differences in demographic features and also if the EEG patterns corroborated with our previous findings. Table 7.2 shows the demographics the patients stratified according to the diagnosis of MCI. MCI and non-MCI patients did not differ in their age, education, UPDRS III and Hoehn and Yahr scores. UPDRS III scores recorded reflect the condition of patients under medication. The disease duration was also similar in both groups; so all patients were at a relatively early stage of the disease. As expected, they had significant differences in their MMSE scores.

Self- reported sleepiness scores indicated alertness for majority of the patients, with median value 3 on the 1 to 9- sleepiness scale.

Parameters	**PD patients(n=70)**		
	MCI (n=27) (21 M, 6 F)	**Non-MCI(n=43)(26 M, 17 F)**	**p-value**
Age	67[53,84]	67[46,82]	n.s.
Education	16[9,20]	15[9,21]	n.s
MMSE	29[24,30]	29[27,30]	0.02
UPDRS III	15[0,41]	15[0,36]	n.s.
Hoehn and Yahr	2[0,5]	2[0,4]	n.s
Disease duration (years)	5[0,23]	4[0,17]	n.s
Levodopa Dosage (mg/day)	650[0,1875]	525[0,2129.5]	n.s
Karolinska Sleepiness Scale	3[1,7.7]	3 [1,7]	n.s.

Table 7.2: Patient demographics, showing Median [Min, Max].

7.3.2 EEG features in PD-MCI and non-MCI patients

While inspecting the differences in the global EEG features in the two groups, relative median spectral power in theta ($p<.05$) and beta bands ($p<.05$) differed significantly between MCI and Non-MCI patient groups as did PLI in theta band ($p<.05$) (Figure 7.1). This aligned with our previous understanding of theta power being highly associated with cognitive decline.

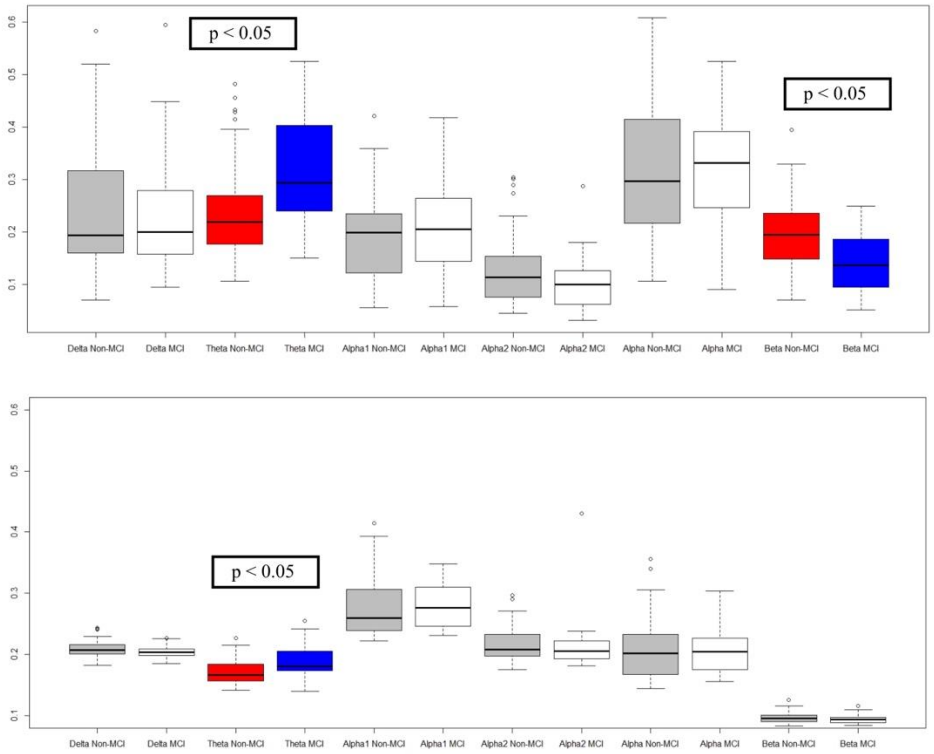

Figure 7.1: (Top) Global spectral powers and PLI measures in Delta, Theta, Alpha1, Alpha2, Alpha, Beta bands between PD Non -MCI and PD MCI patients. **(Bottom)**Theta, Beta global powers and Theta global PLI differed significantly in the two groups.

7.3.3 Classifying PD patients according to MCI using PLI and spectral measures

We proceeded to carry out the classification between the two groups and obtained the ROC-curves using PLI and frequency measures, separately and in combination. The demographics and clinical features assessed earlier were also included, to verify yet again if any of these features would be ranked as highly influential in the classification. The mean AUC values obtained for frequency measures after cross-validation (0.64 +/- 0.15) were lower than those obtained for PLI (0.74 +/- 0.17) and for the combination of Frequency, PLI (0.73 +/- 0.16). The range of AUC values in these three cases is depicted in Figure 7.2.

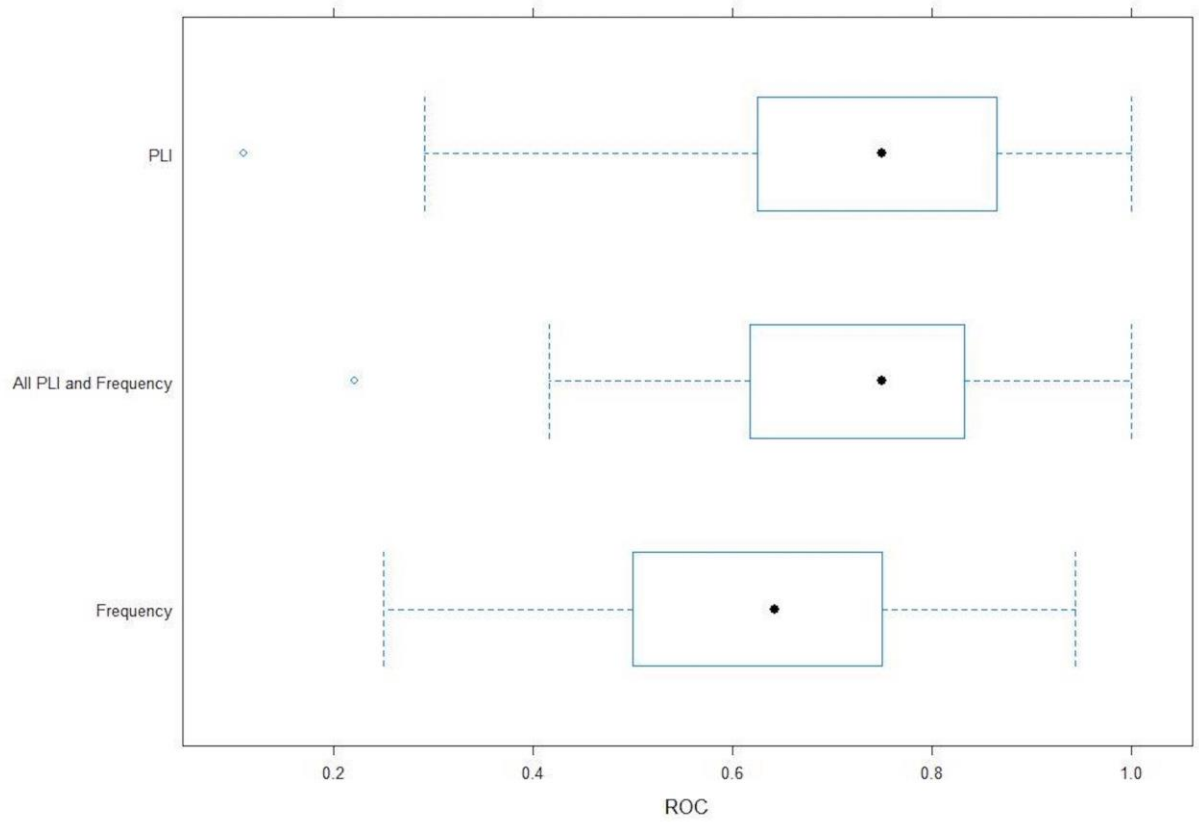

Figure 7.2: AUC spreads showing model performance while using PLI, Frequency and a combination of PLI, Frequency measures mapped to 10 regions.

We then wanted to test if AUC values obtained from these 3 groups have any significant differences, so as to understand if the classification performance would truly improve while using PLI measures instead of frequency. Friedman test showed overall group differences to be significant and then, the Friedman posthoc testing showed that the classification performance using PLI was statistically different than using frequency measures but similar to performance obtained when combining frequency and PLI. This is depicted in Table 7.3.

EEG features comparisons	**p-value**
PLI vs Frequency	7.7e-05
Frequency + PLI vs Frequency	0.0005
Frequency + PLI vs PLI	0.8

Table 7.3: Statistical significances between AUC measures obtained during classification using frequency, PLI measures and combining them together.

On an external unseen test set, AUC values of 0.65, 0.65 and 0.71 were obtained respectively for the three cases. With regards to identifying the most critical variables to identify MCI in PD patients, more PLI measures than spectral measures were ranked amongst the most important ones. In the model constructed using PLI features, measures in theta, delta, beta bands, especially in the Temporal, Central and Parietal regions were ranked high. The clinical features were not ranked amongst the top 20 variables influential for the prediction accuracy of the model but Hoehn and Yahr stage came up as important feature while using frequency features alone. When considering all frequency and PLI measures together, theta powers in the parietal, central, regions and alpha1 power in central region were ranked at the top, along with PLI measures. Figures 7.3, 7.4 show the top 20 PLI and all frequency and PLI combined measures, ranked according to their effect on the accuracy of the model by Random Forest respectively.

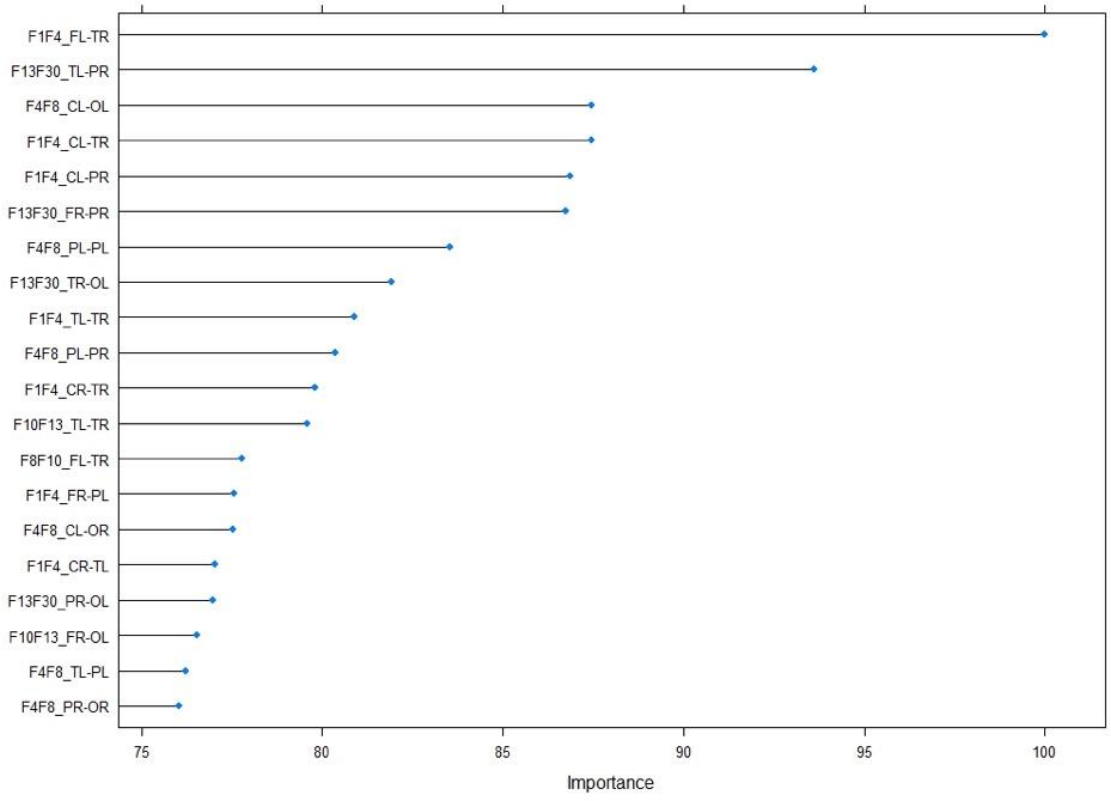

Figure 7.3: Top Selected features by Random Forest while building the model with PLI measures mapped to 10 regions. The x-axis shows the relative importance of the features as percentages. The y-axis denotes the features corresponding to the power band [1–4 (delta), 4–8 (theta), 8–10 (alpha1), 10–13 (alpha2), 8–13 (alpha), 13–30 (beta)] and the connectivity between two regions. E.g.: F1F4_FL-TR denotes the PLI in the delta band between the frontal left and temporal right regions.

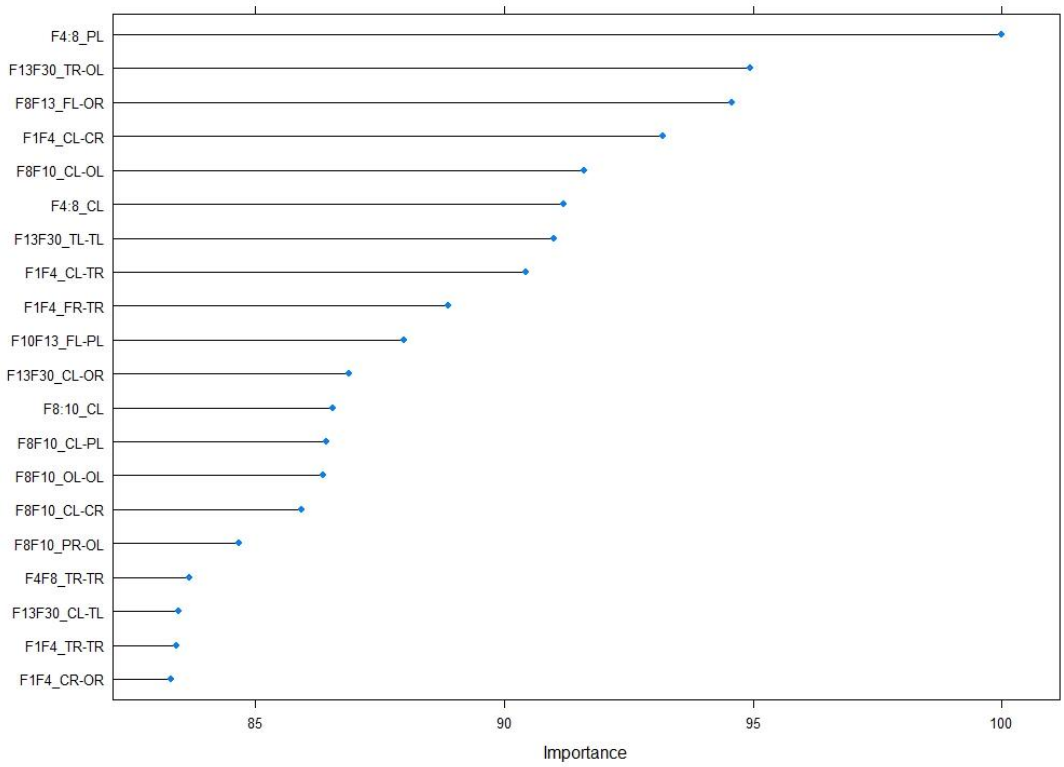

Figure 7.4: Top Selected features by Random Forest while building the model with PLI and frequency measures mapped to 10 regions. The x-axis shows the relative importance of the features as percentages. The y-axis denotes the features corresponding to the power band and the spectral power in a specific region (e.g.: PL denotes parietal left) or PLI between two regions (e.g.: TR-OL denotes the connectivity between temporal right and occipital left regions).

These results indicate that PLI measures perform better while classifying MCI from Non-MCI patients. We found no added benefit in performance while adding on the frequency measures to the PLI features. So, for classification purposes, using this data, we can say that PLI would be the preferred choice of EEG measure over frequency. In line with our previous understanding and assumptions, theta, beta power bands and theta PLI showed the major differences in the two groups. We also observed Alpha frequency and Delta PLI measures amongst the top influential variables selected by Random Forest.

Additionally, we also investigated the effect of using all 256 electrodes, without mapping to corresponding anatomical brain regions, for the development of prediction models and classifying PD MCI from PD non-MCI patients. In this case, we retrieved 1278 frequency measures and

136846 non-zero PLI measures. AUC values from the model developed using frequency measures during cross-validation (0.65+/-0.15) did not differ much when using PLI measures (0.696+/-0.145) or combining all frequency and PLI measures (0.7+/-0.14) during cross-validation. There were no statistical differences in AUC's, as depicted in Table 7.4.

EEG features comparisons	**p-val**
PLI vs Frequency	0.54
Frequency + PLI vs Frequency	0.17
Frequency + PLI vs PLI	0.74

Table 7.4: Statistical significances between AUC measures obtained during classification using frequency, PLI measures (without mapping to regions) and combining them.

Figure 7.5 shows the higher influence of Theta and Delta PLI in the classification using all PLI and frequency measures. Most of the electrodes ranked at the top corresponded to the Temporal, Parietal and Central Regions, aligned with our previous findings. The only frequency feature ranked amongst the top 20 variables corresponded to Theta power in the Temporal Right region. On an unseen external test, AUC values of 0.74, 0.85 and 0.875 were obtained for the three models respectively

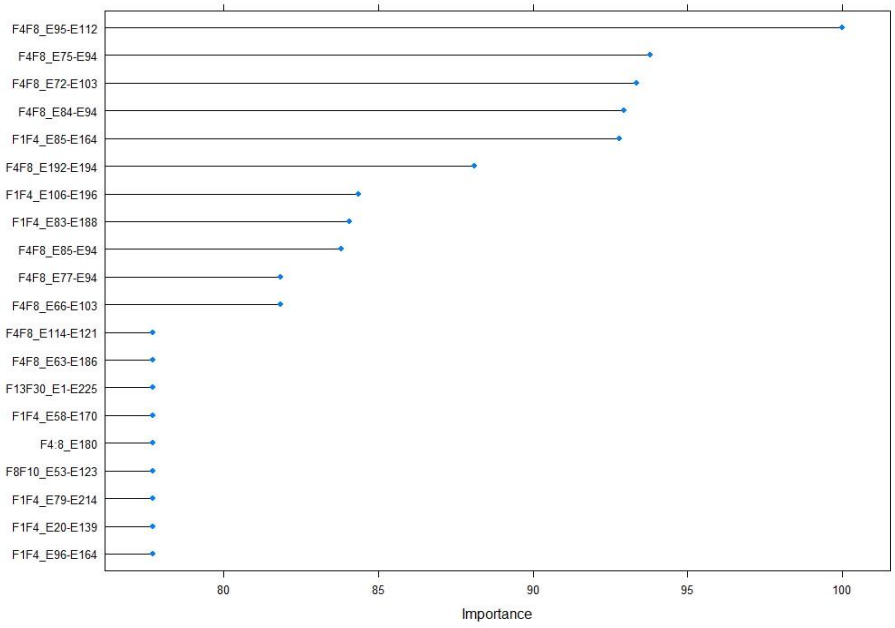

Figure 7.5: Top Selected features by Random Forest while building the model with PLI and frequency measures, without any mapping to regions. The x-axis shows the relative importance of the features as percentages. The y-axis denotes the EEG features in power bands corresponding to specific electrode numbers from the 256-electrode placement. E.g.: F4F8_E95-E112 represents the PLI in theta band between electrode numbers 95 and 112. F4:8_E180 denotes theta power in electrode 180.

However, when comparing the runtime complexities for different models, we noted that using all PLI and frequency features without mapping to regions took maximum time (40,620.02 seconds or about 11 hours) while doing so with the mapped 10 regions took 64.45 seconds. The model using PLI features mapped to 10 regions took 53.79 seconds while using all PLI features without mapping took 32,924 seconds. Models built using 256 electrodes, in general, took more runtime, which should be taken into consideration while building similar models in the future. Time taken by each of the six models can be seen in Table 7.5.

Models	**Run time (seconds)**
Frequency-10 regions	20.78
PLI-10 regions	53.79
Frequency + PLI (10 regions)	64.45
Frequency – 214 electrodes (no mapping)	154.45
PLI- 214 electrodes (no mapping)	32924.44
Frequency +PLI (214 electrodes- no mapping)	40620.02

Table 7.5: Run time of each cross-validated classification model

7.3.4 Correlation of Cognitive domains and EEG features

Now that we determined PLI to be an effective measure for identifying PD patients with MCI, we wanted to assess correlations between each of the 5 cognitive domains and the Overall Cognitive Score (Attention + Working Memory, Executive Function, Memory, Visuo-Spatial Function, Language) and global PLI measures to get some additional insights into cognitive decline. The strongest correlations were seen for Theta PLI with Memory(r=-0.4), Attention (r=-0.38).

While checking for which of these correlations remain significant, we found alpha2 PLI to be correlated with Memory at p=0.05, theta PLI with Attention + Working Memory at p=0.05, alpha1 PLI with Visuo-Spatial Function at p=0.01, beta PLI with Attention + Working Memory and theta PLI with Memory at p=0.001 (Figure 7.6). After adjusting the correlation p-values using Holm correction we identified the most significant correlation for Memory domain with theta PLI (p=0.04).

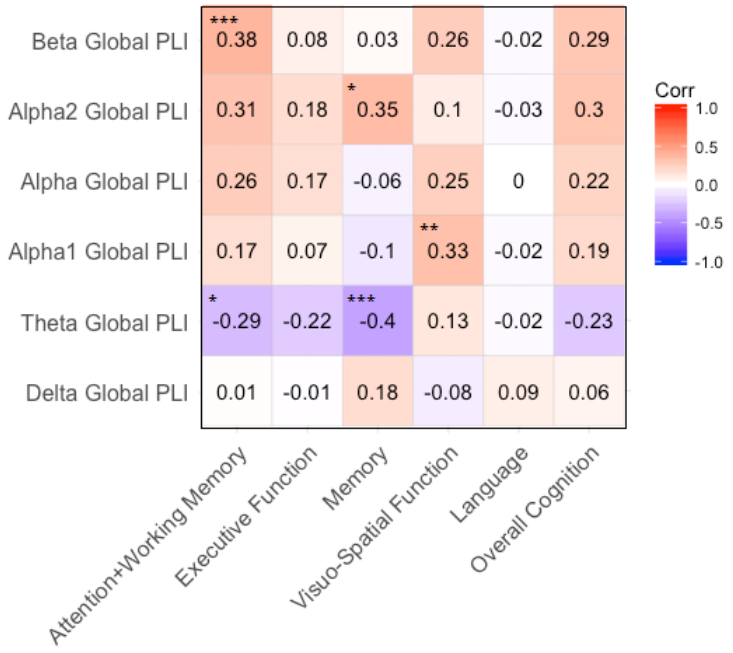

Figure 7.6: Spearman rank correlations for cognitive domains and PLI measures in each power band. (* P ≤ 0.05, ** P ≤ 0.01, *** P≤ 0.001)

The p-values and confidence intervals for correlations between the cognitive domains and all PLI global measures can be seen in Table 7.6.

PLI-Cog domain	**lower**	**R = correlation coefficient**	**upper**	**p**
TGPLI-Memory	-0.4659	-0.39897	-0.32749	6.24E-04
TGPLI-Attn.	-0.44406	-0.37556	-0.30269	1.36E-03
BGPLI-Attn.	0.292741	0.366145	0.435258	1.83E-03
A2GPL-Memry	0.276027	0.350293	0.420402	2.95E-03
A2GPL-OvrlC	0.204659	0.282128	0.356084	1.80E-02
BGPLI-OvrlC	0.197014	0.274779	0.349108	2.13E-02

A2GPL-Attnt	0.170983	0.249689	0.325229	3.71E-02
AGPLI-Attn.	0.142141	0.221765	0.298538	6.50E-02
BGPLI-Visuo	0.130488	0.210446	0.287685	8.04E-02
A1GPL-OvrlC	0.120005	0.200245	0.277886	9.65E-02
TGPLI-Exfnc	-0.26927	-0.19129	-0.11081	1.13E-01
A1GPL-Visuo	0.109306	0.189816	0.267852	1.16E-01
DGPLI-Memory	0.103141	0.183798	0.262055	1.28E-01
AGPLI-OvrlC	0.092079	0.172986	0.251623	1.52E-01
A2GPL-Exfnc	0.089755	0.170711	0.249427	1.58E-01
TGPLI-Wrk_M	0.087849	0.168846	0.247624	1.62E-01
TGPLI-OvrlC	-0.24023	-0.16119	-0.08004	1.83E-01
A1GPL-Wrk_M	0.075876	0.157112	0.236276	1.94E-01
A2GPL-Wrk_M	0.053564	0.135185	0.215011	2.65E-01
AGPLI-Wrk_M	0.044126	0.125886	0.20597	2.99E-01
TGPLI-Visuo	0.035059	0.116938	0.197257	3.35E-01
BGPLI-Wrk_M	0.022992	0.10501	0.185623	3.87E-01
DGPLI-Wrk_M	0.022957	0.104975	0.185589	3.87E-01
A1GPL-Memry	-0.1852	-0.10458	-0.02255	3.89E-01
AGPLI-Exfnc	0.012378	0.094497	0.175351	4.36E-01
A1GPL-Attnt	0.000739	0.08295	0.164047	4.95E-01
A2GPL-Visuo	0.000411	0.082625	0.163728	4.97E-01
AGPLI-Visuo	-0.00719	0.075066	0.156317	5.37E-01
BGPLI-Exfnc	-0.01763	0.064684	0.146123	5.95E-01
AGPLI-Memory	-0.14299	-0.0615	0.020822	6.13E-01
DGPLI-Exfnc	-0.02261	0.059715	0.141237	6.23E-01
DGPLI-OvrlC	-0.02367	0.058665	0.140205	6.30E-01
DGPLI-Attnt	-0.13118	-0.0495	0.032853	6.84E-01
BGPLI-Memory	-0.05618	0.026157	0.10814	8.30E-01

DGPLI-Visuo	-0.1056	-0.02359	0.058743	8.46E-01
A1GPL-Exfnc	-0.07796	0.004287	0.086472	9.72E-01

Table 7.6: The p-values and confidence intervals for correlations between the cognitive domains and all PLI global measures.

7.4 Discussion

In this study, we analysed the capacity of quantitative EEG to identify MCI in patients with Parkinson's disease. It is considerable to note that though PD-MCI is a common condition, it could result from a mixture of complex pathophysiologies, rather than being a distinct pathologic entity, as shown in some studies (Wen *et al.*, 2017). Identifying clinical features or biomarkers associated with this condition can be useful in early risk assessment of dementia.

Patients with MCI in our study, in comparison to those without MCI, had statistically significant differences in the following frequency measures: higher theta spectral power, and lower beta power; and following connectivity measures: higher PLI in theta band. This corresponds to studies reporting higher theta and lower beta powers in PD- MCI patients (He *et al.*, 2016). PLI measures in theta, delta bands came up ranked high as important variables while classifying PD- MCI from PD non-MCI patients.

When considering model performance with AUC as a criterion in this dataset, cross-validated classification performance was better with PLI than frequency and this was comparable to the performance obtained while combining PLI and frequency measures. This shows us that PLI features are not inferior to frequency measures and may contain additional information for understanding and detecting disease progression.

In a previous analysis, we had identified theta spectral power as predictor of general cognitive decline in a cohort of PD patients (Cozac *et al.*, 2016*a*), but we had not investigated connectivity measures (PLI) with regard to MCI. Considering the EEG features ranked high in the classification and looking at the correlations between EEG features and cognitive domains, we see that theta PLI is highly correlated with Memory cognitive domain. These results confirm previous findings of cognitive domains like memory being associated with EEG features like theta power (Jacobs *et al.*, 2006; Han *et al.*, 2017). They may also provide additional evidence to the concept of consecutive cognitive decline and as shown in several studies, MCI is a risk factor of progression to dementia in PD (Caviness *et al.*, 2007; Hobson and Meara, 2015; Wood *et al.*, 2016).

We also re-ran the classification analysis using signals from all electrodes, without mapping to ten regions of interest in the brain, although excluding the electrodes placed on neck, cheeks, and ear lobes. Using all PLI and frequency features, we found that the most important variables ranked at the top were those from Theta, Delta PLI, corresponding to Temporal, Parietal, Central regions and Theta power in the Temporal region. This aligned with results obtained from creating models with features mapped to regions, in which the number of features is much reduced. Through this analysis, we also saw how computationally expensive it can be to deal with vast amounts of data, as with more than 130,000 PLI features.

The limitations of this study arise due to the small number of patients, especially those diagnosed with MCI. However, the study also has some strengths. As this data was recorded at baseline and patients had mild cognitive impairment, they also had low dosages of medication which could not have had a substantial altering effect on the EEG. Patients at advanced stages of the disease can potentially be on medication for several issues such as sleep, bladder, etc. which could affect the EEG recordings. We also had extensive neuropsychological testing which served as reliable scores for overall cognition and the different domains. The EEG features identified in this study could be characteristic of cognitive impairment and help us investigate cognitive decline while following up with the patients in the next steps.

8.Theta as a potential prognostic marker

Evidence from all the cross-sectional studies pointed towards features from the theta band holding predictive value for Parkinson's disease. The Basel PD cohort was followed up for three years and the five-year follow-up is underway. In a first follow-up study after three years, we investigated clinical and qEEG parameters as predictors of severe cognitive decline in PD. Our hypothesis was that qEEG variables at baseline are able to predict severe cognitive decline, and these qEEG variables are not influenced by clinical and demographic parameters. Section 8.1 is based on a publication by Cozac et. al (Cozac *et al.*, 2016*a*). Section 8.2 follows up on the results and includes Theta PLI to investigate both these variables as predictors at 5 years follow-up.

8.1 Theta spectral power as a predictor of cognitive decline at 3 years

At the time of this study, we could acquire data from 37 patients with Parkinson's disease at baseline and 3-year follow-up. Patients had no severe cognitive impairment at baseline. We used a summary score of cognitive tests as the outcome at follow-up, using 14 tests covering six cognitive domains. The difference in the overall cognitive score and in each domain from baseline to 3 years can be seen in Figure 8.1.

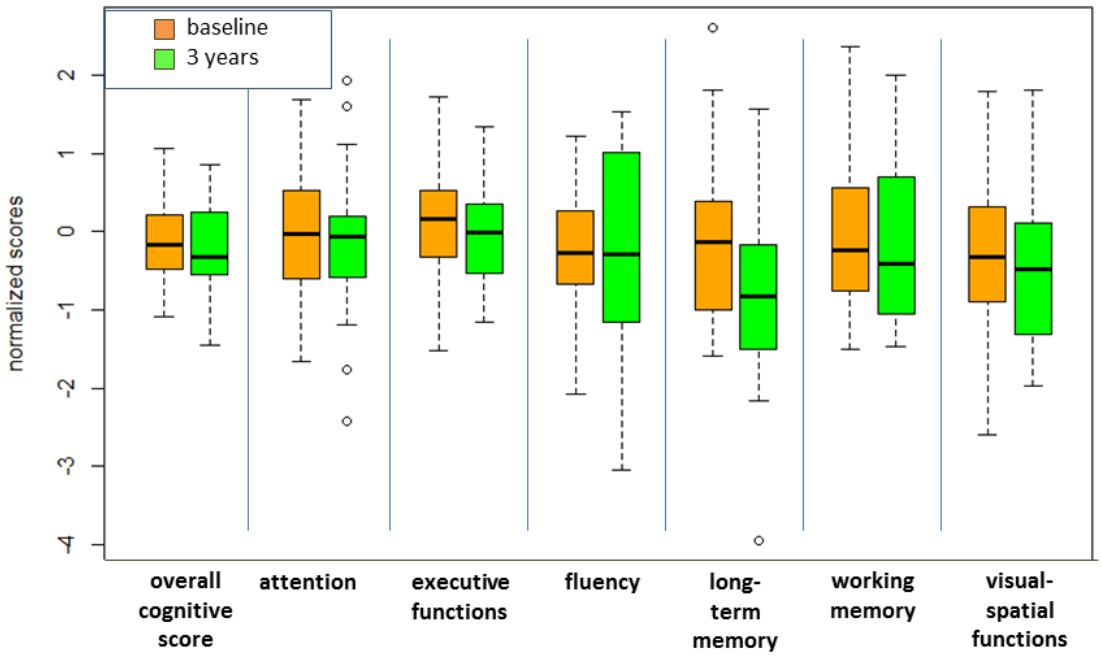

Figure 8.1: Cognitive domains and overall cognitive score of the sample at baseline and after 3 years.

We used linear regression models to evaluate the relation of baseline parameters with cognitive deterioration. The influence of the baseline parameters on cognitive state at follow-up was checked with univariate and multivariate linear regression models with backward elimination. Prediction accuracy was checked with receiver operating characteristic (ROC) curves. Additionally, regression using Random Forest was applied. The level of statistical significance
was set at 0.05. Regression analyses identified three baseline parameters which had significant influence on CI-OCS: Global relative median power (GRMP) theta (β = -3.16, $p < 0.001$), executive functions (β = 0.54, $p < 0.001$), working memory (β = 0.19, $p < 0.05$), adjusted R squared = 0.64, $p < 0.001$.

Explained variance of the overall model was 66.9%, of which "executive functions" made 27.5%, GRMP theta – 25.8%, and "working memory" – 13.6%. Furthermore, we checked if age, sex, and education had confounding effect on each of the three significant variables (GRMP theta, "executive functions," and "working memory"). No confounding effects were identified.

Predictor	**Estimate**	**Standard error**	**t value**	**p-value**	**Variance importance metrics, %**
theta.baseline	-3.157	0.641	-4.920	2.33e-05 *	25.79
exec.functions.baseline	0.544	0.106	5.127	1.27e-05 *	27.52
work.memory.baseline	0.187	0.072	2.588	0.0142 *	13.61
Residual standard error: 0.4057, F-statistic: 22.280 on 3 and 33 DF, Adjusted R-squared: 0.6394, p-value: 4.542e-08 Proportion of variance explained by model: 66.92%, metrics are not normalized.					

Table 8.1 Multivariate regression model with significant qEEG spectral and cognitive predictors. "Change index of the overall cognitive score" was introduced as dependent variable.

Receiver operating characteristic were built using the selected variables: GRMP theta, "executive functions," and "working memory." Best accuracy was identified in GRMP theta: AUC = 75%, specificity = 63%, specificity = 77%. The ROC curves for each of the selected variables can be seen in Figure 8.2 and the corresponding values are shown in Table 8.2.

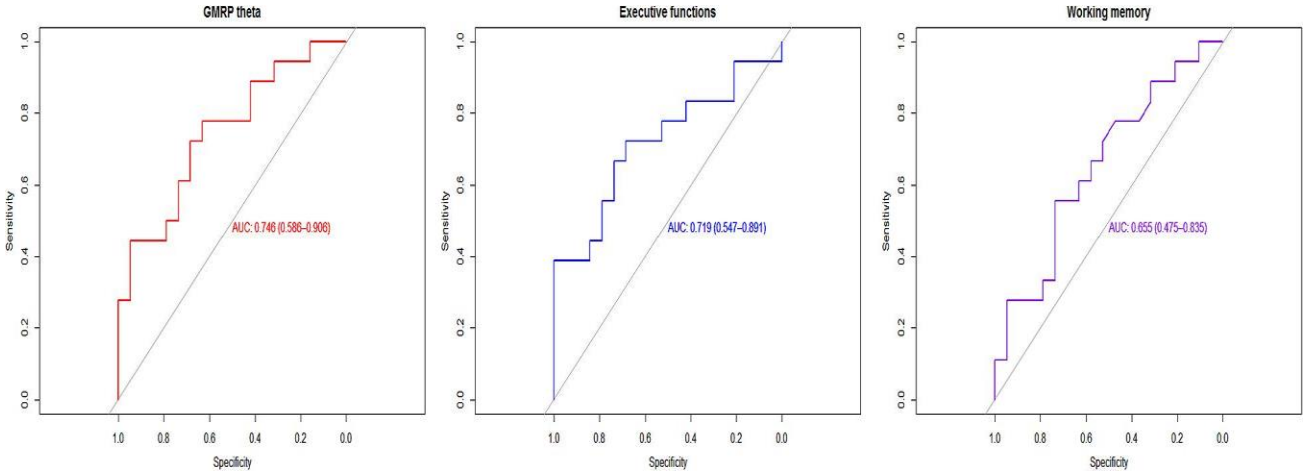

Figure 8.2: ROC curves using theta global power, executive function and working memory

Coordinates	**GMRP theta**	**Executive functions**	**Working memory**
Area under the curve	0.746	0.719	0.655
Specificity	0.631	0.684	0.736
Sensitivity	0.777	0.722	0.555
Positive predictive value	0.666	0.684	0.666
Negative predictive value	0.750	0.722	0.636

Table 8.2: Prediction values for ROC curves using theta global power, executive function and working memory

While using Random Forest Regression, global relative median power theta was classified as the most important variable (MDA = 7.49, MDGC = 1.63). The complete list of ranked variables is shown in Table 8.3.

Predictors	**Mean Decrease Accuracy**	**Mean Decrease Gini Coefficient**
theta.baseline	7.49	1.63
alpha2.baseline	4.28	1.20
beta.baseline	4.98	1.29
median.freq.baseline	1.79	1.27
attention.baseline	2.91	1.40
exec.functions.baseline	7.29	1.67
fluency.baseline	4.39	1.51
work.memory.baseline	3.69	1.51
long.memory.baseline	1.38	1.25
vis.spat.funct.baseline	4.58	1.43
Type of random forest: regression Number of trees: 1000 No. of variables tried at each split: 1 Mean of squared residuals: 0.2796442, % Var explained: 37.03		

Table 8.3: Important predictors using Random Forest regression

Concluding Remark: At three years, we found increased theta global power, especially when combined with low scores in the executive function and working memory domains to be strong predictors of change in overall cognition.

8.2 Theta Global PLI and spectral power as predictors of cognitive decline at 5 years

At the 5-year follow-up, we assessed the relative change in overall cognition and obtained change scores for 37 patients. The aim was to investigate if theta PLI and spectral powers would be associated with cognitive decline at 5 years, based on previous findings.
For this purpose, at first, Spearman's rank correlation tests were carried out for theta global PLI and theta global powers with the reliable change index score (RCI). Both measures correlated significantly with cognitive decline. This is seen in Table 8.4.

Predictor	**Rho**	**p-value**
Theta global spectral power	-0.61	7.878e-05
Theta global PLI	-0.49	0.002251

Table 8.4: Correlation coefficients of theta global power and theta global PLI with Reliable change index in overall cognition at 5 years

Linear regression was carried out to check for the individual association of both these measures with the RCI. This association is depicted in Figures 8.3 and 8.4, where the grey areas around the slope depict the 95% confidence intervals. A confidence band provides a representation of the uncertainty about the regression line. In univariate models as well as when combined, both measures were found to be significantly associated with the RCI. However, the model improved (adjusted R-square) while using theta global spectral power instead of theta global PLI and further enhanced when combining both in a single model.

Predictor	**p-value**	**Adjusted R-Squared**
Theta global PLI	0.0222	0.1161
Theta global power	5.68e-05	0.3568
Theta global PLI+ theta global power	4.436e-05	0.4128

Table 8.5: Comparison of linear regression models using RCI as the dependent variable

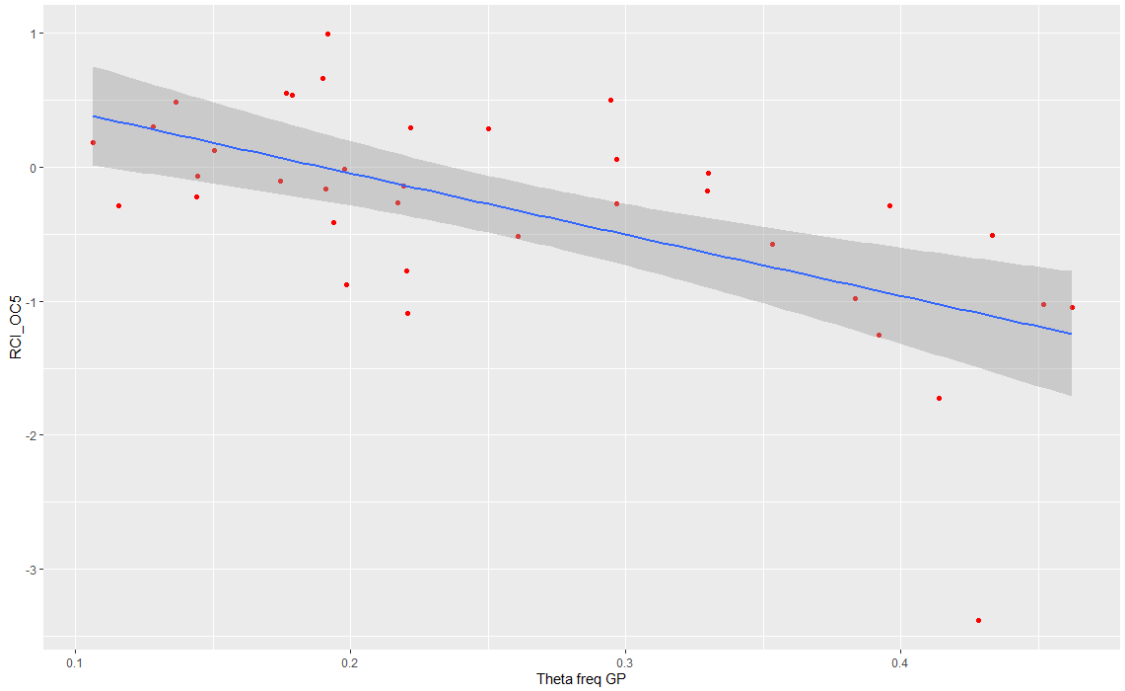

Figure 8.3: Association of theta global spectral power with Reliable change index at 5 years.

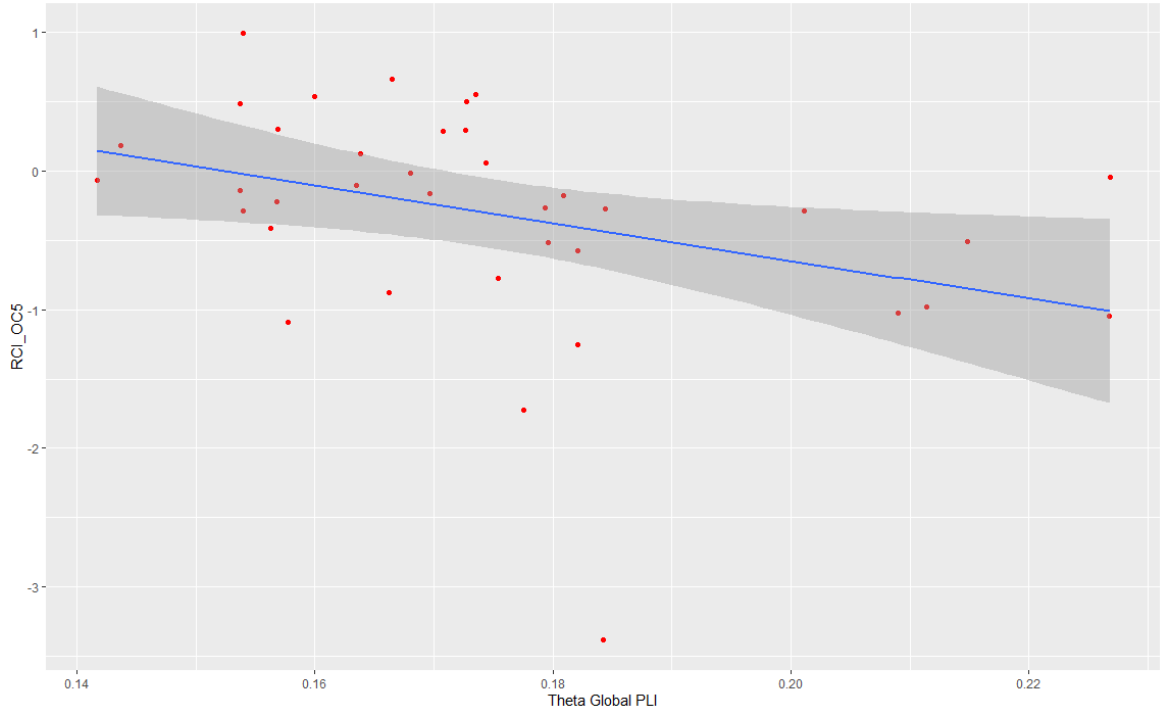

Figure 8.4: Association of theta global PLI with Reliable change index at 5 years.

To check for confounders, variables like age, education, gender, disease duration, medication were assessed in separate models but were also included in a stepwise regression model with theta PLI and global theta power. This model is described in Table 8.5.

Predictor	**Estimate**	**Standard error**	**t value**	**p-value**
Intercept	0.5270689	1.4756915	0.357	0.72339
Theta global PLI	15.2127046	8.2339940	1.848	0.0742
Theta global power	5.8759281	1.8052430	-3.255	0.00274 **
Age	-0.0217180	0.0139083	-1.562	0.12856
UPDRS III	-0.0213079	0.0086264	-2.470	0.01921 *
LEDD	0.0002833	0.0002122	-1.335	0.19153
Residual standard error: 0.5627 on 31 degrees of freedom Multiple R-squared: 0.5639, Adjusted R-squared: 0.4936 F-statistic: 8.017 on 5 and 31 DF, p-value: 6.065e-05				

Table 8.5: Stepwise regression model with theta features, age, medication, motor scores

Besides this, an extreme group analysis was also carried out on these 37 patients. A subset of patients falling in the top and bottom quantiles was obtained, representing ten patients who showed the maximum deterioration (Biggest cognitive decline) and 10 others who showed an improvement in cognition (Cognitive improvement). Their corresponding EEG frequency values at baseline were checked to see how the two groups differed.

The graphs here in Figures 8.5 and 8.6 show the mapping band power median relative values and can be seen as representative of percentages. We observe the biggest difference in theta power in these two groups. Patients who had the most significant cognitive decline had a much higher global theta power at baseline; more than 40% of their relative spectral powers were constituted of theta. With regards to Phase Lag Index, the two groups differed in theta PLI the most. The coloured boxes are representative of the interquartile range, and the horizontal line in the boxplots show the median values.

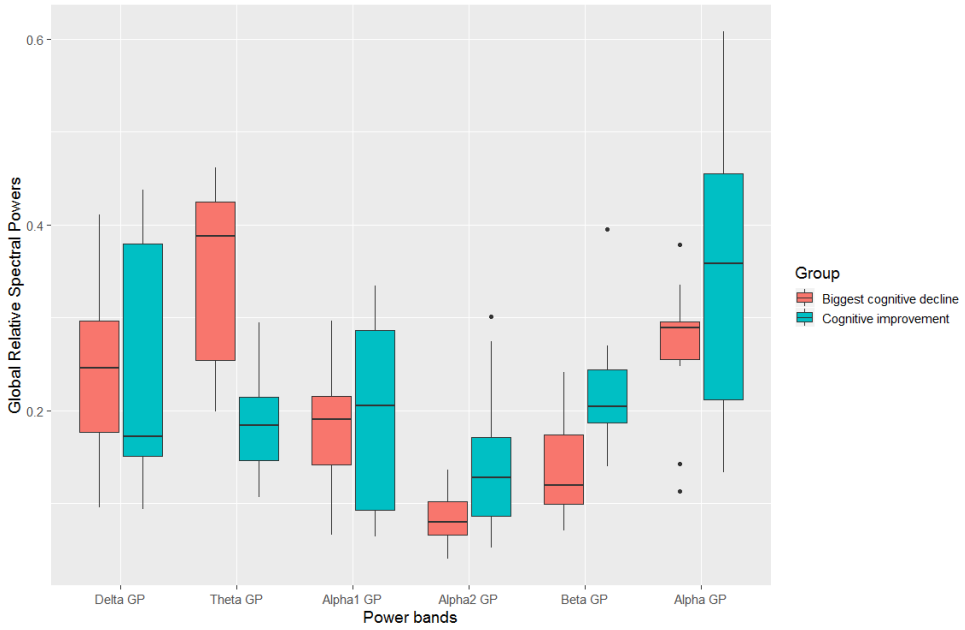

Figure 8.5: Difference in spectral powers at baseline between PD patients who had the most and least cognitive decline in 5 years.

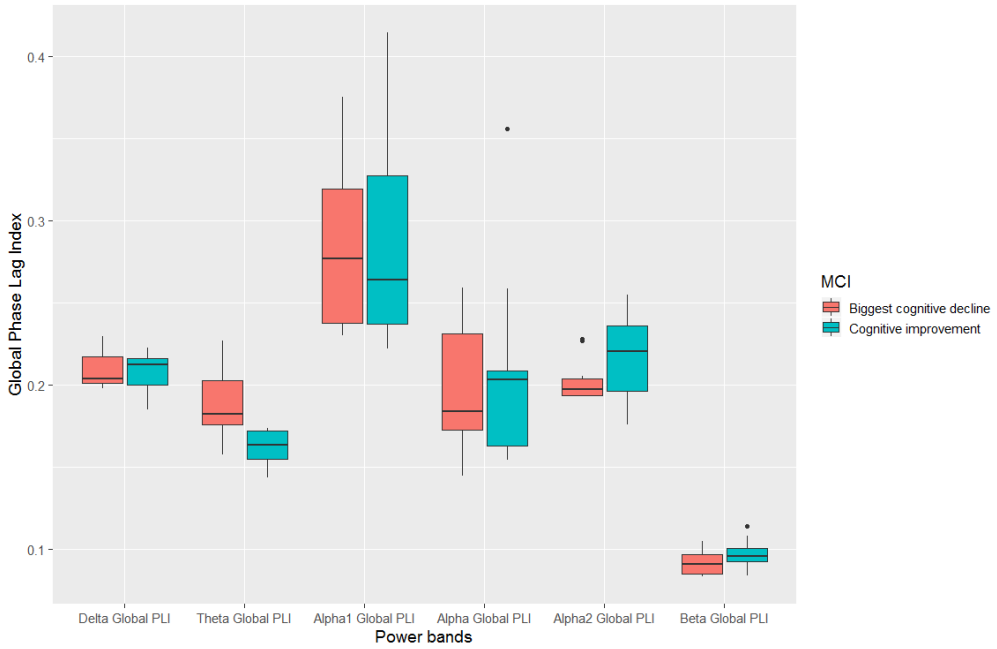

Figure 8.6: Difference in Phase. Lag index at baseline between PD patients who had the most and least cognitive decline in 5 years.

This shows the potential of theta band as a prognostic marker and reiterates our findings on its importance as a biomarker for cognitive decline.

In general, over a period of 5 years, we observed a reduction in overall alpha, beta powers and increase in delta, theta powers. However, there were no significant differences in this cohort. Alpha and delta bands had shown trends with p=0.06 and p=0.07. This is based on comparing 27 patients who had EEG's at both time points- and amongst those, 8 were detected as MCI at Baseline and 19 as Non-MCI. The general overall results are more representative of Non-MCI patients as they constitute the majority in the cohort and are depicted in Figures 8.7, 8.8. However, what it points towards is the fact that for most patients, the EEG patterns remained consistent but changes in specific bands started occurring early on in those who progressed to dementia at a later stage.

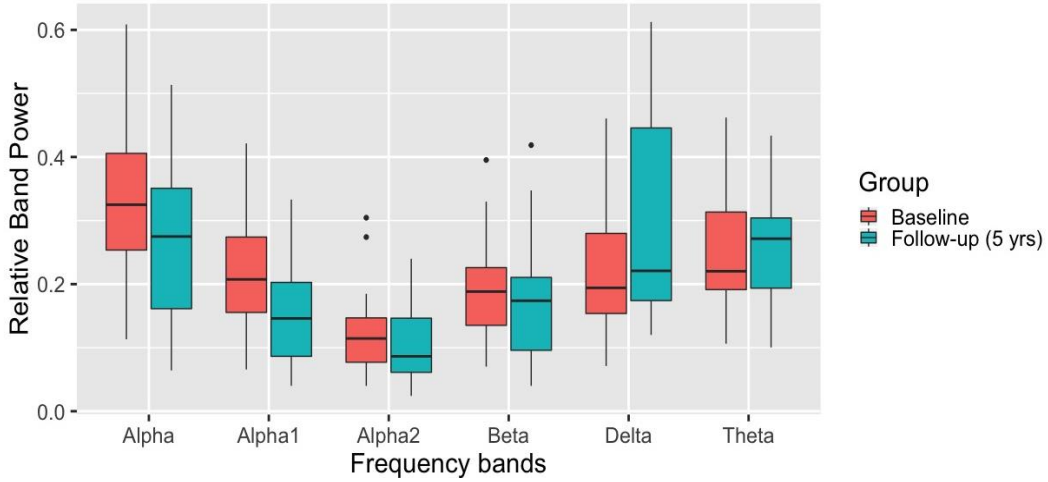

Figure 8.7: Differences in spectral powers in PD patients at baseline and at 5 years

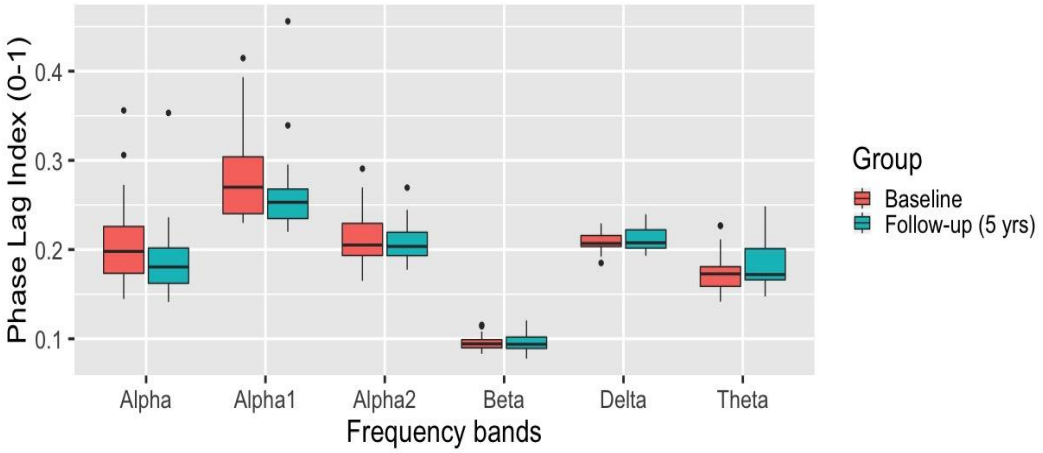

Figure 8.8: Changes in PLI in PD patients at baseline and 5 years

Conclusion: We observe theta as a significant predictor of cognitive decline at 5 years, with spectral power to have a higher substantial effect but improves the prediction model when combined with theta PLI and considering factors like UPDRS III, age, levodopa dosage.

9.Integrated discussion and conclusion

In this thesis, we investigated a cohort of healthy individuals, Parkinson's disease patients at a prodromal stage, PD patients at an early stage with normal cognition and PD patients with mild cognitive impairment to investigate potential EEG biomarkers for predicting cognitive decline in PD patients, leading to dementia. What we learnt can be categorized into two main categories: technical considerations and clinical implications.

9.1 Technical considerations

EEG Recording systems

EEF recording systems can have varying numbers of electrodes, resulting in usable data from 18, 21 or 214 electrodes, for instance. A big challenge is combining data from different recording systems, especially if the aim is to pool data in a multi-centre study to have an increased sample size.

EEG processing

Differences in methods of processing the data, such as automated processing or semi-automated with visual inspection, or even altering settings like filters, amplifiers, post processing can impact the quantified results. In order to have consistency and reproducibility in results, it is vital to follow a specific protocol and to have it accessible by all members of the group to avoid any confusion.

Grouping into regions

While using a high-density EEG system, one can obtain signals from 214 usable electrodes, but the features obtained from every single electrode increase the complexity of the analysis and processing manifold. To make the data meaningful and interpretable, we often average the signals from electrodes into 10 or 22 regions of interest, corresponding to the brain regions. However, a consistent question we get is if it makes sense to group these electrodes into regions.
In Chapter 7, while investigating patients with PD MCI, we re-performed the analysis for frequency and PLI measures taking 214 electrodes to see if the classification performance improved and which features would come up as the most influential ones if we didn't group them into regions. We noted comparable performance on the cross-validated data, although an improvement while predicting on a small, unseen external set. The most important variables for frequency were primarily from theta and beta bands, corresponding to the occipital, temporal regions, mid-auricular line. In case of PLI, we obtained 136,846 features excluding the PLI=0 features in the diagonal of the matrix, which was computationally expensive while running cross-validations and other analysis. The most important PLI features corresponded to those in theta and

delta bands, similar to the observations with the grouped features. However, the run time of 11 hours is too computationally expensive if machine-learning algorithms like random forest would need to be carried out multiple times on all the PLI data for all electrodes.

While post-processing EEG using inverse solution with 76 regions of interest (based on the AAL atlas), it is possible to either carry out an analysis with connectivity between all 76 regions or average them into 8 regions at the end for simplicity and ease of interpretation. Including connectivity between 76 regions would result in big amounts of data, which would be computationally expensive and more difficult to interpret, while grouping all connectivity measures into 8 regions might not give a nuanced view of the condition. Therefore, it is important to keep the main research question in mind before deciding on the form of data to be used.

Inverse solutions can also be applied using different methods for calculating the regions of interests and this can impact the results, especially if there is lack of uniformity while pooling different data or using data processed at different times. To have a uniform method processing and acquiring comparable results, it is suggested to use the 'center' method, which computes the centre voxel for every region instead of computing the voxel with maximal power in different bands as is with the 'maxpower' method.

Dealing with the p<<n problem of sparse data

With EEG data, one of the main challenges is the dimension of the dataset, especially when dealing with a small group of patients but evaluating EEG features from different regions, which amounts to the classic p<<n problem of sparse data. If the number of variables or features used are much greater than the number of observations or patients, it can lead to problems like overfitting and inaccurate, unstable results. For this reason, we need to adjust the regression or classification methods accordingly. In studies conducted as part of this project, penalized regression was applied using LASSO to overcome the issue and Random Forest was the only other standard machine learning algorithm that was found suitable to handle this kind of data. In a separate study conducted (Eckl, Florian, 2017) using the same data as shown in Chapter 5.1, group LASSO was applied and both methods were compared. While the latter was seen to have an improved prediction accuracy, the main features selected by both methods were similar. This shows that there may be scope of adjusting the penalties further but a regularized regression method is still a good choice for feature selection on sparse data.

Solving the issue of imbalanced data

In statistical classification tasks, dataset is considered imbalanced data if it is not evenly distributed amongst the classes and one class constitutes the minority or 'rare' sample. At the same time, the rare class represents the interest and needs to be identified accurately (Krawczyk, 2016). In

practical scenarios, such problems can arise in cases of fraud detection (Fawcett and Provost, 1997) diagnosing rare diseases and associated genetic variants (Schubach *et al.*, 2017). Applying the standard general classification algorithms may not have good results as they work towards minimizing the overall classification error rate, instead of considering the true classification rate of the minority class. Several studies have investigated imbalanced learning with different types of data (Haixiang *et al.*, 2017). To solve the issue of imbalanced data, two mathematical approaches can be used:

- "cost-sensitive" learning – this is assigning a high cost to misclassification of the minority class, and trying to minimize the overall cost (Domingos, 1999).
- sampling techniques - Either down-sampling the majority class or over sampling the minority class, or both.

In one of the studies, the aim was to identify PD-D patients from a pool of PD patients with and without PD-D, and the number of PD-D patients was about 4 times lesser than the number of dementia-free patients. So, Random Forest (Breiman, 2001*a*) algorithm was adapted for imbalanced learning (Chen Chao and Liaw Andy, 2004) using stratified sampling. This proved to be better than using the standard implementation of the algorithm.

9.2 Clinical implications and challenges

"Knowledge isn't power until it is applied." – Dale Carnegie

Through all the studies carried out, innumerable trial and error sessions and technical challenges, the focus of this thesis was to see how the findings can be potentially applied in a clinical environment and accelerate the diagnostic process in the future while coming up with prognostic biomarkers for cognitive decline in Parkinson's disease. The main findings and future prospects are outlined below.

Predictive value of EEG for early diagnosis of PD

In order to eventually investigate cognitive decline, we started by investigating how Parkinson's patients differ from healthy individuals in terms of EEG patterns. We took all the spectral powers into consideration and came up with two regression models, one while using a 256 electrode EEG system with electrodes grouped into 10 regions of interest (Chapter 5), and the other while using a standard 10-20 system (Chapter 6).

The challenge lay in handling a large group of EEG features from a small group of patients, which refers to the p<<n problem. We wanted to obtain models with only a few EEG features, so that it could be easy to implement in the future and would avoid the problems of multicollinearity as well as overfitting. After applying a selection of machine learning methods, we chose to work with a

penalized regression model, applying the LASSO penalty. LASSO was seen effective in solving problems in different fields such as, fraud detection in banks or genetic analysis (Wu *et al.*, 2009; Fontanarosa and Dai, 2011; Wang *et al.*, 2015). We also found it to be effective in dealing with EEG data.

EEG Risk model using high-density systems

The penalized logistic regression method (LASSO) applied for classifying Parkinson's disease patients from healthy individuals using seventy-nine features resulted in a subset of six features, reflecting differences in theta, alpha2, beta power, and alpha1/theta ratio in certain regions. **Two of the most influential features included theta power in the temporal left region and alpha1/theta ratio in central left region.** Implementing these coefficients in an equation would look like:

(Theta_TL *8.77)+ (Theta_PL*3.32)+(Alpha2_FL*0.83) + (Alpha1_CL* -1.04) + (Delta_FL*-2.1) + (Beta_PR*-2.74) + (Alpha1_OL* +6.32) + 0.46

EEG Risk model using 10-20 system

Using a 10-20 standard EEG system, **we shortlisted two features from the theta and alpha bands in an optimal risk score model.** We identified theta power in the right occipital lobe (O2) and alpha1 activity in the left parietal lobe (P3) as primary factors differentiating controls from PD. This resulted in a risk score obtained from the following equation: (1.62*Theta_O2) + (0.75*Alpha1_P3) + 3.75.

The probability of each patient being diagnosed as PD or the predicted risk can be obtained by applying the formula: exponential (patient's risk score) ÷ (1 + exponential (patient's risk score)). **Theta spectral power (in the temporal and occipital regions) was found to be the most important feature in both cases.**

Theta and alpha powers, especially in the occipital, parietal and temporal regions, are reported as characteristics of PD patients in several studies. One study investigating 15 early-stage PD patients and 15 healthy individuals had found an increase in delta and theta bands in PD patients with a decrease in alpha, beta bands (Han *et al.*, 2013). Theta power in the left occipital region was found to be associated with disease severity in PD patients and also differed significantly between PD patients with and without mild cognitive impairment (He *et al.*, 2016). One MEG study (Bosboom *et al.*, 2006) had also reported an increase in theta power in the occipital and temporal channels to be associated with lower cognitive performance in PD patients without dementia. In Alzheimer's disease, the alpha/theta ratio was seen to be indicative of the condition too, with potential to distinguish between the diseased and the healthy group(Schmidt *et al.*, 2013). Our current data

supports these patterns as being reliable enough for implementation in an easy to use tool in the future to help in early diagnosis.

As the penalized logistic regression method picks out features that are not highly correlated to each other, the final selected features may not represent the only possible solution, but rather an optimal model resulting in a considerable classification accuracy. This could explain why some studies found power in theta temporal left region to be the most effective classifier instead of theta power in temporal right or occipital regions. Signals from electrodes placed close to each other can be more correlated than those further away, which would lead to selection of only one amongst the cluster.

EEG reflects dopaminergic loss associated with Parkinson's disease

We investigated for the first time the potential of EEG as a biomarker for Parkinson's disease in individuals potentially at high risk for PD.

When subtle signs of PD are present in a patient but do not fulfil the diagnostic criteria of the disease, it is referred to as prodromal PD (Hughes *et al.*, 1993, Berg *et al.*, 2015*a*; Heinzel *et al.*, 2016). A better understanding of the prodromal period is essential for the early diagnosis of PD, with the future aim to apply neuroprotective treatment in individuals at high risk for PD, once it is available. After obtaining the risk score model for early PD patients, this study applied it on a group of patients suspected to be in the prodromal stage. The premise of the study was that symptoms start appearing many years before a clear diagnosis can be made, and if the patients are identified early on, it could help improve their quality of life in the long run. As the pre-clinical symptoms of PD are heterogenic as an expression of the underlying neurodegenerative process (Dauer and Przedborski, 2003; Grosch *et al.*, 2016), biomarkers indicating a high risk for PD conversion reflecting in vivo PD specific brain changes are needed to identify a high-risk PD group. The method used for identifying this group , Transcranial Sonography, has been used in various studies, not only to confirm PD diagnosis (Li *et al.*, 2016) but also to encompass a high-risk group for future onset of PD (Berg *et al.*, 2011).

The high-risk group had a higher amount of theta power than the healthy individuals and lesser than the PD group, indicating that theta power changes can already be measured in the prodromal stage. After two years, motor symptoms worsened in several of these patients and EEG was also found associated with olfactory test scores as well as cognitive functions like attention, executive function. As we know, loss of the sense of smell is a well-known symptom of early PD(Berendse and Ponsen, 2006; Morley *et al.*, 2018; Pak *et al.*, 2018) and cognitive decline occurs in several PD patients in the long run (de la Riva *et al.*, 2014; Chahine *et al.*, 2018).

Currently, one of the only ways to measure the dopaminergic loss in a human brain is by using a 123I-FP-CIT-SPECT or DAT Scan, and some of the patients underwent this imaging procedure. It was interesting to find the theta power correlated with the uptake of the tracer in the caudate and putamen, showing that EEG reflects dopaminergic loss associated with PD.

These findings suggest that theta activity might be a potential prodromal marker for Parkinson's disease and can be useful for predicting PD-related motor symptoms.

EEG markers for Mild Cognitive Impairment in PD patients

The study described in Chapter 7 analysed the capacity of quantitative EEG to identify MCI in patients with Parkinson's disease. Mild Cognitive Impairment (MCI) is the intermediate condition between non-altered cognition and Parkinson's disease dementia (PD-D). PD-MCI is a common condition, but it could result from a mixture of complex pathophysiology, rather than being a distinct pathologic entity (Wen *et al.*, 2017). Identifying clinical features or biomarkers associated with this condition can be useful in early risk assessment of dementia.

Patients with MCI in this study, in comparison to those without MCI, had significantly **higher theta spectral power, lower beta power and higher PLI in theta band.** This corresponds to studies reporting higher theta and lower beta powers in PD-MCI patients (He *et al.*, 2016). PLI measures in theta and delta bands differ between PD-MCI from PD non-MCI patients. Connectivity measures classified MCI patients from non-MCI PD patients better than spectral power when used alone but had comparable performance when combined.

It is interesting to note that the criteria for determining the MCI status of a patient can vary across clinics, populations, demographics and studies report varying MCI prevalence as well as progression rates. For instance, one study showed prevalence of MCI in about 40% of newly diagnosed PD patients (Monastero *et al.*, 2018) and another reported 15% to 53% prevalence across different centres(Yarnall *et al.*, 2013). The MDS Task Force's Level I criteria can be applied on global cognition scales or using fewer than two tests in each of five cognitive domains (attention/working memory; executive function; episodic memory; visuospatial function; language) or when fewer than five cognitive domains are assessed. The Level II criteria requires more than one test in each of the cognitive domains and PD-MCI is confirmed when any two (or more) neuropsychological test scores are 1-2 S.D below normative data(Litvan *et al.*, 2012). The study described was based on the Litvan Level 2 criteria and impaired scores were assessed with a 1.5 S. D cut-off. This should be kept in mind while replicating studies or designing any future studies.

Association between EEG and cognitive function

Through the different studies showcased in Chapters 5, 6, 7, consistent findings showed association of EEG with attention and memory domains. With regards to spectral power, theta and beta powers, especially in the temporal and parietal regions respectively, apart from global powers, had the strongest correlation with attention and memory. For patients identified to be in the prodromal stage, lower test performance in these domains was associated with higher EEG risk scores reflecting a higher probability of resembling the PD specific EEG profile. Following up this group for two years indicated attention and executive problems were significantly associated with the baseline EEG risk score. Attention and memory, along with visuo-constructive domains were also amongst the most influential domains while classifying the PD group from the healthy individuals.

Moving on to connectivity features like Phase Lag Index, the strongest correlation was seen between theta PLI and memory, followed by beta and theta PLI with attention+working memory while investigating Parkinson's disease patients with and without MCI. In line with Section 5.3, the idea of association between alpha band and visuo-spatial function was reiterated also in the case of PLI as seen in Chapter 7.

These results confirm previous findings of cognitive domains like memory being associated with EEG features like theta power (Jacobs *et al.*, 2006; Han *et al.*, 2017). They may also provide additional evidence to the concept of consecutive cognitive decline and as shown in several studies, MCI is a risk factor of progression to dementia in PD (Caviness *et al.*, 2007; Hobson and Meara, 2015; Wood *et al.*, 2016).

Theta as a potential prognostic marker

Evidence from all the cross-sectional studies pointed towards features from the theta band holding predictive value for Parkinson's disease. The Basel PD cohort was followed up for three years and the five-year follow-up was carried out for 37 patients. In a first follow-up study (Cozac *et al.*, 2016*a*), increased theta global power, especially when combined with low scores in the executive function and working memory domains were found to be strong predictors of change in overall cognition after three years. Some studies have reported the progression rate of MCI to PD-D over 4 – 12 years to be 40-60% (Williams-Gray *et al.*, 2013; Wood *et al.*, 2016; Pedersen *et al.*, 2017; Weil *et al.*, 2018). But this is not what we observed in our cohort. Only five patients from our cohort progressed to dementia in three years and there wasn't much of a change at five years. In fact, to investigate how EEG patterns might vary early on in patients who progressed to dementia, an extreme group analysis was carried out.

This shows the potential of theta band as a prognostic marker and reiterates our findings on its importance as a biomarker for cognitive decline.

Rate of cognitive decline

When looking at a group of 46 PD patients who were followed up, 15 were evaluated to have Mild Cognitive Impairment (MCI) at baseline. This number grew to 19 after three years. Nine patients converted to MCI in three years and five MCI patients were seen to re-convert to normal cognition at the time of the follow-up study. At baseline, MCI and Non-MCI patients did not differ in their demographics except for disease duration. However, after three years, MCI and Non-MCI patients had significant differences in their MMSE and UPDRS III scores. Table 1 shows the demographics of MCI and Non-MCI patients at Baseline and at three years.

Parameters	**Baseline (n=46)**			**3 Year Follow up(n=46)**		
	MCI (10 M, 5 F)	**Non-MCI (19 M, 12 F)**	**p-value**	**MCI (12 M, 7 F)**	**Non-MCI (17 M, 10 F)**	**p-value**
Age	67.4+/- 8.6	67.4+/-7.2	n.s.	71.4+/-7.8	69.7+/-7.4	n.s
Education	15.2+/-3.5	14.4+/-3	n.s	15+/-3.5	14.4+/-2.9	n.s.
MMSE	28.4+/-1.5	28.9+/-0.8	n.s.	26.8+/-2.5	29.18+/-1	0.0002
UPDRS III	15.7+/-11	15.9+/-11.8	n.s.	25.5+/-11.1	15.7+/-12.3	0.005
Disease Duration	6.46+/-5.8	3.95+/-3.8	n.s	8.3+/-4.4	7.4+/-4.94	n.s.

Table 9.1: Patient demographics

MCI can be a stable stage for many patients, as is demonstrated in a longitudinal study over three years (Lawson *et al.*, 2017). As discussed previously, different clinics may be applying variations of cut off scores for diagnosing MCI and for determining the dementia status. MCI is considered a risk marker for dementia, but if there is a lack of uniformity in scales, it can be challenging to compare studies and arrive at the same conclusions. Based on literature review, we expected a much higher proportion of our cohort to progress to dementia. But we found that the rate of cognitive decline was exceptionally low in our case. In comparison, when working on a collaborative project with patients from Italy, many more dementia patients were observed and a

huge difference in education was observed between the two cohorts. We know that a longer span of education does influence a higher cognitive reserve which prevents a rapid cognitive decline (Meng and D'Arcy, 2012) , but we are unsure of what other factors might have facilitated the preservation of cognitive health of our patients.

9.3 Significance for patients and future direction

To implement a biomarker in practice, it is important for it to be stable and reliable. EEG is seen to have a high test-retest reliability, is seen to be stable and we have seen patterns emerging and staying consistent throughout the disease progression. In our case, theta, in particular, has proven to be an effective measure of identifying early PD, MCI and eventually dementia. Its strong association with memory and attention domains make it a good indicator of cognitive decline. This was also observed in the prodromal PD group and as discussed, the prodromal stage begins several years before a clear clinical diagnosis is feasible for PD.

An effective implementation might be to find out optimal cut-off points pertaining to different phases of progression and using it in the clinic for facilitating decision making with regards to patient therapy, care and treatment.

Improving the quality of life of patients and helping them overcome problems in daily life has been one of the main visions and drivers of this project. If we are able to effectively implement tools using cut-off scores from selected EEG and neuropsychological tests, we might be able to identify patients at risk at an early stage and provide them with relevant regular therapy to improve, stabilize and possibly revert their condition. As observed, a few patients did revert to normal cognition, although it is not fully clear how well they stuck to a routine or practised physical/mental exercises at home throughout. One study carried out at our centre had used the Wii gaming console to train patients thrice a week for six months (Zimmermann *et al.*, 2015*b*) and noted an improvement in cognitive performance for some of the patients. Some other patients are given dance therapy, speech therapy or cognitive behavioural therapy in a group, depending on each one's needs and condition.

REFERENCES

Aarsland D, Andersen K, Larsen JP, Lolk A, Nielsen H, Kragh–Sørensen P. Risk of dementia in Parkinson's disease. Neurology 2001; 56: 730.

Aarsland D, Creese B, Politis M, Chaudhuri KR, Ffytche DH, Weintraub D, et al. Cognitive decline in Parkinson disease. Nat Rev Neurol 2017; 13: 217.

Abbott DF. Probing the Human Brain Functional Connectome with Simultaneous EEG and fMRI [Internet]. Front Neurosci 2016; 10[cited 2019 Aug 22] Available from: https://www.frontiersin.org/articles/10.3389/fnins.2016.00302/full

Açıcı K, Erdaş ÇB, Aşuroğlu T, Toprak MK, Erdem H, Oğul H. A Random Forest Method to Detect Parkinson's Disease via Gait Analysis. In: Boracchi G, Iliadis L, Jayne C, Likas A, editor(s). Engineering Applications of Neural Networks. Springer International Publishing; 2017. p. 609–19

Adler CH, Beach TG. Neuropathological Basis of Non-Motor Manifestations of Parkinson's Disease. Mov Disord Off J Mov Disord Soc 2016; 31: 1114–9.

Aebi S, Mistridis P. Die komplexe Figur von Rey-Osterrieth. Eine Normierungsstudie zur Bewertung der Reproduktionsgenauigkeit nach deutschen Kriterien. 2009

Agrawal M, Biswas A. Molecular diagnostics of neurodegenerative disorders [Internet]. Front Mol Biosci 2015; 2[cited 2019 Nov 20] Available from: https://www.frontiersin.org/articles/10.3389/fmolb.2015.00054/full

Akbani R, Kwek S, Japkowicz N. Applying Support Vector Machines to Imbalanced Datasets. In: Boulicaut J-F, Esposito F, Giannotti F, Pedreschi D, editor(s). Machine Learning: ECML 2004. Springer Berlin Heidelberg; 2004. p. 39–50

Åkerstedt T, Gillberg M. Subjective and Objective Sleepiness in the Active Individual. Int J Neurosci 1990; 52: 29–37.

Aleman A, Van'T Wout M. Repetitive transcranial magnetic stimulation over the right dorsolateral prefrontal cortex disrupts digit span task performance. Neuropsychobiology 2008; 57: 44–8.

Alexopoulos EC. Introduction to Multivariate Regression Analysis. Hippokratia 2010; 14: 23–8.

Al-Qazzaz NK, Ali SHBMD, Ahmad SA, Chellappan K, Islam MdS, Escudero J. Role of EEG as Biomarker in the Early Detection and Classification of Dementia. Sci World J 2014; 2014: 1–16.

Álvarez JD, Matias-Guiu JA, Cabrera-Martín MN, Risco-Martín JL, Ayala JL. An application of machine learning with feature selection to improve diagnosis and classification of neurodegenerative disorders. BMC Bioinformatics 2019; 20: 491.

Antal A, Bandini F, Kéri S, Bodis-Wollner I. Visuo-cognitive dysfunctions in Parkinson's disease. Clin Neurosci N Y N 1998; 5: 147–52.

Arnaldi D, Campus C, Ferrara M, Famà F, Picco A, De Carli F, et al. What predicts cognitive decline in de novo Parkinson's disease? Neurobiol Aging 2012; 33: 1127.e11-1127.e20.

Aubert-Broche B, Evans AC, Collins L. A new improved version of the realistic digital brain phantom. NeuroImage 2006; 32: 138–45.

Babiloni C, De Pandis MF, Vecchio F, Buffo P, Sorpresi F, Frisoni GB, et al. Cortical sources of resting state electroencephalographic rhythms in Parkinson's disease related dementia and Alzheimer's disease. Clin Neurophysiol 2011; 122: 2355–64.

Babiloni C, Del Percio C, Lizio R, Noce G, Cordone S, Lopez S, et al. Abnormalities of cortical neural synchronization mechanisms in patients with dementia due to Alzheimer's and Lewy body diseases: an EEG study. Neurobiol Aging 2017; 55: 143–58.

Babiloni C, Del Percio C, Lizio R, Noce G, Lopez S, Soricelli A, et al. Levodopa may affect cortical excitability in Parkinson's disease patients with cognitive deficits as revealed by reduced activity of cortical sources of resting state electroencephalographic rhythms. Neurobiol Aging 2019; 73: 9–20.

Baeumler G. FWIT - Farbe-Wort-Interferenztest nach J.R. Stroop (FWIT). Goettingen: Hogrefe 1985. [Internet]. [cited 2019 May 24] Available from: https://www.testzentrale.de/shop/farbe-wort-interferenztest.html

Bago Rožanković P, Rožanković M, Vučak Novosel L, Stojić M. Nonmotor symptoms in de novo Parkinson disease comparing to normal aging. Clin Neurol Neurosurg 2017; 155: 7–11.

Bajaj N, Hauser RA, Grachev ID. Clinical utility of dopamine transporter single photon emission CT (DaT-SPECT) with (123I) ioflupane in diagnosis of parkinsonian syndromes. J Neurol Neurosurg Psychiatry 2013; 84: 1288–95.

Baldereschi M, Di Carlo A, Rocca WA, Vanni P, Maggi S, Perissinotto E, et al. Parkinson's disease and parkinsonism in a longitudinal study: Two-fold higher incidence in men. Neurology 2000; 55: 1358–63.

Barbosa MT, Caramelli P, Maia DP, Cunningham MCQ, Guerra HL, Lima-Costa MF, et al. Parkinsonism and Parkinson's disease in the elderly: A community-based survey in Brazil (the Bambuí study). Mov Disord 2006; 21: 800–8.

Bártová P, Kraft O, Bernátek J, Havel M, Ressner P, Langová K, et al. Transcranial sonography and (123)I-FP-CIT single photon emission computed tomography in movement disorders. Ultrasound Med Biol 2014; 40: 2365–71.

Baştanlar Y, Ozuysal M. Introduction to machine learning. Methods Mol Biol Clifton NJ 2014; 1107: 105–28.

Bastos AM, Schoffelen J-M. A Tutorial Review of Functional Connectivity Analysis Methods and Their Interpretational Pitfalls [Internet]. Front Syst Neurosci 2016; 9[cited 2018 Jan 23] Available from: https://www.frontiersin.org/articles/10.3389/fnsys.2015.00175/full

Benamer HTS, Patterson J, Grosset DG, Booij J, Bruin K de, Royen E van, et al. Accurate differentiation of parkinsonism and essential tremor using visual assessment of [123I]-FP-CIT SPECT imaging: The [123I]-FP-CIT study group. Mov Disord 2000; 15: 503–10.

Benz N, Hatz F, Bousleiman H, Ehrensperger MM, Gschwandtner U, Hardmeier M, et al. Slowing of EEG background activity in Parkinson's and Alzheimer's disease with early cognitive dysfunction. Front Aging Neurosci 2014; 6: 314.

Benz N, Hatz F, Bousleiman H, Ehrensperger MM, Gschwandtner U, Hardmeier M, et al. Slowing of EEG Background Activity in Parkinsonâ€™s and Alzheimerâ€™s Disease with Early Cognitive Dysfunction [Internet]. Front Aging Neurosci 2014; 6[cited 2016 Jan 13] Available from: http://journal.frontiersin.org/article/10.3389/fnagi.2014.00314/abstract

Berendse HW, Ponsen MM. Detection of preclinical Parkinson's disease along the olfactory trac(t). J Neural Transm Suppl 2006: 321–5.

Berendse HW, Stam CJ. Stage-dependent patterns of disturbed neural synchrony in Parkinson's disease. Parkinsonism Relat Disord 2007; 13: S440–5.

Berg D, Behnke S, Seppi K, Godau J, Lerche S, Mahlknecht P, et al. Enlarged hyperechogenic substantia nigra as a risk marker for Parkinson's disease. Mov Disord 2013; 28: 216–9.

Berg D, Behnke S, Walter U. Application of transcranial sonography in extrapyramidal disorders: updated recommendations. Ultraschall Med Stuttg Ger 1980 2006; 27: 12–9.

Berg D, Marek K, Ross GW, Poewe W. Defining at-risk populations for Parkinson's disease: Lessons from ongoing studies. Mov Disord 2012; 27: 656–65.

Berg D, Postuma RB, Adler CH, Bloem BR, Chan P, Dubois B, et al. MDS research criteria for prodromal Parkinson's disease. Mov Disord 2015; 30: 1600–11.

Berg D, Postuma RB, Adler CH, Bloem BR, Chan P, Dubois B, et al. MDS research criteria for prodromal Parkinson's disease: MDS Criteria for Prodromal PD. Mov Disord 2015; 30: 1600–11.

Berg D, Seppi K, Behnke S, Liepelt I, Schweitzer K, Stockner H, et al. Enlarged substantia nigra hyperechogenicity and risk for Parkinson disease: a 37-month 3-center study of 1847 older persons. Arch Neurol 2011; 68: 932–7.

Berrar D. Cross-Validation. In: Ranganathan S, Gribskov M, Nakai K, Schönbach C, editor(s). Encyclopedia of Bioinformatics and Computational Biology. Oxford: Academic Press; 2019. p. 542–5

Berres M, Monsch AU, Bernasconi F, Thalmann B, Stähelin HB. Normal ranges of neuropsychological tests for the diagnosis of Alzheimer's disease. Stud Health Technol Inform 2000; 77: 195–9.

Bertrand J-A, McIntosh AR, Postuma RB, Kovacevic N, Latreille V, Panisset M, et al. Brain Connectivity Alterations Are Associated with the Development of Dementia in Parkinson's Disease. Brain Connect 2016; 6: 216–24.

Biswal BB, Mennes M, Zuo X-N, Gohel S, Kelly C, Smith SM, et al. Toward discovery science of human brain function. Proc Natl Acad Sci 2010; 107: 4734–9.

Biundo R, Weis L, Bostantjopoulou S, Stefanova E, Falup-Pecurariu C, Kramberger MG, et al. MMSE and MoCA in Parkinson's disease and dementia with Lewy bodies: a multicenter 1-year follow-up study. J Neural Transm Vienna Austria 1996 2016; 123: 431–8.

Bočková M, Rektor I. Impairment of brain functions in Parkinson's disease reflected by alterations in neural connectivity in EEG studies: A viewpoint. Clin Neurophysiol 2019; 130: 239–47.

Bonanni L, Thomas A, Tiraboschi P, Perfetti B, Varanese S, Onofrj M. EEG comparisons in early Alzheimer's disease, dementia with Lewy bodies and Parkinson's disease with dementia patients with a 2-year follow-up. Brain 2008; 131: 690–705.

Bosboom JLW, Stoffers D, Stam CJ, van Dijk BW, Verbunt J, Berendse HW, et al. Resting state oscillatory brain dynamics in Parkinson's disease: an MEG study. Clin Neurophysiol Off J Int Fed Clin Neurophysiol 2006; 117: 2521–31.

Boser BE, Guyon IM, Vapnik VN. A Training Algorithm for Optimal Margin Classifiers. In: Proceedings of the Fifth Annual Workshop on Computational Learning Theory. New York, NY, USA: ACM; 1992. p. 144–152

Bosl WJ, Tager-Flusberg H, Nelson CA. EEG Analytics for Early Detection of Autism Spectrum Disorder: A data-driven approach. Sci Rep 2018; 8: 1–20.

Bousleiman Ha, Chaturvedi M, Gschwandtner U, Hatz F, Schindler C, Zimmermann R, et al. Alpha1/theta ratio from quantitative EEG (qEEG) as a reliable marker for mild cognitive impairment (MCI) in patients with Parkinson's disease (PD) (P2.081). Neurology 2015; 84: P2.081.

Braak H, Del Tredici K. Neuropathological Staging of Brain Pathology in Sporadic Parkinson's disease: Separating the Wheat from the Chaff. J Park Dis 2017; 7: S71–85.

Braak H, Rüb U, Gai WP, Del Tredici K. Idiopathic Parkinson's disease: possible routes by which vulnerable neuronal types may be subject to neuroinvasion by an unknown pathogen. J Neural Transm Vienna Austria 1996 2003; 110: 517–36.

Breiman L. Bagging Predictors. Mach Learn 1996; 24: 123–40.

Breiman L. Random Forests. Mach Learn 2001; 45: 5–32.

Breiman L. Random Forests. Mach Learn 2001; 45: 5–32.

Breiman L, Friedman JH, Olshen RA, Stone CJ. Classification and Regression Trees. Chapman & Hall; 1984

Brodaty H, Moore CM. The clock drawing test for dementia of the Alzheimer's type: A comparison of three scoring methods in a memory disorders clinic. Int J Geriatr Psychiatry 1997; 12: 619–27.

Buter TC, van den Hout A, Matthews FE, Larsen JP, Brayne C, Aarsland D. Dementia and survival in Parkinson disease: A 12-year population study. Neurology 2008; 70: 1017–22.

Cahn-Weiner DA, Sullivan EV, Shear PK, Fama R, Lim KO, Yesavage JA, et al. Brain structural and cognitive correlates of clock drawing performance in Alzheimer's disease. J Int Neuropsychol Soc 1999; 5: 502–9.

Cai H, Han J, Chen Y, Sha X, Wang Z, Hu B, et al. A Pervasive Approach to EEG-Based Depression Detection [Internet]. Complexity 2018[cited 2019 Aug 22] Available from: https://www.hindawi.com/journals/complexity/2018/5238028/

Carmona Arroyave JA, Tobón Quintero CA, Suárez Revelo JJ, Ochoa Gómez JF, García YB, Gómez LM, et al. Resting functional connectivity and mild cognitive impairment in Parkinson's disease. An electroencephalogram study. Future Neurol 2019; 14: FNL18.

Carmona J, Suarez J, Ochoa J. Brain Functional Connectivity in Parkinson's disease – EEG resting analysis. In: Torres I, Bustamante J, Sierra DA, editor(s). VII Latin American Congress on Biomedical Engineering CLAIB 2016, Bucaramanga, Santander, Colombia, October 26th -28th, 2016. Springer Singapore; 2017. p. 185–8

Carroll WM. The global burden of neurological disorders. Lancet Neurol 2019; 18: 418–9.

Caviness JN, Hentz JG, Belden CM, Shill HA, Driver-Dunckley ED, Sabbagh MN, et al. Longitudinal EEG Changes Correlate with Cognitive Measure Deterioration in Parkinson's Disease. J Park Dis 2015; 5: 117–24.

Caviness JN, Hentz JG, Evidente VG, Driver-Dunckley E, Samanta J, Mahant P, et al. Both early and late cognitive dysfunction affects the electroencephalogram in Parkinson's disease. Parkinsonism Relat Disord 2007; 13: 348–54.

Caviness JN, Utianski RL, Hentz JG, Beach TG, Dugger BN, Shill HA, et al. Differential spectral quantitative electroencephalography patterns between control and Parkinson's disease cohorts. Eur J Neurol 2016; 23: 387–92.

Chahine L, Stern M, Chen-Plotkin A. Blood-Based Biomarkers for Parkinson's Disease. Parkinsonism Relat Disord 2014; 20: S99-103.

Chahine LM, Urbe L, Caspell-Garcia C, Aarsland D, Alcalay R, Barone P, et al. Cognition among individuals along a spectrum of increased risk for Parkinson's disease. PLOS ONE 2018; 13: e0201964.

Chang C-C, Lin C-J. LIBSVM: A library for support vector machines. ACM Trans Intell Syst Technol 2011; 2: 1–27.

Charan J, Biswas T. How to Calculate Sample Size for Different Study Designs in Medical Research? Indian J Psychol Med 2013; 35: 121–6.

Chase TN, Fedio P, Foster NL, Brooks R, Chiro G, Mansi L. Wechsler Adult Intelligence Scale Performance: Cortical Localization by Fluorodeoxyglucose F18-Positron Emission Tomography. Arch Neurol 1984; 41: 1244–7.

Chaturvedi M, Guy Bogaarts J, Kozak (Cozac) VV, Hatz F, Gschwandtner U, Meyer A, et al. Phase Lag Index and Spectral power as QEEG features for identification of patients with Mild Cognitive Impairment in Parkinsońs disease [Internet]. Clin Neurophysiol 2019[cited 2019 Aug 13] Available from: http://www.sciencedirect.com/science/article/pii/S1388245719311630

Chaturvedi M, Hatz F, Gschwandtner U, Bogaarts JG, Meyer A, Fuhr P, et al. Quantitative EEG (QEEG) measures differentiate Parkinson's disease (PD) patients from healthy controls (HC) [Internet]. Front Aging Neurosci 2017; 9[cited 2017 Jan 13] Available from: http://journal.frontiersin.org/article/10.3389/fnagi.2017.00003/full#supplementary-material

Chen Chao, Liaw Andy. Using Random Forest to Learn Imbalanced Data. [Internet]. 2004Available from: https://www.semanticscholar.org/paper/Using-Random-Forest-to-Learn-Imbalanced-Data-Chen-Liaw/2138b37bfced70599d26dfccbf93a8e7a4b7ad85?tab=abstract

Cheng H-C, Ulane CM, Burke RE. Clinical progression in Parkinson disease and the neurobiology of axons. Ann Neurol 2010; 67: 715–25.

Coravos A, Khozin S, Mandl KD. Developing and adopting safe and effective digital biomarkers to improve patient outcomes [Internet]. NPJ Digit Med 2019; 2[cited 2019 Nov 28] Available from: https://www.ncbi.nlm.nih.gov/pmc/articles/PMC6411051/

Cortes C, Vapnik V. Support-vector networks. Mach Learn 1995; 20: 273–97.

Cozac VV. Quantitative Electroencephalography and genetics as biomarkers of dementia in Parkinson's disease [Internet]. 2017[cited 2019 Jan 24] Available from: http://edoc.unibas.ch/diss/DissB_12696

Cozac VV, Auschra B, Chaturvedi M, Gschwandtner U, Hatz F, Meyer A, et al. Among Early Appearing Non-Motor Signs of Parkinson's Disease, Alteration of Olfaction but Not Electroencephalographic Spectrum Correlates with Motor Function [Internet]. Front Neurol 2017; 8[cited 2018 Apr 9] Available from: https://www.frontiersin.org/articles/10.3389/fneur.2017.00545/full

Cozac VV, Chaturvedi M, Hatz F, Meyer A, Fuhr P, Gschwandtner U. Increase of EEG Spectral Theta Power Indicates Higher Risk of the Development of Severe Cognitive Decline in Parkinson's Disease after 3 Years [Internet]. Front Aging Neurosci 2016; 8[cited 2017 Jan 13] Available from: http://journal.frontiersin.org/article/10.3389/fnagi.2016.00284/abstract

Cozac VV, Gschwandtner U, Hatz F, Hardmeier M, Rüegg S, Fuhr P. Quantitative EEG and Cognitive Decline in Parkinson's Disease [Internet]. Park Dis 2016; 2016[cited 2018 Sep 11] Available from: https://www.ncbi.nlm.nih.gov/pmc/articles/PMC4842380/

Cummings JL, Fine MJ, Grachev ID, Jarecke CR, Johnson MK, Kuo PH, et al. Effective and efficient diagnosis of parkinsonism: the role of dopamine transporter SPECT imaging with ioflupane I-123 injection (DaTscan™). Am J Manag Care 2014; 20: S97-109.

Dauer W, Przedborski S. Parkinson's Disease: Mechanisms and Models. Neuron 2003; 39: 889–909.

Delis D, Kramer J, Ober B, Kaplan E. The California Verbal Learning Test: Administration and interpretation. San Antonio, TX: Psychological Corporation; 1987

DeLong M, Wichmann T. Changing Views of Basal Ganglia Circuits and Circuit Disorders. Clin EEG Neurosci 2010; 41: 61–7.

Delorme A, Makeig S. EEGLAB: an open source toolbox for analysis of single-trial EEG dynamics including independent component analysis. J Neurosci Methods 2004; 134: 9–21.

Demšar J. Statistical Comparisons of Classifiers over Multiple Data Sets. J Mach Learn Res 2006; 7: 1–30.

Dimitriadis SI, Liparas D. How random is the random forest? Random forest algorithm on the service of structural imaging biomarkers for Alzheimer's disease: from Alzheimer's disease neuroimaging initiative (ADNI) database. Neural Regen Res 2018; 13: 962–70.

Dimitriadis SI, Liparas D, Tsolaki MN. Random forest feature selection, fusion and ensemble strategy: Combining multiple morphological MRI measures to discriminate among healhy elderly, MCI, cMCI and alzheimer's disease patients: From the alzheimer's disease neuroimaging initiative (ADNI) database. J Neurosci Methods 2018; 302: 14–23.

Domingos P. MetaCost: A General Method for Making Classifiers Cost-sensitive. In: Proceedings of the Fifth ACM SIGKDD International Conference on Knowledge Discovery and Data Mining. New York, NY, USA: ACM; 1999. p. 155–164

Dorsey ER, Elbaz A, Nichols E, Abd-Allah F, Abdelalim A, Adsuar JC, et al. Global, regional, and national burden of Parkinson's disease, 1990–2016: a systematic analysis for the Global Burden of Disease Study 2016. Lancet Neurol 2018; 17: 939–53.

Doshi-Velez F, Kim B. Towards A Rigorous Science of Interpretable Machine Learning [Internet]. ArXiv170208608 Cs Stat 2017[cited 2019 Nov 22] Available from: http://arxiv.org/abs/1702.08608

Drouin-Ouellet J, Cicchetti F. Inflammation and neurodegeneration: the story 'retolled'. Trends Pharmacol Sci 2012; 33: 542–51.

Dubbelink KTEO, Hillebrand A, Twisk JWR, Deijen JB, Stoffers D, Schmand BA, et al. Predicting dementia in Parkinson disease by combining neurophysiologic and cognitive markers. Neurology 2014; 82: 263–70.

Duley JF, Wilkins JW, Hamby SL, Hopkins DG, Burwell RD, Barry NS. Explicit scoring criteria for the Rey-Osterrieth and Taylor complex figures. Clin Neuropsychol 1993; 7: 29–38.

Eckl, Florian. Application of the Group Lasso in the classification of Parkinson's disease. 2017

Eichelberger D, Calabrese P, Meyer A, Chaturvedi M, Hatz F, Fuhr P, et al. Correlation of Visuospatial Ability and EEG Slowing in Patients with Parkinson's Disease [Internet]. Park Dis 2017[cited 2019 Jun 10] Available from: https://www.hindawi.com/journals/pd/2017/3659784/

Elderkin-Thompson V, Boone KB, Hwang S, Kumar A. Neurocognitive profiles in elderly patients with frontotemporal degeneration or major depressive disorder. J Int Neuropsychol Soc 2004; 10: 753–71.

Emre M. Dementia associated with Parkinson's disease. Lancet Neurol 2003; 2: 229–37.

Emre M. Dementia associated with Parkinson's disease. Lancet Neurol 2003; 2: 229–37.

Emre M, Aarsland D, Brown R, Burn DJ, Duyckaerts C, Mizuno Y, et al. Clinical diagnostic criteria for dementia associated with Parkinson's disease. Mov Disord Off J Mov Disord Soc 2007; 22: 1689–707; quiz 1837.

Erro R, Picillo M, Vitale C, Amboni M, Moccia M, Santangelo G, et al. The non-motor side of the honeymoon period of Parkinson's disease and its relationship with quality of life: a 4-year longitudinal study. Eur J Neurol 2016; 23: 1673–9.

European Medicines Agency. DaTSCAN [Internet]. Eur Med Agency 2018[cited 2019 Aug 13] Available from: https://www.ema.europa.eu/en/medicines/human/EPAR/datscan

Fawcett T, Provost F. Adaptive Fraud Detection. Data Min Knowl Discov 1997; 1: 291–316.

FDA-NIH Biomarker Working Group. BEST (Biomarkers, EndpointS, and other Tools) Resource [Internet]. Silver Spring (MD): Food and Drug Administration (US); 2016[cited 2019 Nov 28] Available from: http://www.ncbi.nlm.nih.gov/books/NBK326791/

Feigin VL, Nichols E, Alam T, Bannick MS, Beghi E, Blake N, et al. Global, regional, and national burden of neurological disorders, 1990–2016: a systematic analysis for the Global Burden of Disease Study 2016. Lancet Neurol 2019; 18: 459–80.

Fereshtehnejad S-M, Montplaisir JY, Pelletier A, Gagnon J-F, Berg D, Postuma RB. Validation of the MDS research criteria for prodromal Parkinson's disease: Longitudinal assessment in a REM sleep behavior disorder (RBD) cohort: Validation of the MDS Prodromal Parkinson Research Criteria. Mov Disord 2017; 32: 865–73.

Folstein MF, Folstein SE, McHugh PR. 'Mini-mental state'. A practical method for grading the cognitive state of patients for the clinician. J Psychiatr Res 1975; 12: 189–98.

Fonseca LC, Tedrus GMAS, Letro GH, Bossoni AS. Dementia, Mild Cognitive Impairment and Quantitative EEG in Patients with Parkinson's Disease. Clin EEG Neurosci 2009; 40: 168–72.

Fontanarosa JB, Dai Y. Using LASSO regression to detect predictive aggregate effects in genetic studies. BMC Proc 2011; 5: S69.

Friedman M. A Comparison of Alternative Tests of Significance for the Problem of m Rankings. Ann Math Stat 1940; 11: 86–92.

Galbiati A, Verga L, Giora E, Zucconi M, Ferini-Strambi L. The risk of neurodegeneration in REM sleep behavior disorder: A systematic review and meta-analysis of longitudinal studies. Sleep Med Rev 2019; 43: 37–46.

Galvan A, Wichmann T. Pathophysiology of parkinsonism. Clin Neurophysiol Off J Int Fed Clin Neurophysiol 2008; 119: 1459–74.

Gao L, Wu T. The study of brain functional connectivity in Parkinson's disease [Internet]. Transl Neurodegener 2016; 5[cited 2018 Oct 31] Available from: https://www.ncbi.nlm.nih.gov/pmc/articles/PMC5086060/

Gelfand SB, Ravishankar CS, Delp EJ. An iterative growing and pruning algorithm for classification tree design. In: Conference Proceedings., IEEE International Conference on Systems, Man and Cybernetics. 1989. p. 818–23 vol.2

Geraedts VJ, Boon LI, Marinus J, Gouw AA, van Hilten JJ, Stam CJ, et al. Clinical correlates of quantitative EEG in Parkinson disease: A systematic review. Neurology 2018; 91: 871–83.

Geraedts VJ, Marinus J, Gouw AA, Mosch A, Stam CJ, van Hilten JJ, et al. Quantitative EEG reflects non-dopaminergic disease severity in Parkinson's disease. Clin Neurophysiol 2018; 129: 1748–55.

Gerfen CR. The neostriatal mosaic: multiple levels of compartmental organization. Trends Neurosci 1992; 15: 133–9.

Gerfen CR, Keefe KA, Gauda EB. D1 and D2 dopamine receptor function in the striatum: coactivation of D1- and D2-dopamine receptors on separate populations of neurons results in potentiated immediate early gene response in D1-containing neurons. J Neurosci Off J Soc Neurosci 1995; 15: 8167–76.

Gerton BK, Brown TT, Meyer-Lindenberg A, Kohn P, Holt JL, Olsen RK, et al. Shared and distinct neurophysiological components of the digits forward and backward tasks as revealed by functional neuroimaging. Neuropsychologia 2004; 42: 1781–7.

Gibb WR, Lees AJ. The relevance of the Lewy body to the pathogenesis of idiopathic Parkinson's disease. J Neurol Neurosurg Psychiatry 1988; 51: 745–52.

Girotti F, Soliveri P, Carella F, Piccolo I, Caffarra P, Musicco M, et al. Dementia and cognitive impairment in Parkinson's disease. J Neurol Neurosurg Psychiatry 1988; 51: 1498–502.

Goeman JJ. L1 Penalized Estimation in the Cox Proportional Hazards Model. Biom J 2010; 52: 70–84.

Goetz CG. Unified Parkinson's Disease Rating Scale (UPDRS) and The Movement-Disorder Society Sponsored-unified Parkinson's Disease Rating Scale (MDS-UPDRS). In: Kompoliti K, Metman LV, editor(s). Encyclopedia of Movement Disorders. Oxford: Academic Press; 2010. p. 307–9

Goetz CG, Poewe W, Rascol O, Sampaio C, Stebbins GT, Counsell C, et al. Movement Disorder Society Task Force report on the Hoehn and Yahr staging scale: Status and recommendations The Movement Disorder Society Task Force on rating scales for Parkinson's disease. Mov Disord 2004; 19: 1020–8.

Goldman JG, Litvan I. Mild Cognitive Impairment in Parkinson's Disease. Minerva Med 2011; 102: 441–59.

Goldman JG, Vernaleo BA, Camicioli R, Dahodwala N, Dobkin RD, Ellis T, et al. Cognitive impairment in Parkinson's disease: a report from a multidisciplinary symposium on unmet needs and future directions to maintain cognitive health. Npj Park Dis 2018; 4: 1–11.

Gongora M, Velasques B, Cagy M, Teixeira S, Ribeiro P. EEG coherence as a diagnostic tool to measure the initial stages of Parkinson Disease. Med Hypotheses 2019; 123: 74–8.

Gratwicke J, Jahanshahi M, Foltynie T. Parkinson's disease dementia: a neural networks perspective. Brain 2015; 138: 1454–76.

Greenland S. On sample-size and power calculations for studies using confidence intervals. Am J Epidemiol 1988; 128: 231–7.

Greffard S, Verny M, Bonnet A-M, Beinis J-Y, Gallinari C, Meaume S, et al. Motor Score of the Unified Parkinson Disease Rating Scale as a Good Predictor of Lewy Body–Associated Neuronal Loss in the Substantia Nigra. Arch Neurol 2006; 63: 584–8.

Grosch J, Winkler J, Kohl Z. Early Degeneration of Both Dopaminergic and Serotonergic Axons – A Common Mechanism in Parkinson's Disease [Internet]. Front Cell Neurosci 2016; 10[cited 2019 Jul 11] Available from: https://www.frontiersin.org/articles/10.3389/fncel.2016.00293/full

Gu Y, Chen J, Lu Y, Pan S. Integrative Frequency Power of EEG Correlates with Progression of Mild Cognitive Impairment to Dementia in Parkinson's Disease. Clin EEG Neurosci 2014

Gu Y, Chen J, Lu Y, Pan S. Integrative Frequency Power of EEG Correlates with Progression of Mild Cognitive Impairment to Dementia in Parkinson's Disease [Internet]. Clin EEG Neurosci 2014[cited 2016 Feb 29] Available from: http://eeg.sagepub.com/lookup/doi/10.1177/1550059414543796

Gupta K, Attri J, Singh A, Kaur H, Kaur G. Basic concepts for sample size calculation: Critical step for any clinical trials! Saudi J Anaesth 2016; 10: 328–31.

Haixiang G, Yijing L, Shang J, Mingyun G, Yuanyue H, Bing G. Learning from class-imbalanced data: Review of methods and applications. Expert Syst Appl 2017; 73: 220–39.

Hall M, Frank E, Holmes G, Pfahringer B, Reutemann P, Witten IH. The WEKA data mining software: an update. ACM SIGKDD Explor Newsl 2009; 11: 10.

Han C-X, Wang J, Yi G-S, Che Y-Q. Investigation of EEG abnormalities in the early stage of Parkinson's disease. Cogn Neurodyn 2013; 7: 351–9.

Han Y, Wang K, Jia J, Wu W. Changes of EEG Spectra and Functional Connectivity during an Object-Location Memory Task in Alzheimer's Disease [Internet]. Front Behav Neurosci 2017; 11[cited 2018 Sep 11] Available from: https://www.ncbi.nlm.nih.gov/pmc/articles/PMC5449767/

Handojoseno AMA, Naik GR, Gilat M, Shine JM, Nguyen TN, Ly QT, et al. Prediction of Freezing of Gait in Patients with Parkinson's Disease Using EEG Signals. Stud Health Technol Inform 2018; 246: 124–31.

Hanley JA. Simple and multiple linear regression: sample size considerations. J Clin Epidemiol 2016; 79: 112–9.

Hardmeier M, Hatz F, Bousleiman H, Schindler C, Stam CJ, Fuhr P. Reproducibility of Functional Connectivity and Graph Measures Based on the Phase Lag Index (PLI) and Weighted Phase Lag Index (wPLI) Derived from High Resolution EEG. PLOS ONE 2014; 9: e108648.

Härtig C, Markowitsch HJ, Neufeld H, Calabrese P, Deisinger K, Kessler J. Wechsler Gedächtnis Test - Revidierte Fassung. Bern: Verlag Hans Huber; 2000

Harvey PO, Le Bastard G, Pochon JB, Levy R, Allilaire JF, Dubois B, et al. Executive functions and updating of the contents of working memory in unipolar depression. J Psychiatr Res 2004; 38: 567–76.

Hassan M, Chaton L, Benquet P, Delval A, Leroy C, Plomhause L, et al. Functional connectivity disruptions correlate with cognitive phenotypes in Parkinson's disease. NeuroImage Clin 2017; 14: 591–601.

Hatz F, Hardmeier M, Bousleiman H, Rüegg S, Schindler C, Fuhr P. Reliability of fully automated versus visually controlled pre- and post-processing of resting-state EEG. Clin Neurophysiol 2015; 126: 268–74.

He R, Yan X, Guo J, Xu Q, Tang B, Sun Q. Recent Advances in Biomarkers for Parkinson's Disease [Internet]. Front Aging Neurosci 2018; 10[cited 2019 Jun 6] Available from: https://www.ncbi.nlm.nih.gov/pmc/articles/PMC6193101/

He X, Zhang Y, Chen J, Xie C, Gan R, Wang L, et al. Changes in theta activities in left posterior temporal region, left occipital region and right frontal region related to mild cognitive impairment in Parkinson's disease patients. Int J Neurosci 2016: 1–18.

He X, Zhang Y, Chen J, Xie C, Gan R, Yang R, et al. The patterns of EEG changes in early-onset Parkinson's disease patients. Int J Neurosci 2017; 127: 1028–35.

Heemels M-T. Neurodegenerative diseases. Nature 2016; 539: 179–179.

Heinik J, Solomesh I, Berkman P. Correlation between the CAMCOG, the MMSE, and three clock drawing tests in a specialized outpatient psychogeriatric service. Arch Gerontol Geriatr 2004; 38: 77–84.

Heinzel S, Berg D, Gasser T, Chen H, Yao C, Postuma RB, et al. Update of the MDS research criteria for prodromal Parkinson's disease. Mov Disord Off J Mov Disord Soc 2019

Heinzel S, Roeben B, Ben-Shlomo Y, Lerche S, Alves G, Barone P, et al. Prodromal Markers in Parkinson's Disease: Limitations in Longitudinal Studies and Lessons Learned [Internet]. Front Aging Neurosci 2016; 8[cited 2019 Jun 6] Available from: https://www.ncbi.nlm.nih.gov/pmc/articles/PMC4916171/

Heisz JJ, McIntosh AR. Applications of EEG Neuroimaging Data: Event-related Potentials, Spectral Power, and Multiscale Entropy. JoVE J Vis Exp 2013: e50131.

Herculano-Houzel S. The Human Brain in Numbers: A Linearly Scaled-up Primate Brain [Internet]. Front Hum Neurosci 2009; 3[cited 2019 Jul 31] Available from: https://www.ncbi.nlm.nih.gov/pmc/articles/PMC2776484/

Herrmann N, Kidron D, Shulman KI, Kaplan E, Binns M, Leach L, et al. Clock Tests in Depression, Alzheimer's Disease, and Elderly Controls. Int J Psychiatry Med 1998; 28: 437–47.

Hobson P, Meara J. Mild cognitive impairment in Parkinson's disease and its progression onto dementia: a 16-year outcome evaluation of the Denbighshire cohort. Int J Geriatr Psychiatry 2015; 30: 1048–55.

Hochrein A, Jonitz L, Plaum E, Engel RR. Kompetenzbeurteilung und Kompetenzmessung bei Dementen — ein Vergleich zwischen Verfahren zur Quantifizierung demenzbedingter Beeinträchtigungen des Alltagsverhaltens. In: Möller H-J, Engel RR, Hoff P, editor(s). Befunderhebung in der Psychiatrie: Lebensqualität, Negativsymptomatik und andere aktuelle Entwicklungen. Vienna: Springer; 1996. p. 113–24

Högl B, Stefani A, Videnovic A. Idiopathic REM sleep behaviour disorder and neurodegeneration — an update. Nat Rev Neurol 2018; 14: 40–55.

Hughes AJ, Daniel SE, Kilford L, Lees AJ. Accuracy of clinical diagnosis of idiopathic Parkinson's disease: a clinico-pathological study of 100 cases. J Neurol Neurosurg Psychiatry 1992; 55: 181–4.

Hughes AJ, Daniel SE, Lees AJ. The clinical features of Parkinson's disease in 100 histologically proven cases. Adv Neurol 1993; 60: 595–9.

Hummel T, Konnerth CG, Rosenheim K, Kobal G. Screening of olfactory function with a four-minute odor identification test: reliability, normative data, and investigations in patients with olfactory loss. Ann Otol Rhinol Laryngol 2001; 110: 976–81.

Iranzo A, Lomeña F, Stockner H, Valldeoriola F, Vilaseca I, Salamero M, et al. Decreased striatal dopamine transporter uptake and substantia nigra hyperechogenicity as risk markers of synucleinopathy in patients with idiopathic rapid-eye-movement sleep behaviour disorder: a prospective study [corrected]. Lancet Neurol 2010; 9: 1070–7.

Isaacs B, Kennie AT. The Set Test as an Aid to the Detection of Dementia in Old People. Br J Psychiatry 1973; 123: 467–70.

Ishihara L, Brayne C. A systematic review of depression and mental illness preceding Parkinson's disease. Acta Neurol Scand 2006; 113: 211–20.

Jacobs J, Hwang G, Curran T, Kahana MJ. EEG oscillations and recognition memory: Theta correlates of memory retrieval and decision making. NeuroImage 2006; 32: 978–87.

Janvin CC, Larsen JP, Aarsland D, Hugdahl K. Subtypes of mild cognitive impairment in parkinson's disease: Progression to dementia. Mov Disord 2006; 21: 1343–9.

Jennings D, Siderowf A, Stern M, Seibyl J, Eberly S, Oakes D, et al. Conversion to Parkinson Disease in the PARS Hyposmic and Dopamine Transporter-Deficit Prodromal Cohort. JAMA Neurol 2017; 74: 933–40.

Jeromin A, Bowser R. Biomarkers in Neurodegenerative Diseases. In: Beart P, Robinson M, Rattray M, Maragakis NJ, editor(s). Neurodegenerative Diseases: Pathology, Mechanisms, and Potential Therapeutic Targets. Cham: Springer International Publishing; 2017. p. 491–528

Jesus-Ribeiro J, Freire A, Sargento-Freitas J, Sousa M, Silva F, Moreira F, et al. Transcranial Sonography and DaTSCAN in Early Stage Parkinson's Disease and Essential Tremor. Eur Neurol 2016; 76: 252–5.

Joachims T. Text categorization with Support Vector Machines: Learning with many relevant features. In: Nédellec C, Rouveirol C, editor(s). Machine Learning: ECML-98. Springer Berlin Heidelberg; 1998. p. 137–42

Johannesen JK, Bi J, Jiang R, Kenney JG, Chen C-MA. Machine learning identification of EEG features predicting working memory performance in schizophrenia and healthy adults [Internet]. Neuropsychiatr Electrophysiol 2016; 2[cited 2016 Oct 19] Available from: http://www.npepjournal.com/content/2/1/3

Johnson DK, Langford Z, Garnier-Villarreal M, Morris JC, Galvin JE. Onset of Mild Cognitive Impairment in Parkinson Disease: Alzheimer Dis Assoc Disord 2016; 30: 127–33.

Jozwiak N, Postuma RB, Montplaisir J, Latreille V, Panisset M, Chouinard S, et al. REM Sleep Behavior Disorder and Cognitive Impairment in Parkinson's Disease [Internet]. Sleep 2017; 40[cited 2019 Aug 13] Available from: https://academic.oup.com/sleep/article/40/8/zsx101/3884498

Kaida K, Takahashi M, Åkerstedt T, Nakata A, Otsuka Y, Haratani T, et al. Validation of the Karolinska sleepiness scale against performance and EEG variables. Clin Neurophysiol 2006; 117: 1574–81.

Kalia LV, Lang AE. Parkinson's disease. The Lancet 2015; 386: 896–912.

Kamei S, Morita A, Serizawa K, Mizutani T, Hirayanagi K. Quantitative EEG analysis of executive dysfunction in Parkinson disease. J Clin Neurophysiol Off Publ Am Electroencephalogr Soc 2010; 27: 193–7.

Karádi K, Lucza T, Aschermann Z, Komoly S, Deli G, Bosnyák E, et al. Visuospatial impairment in Parkinson's disease: The role of laterality. Laterality 2015; 20: 112–27.

Kassambara A. ggcorrplot: Visualization of a Correlation Matrix using ‘ggplot2’ [Internet]. 2018[cited 2018 Oct 18] Available from: https://CRAN.R-project.org/package=ggcorrplot

Khodayari-Rostamabad A, Reilly JP, Hasey GM, de Bruin H, MacCrimmon DJ. A machine learning approach using EEG data to predict response to SSRI treatment for major depressive disorder. Clin Neurophysiol 2013; 124: 1975–85.

Kim J-H. Estimating classification error rate: Repeated cross-validation, repeated hold-out and bootstrap. Comput Stat Data Anal 2009; 53: 3735–45.

Kirby M, Denihan A, Bruce I, Coakley D, Lawlor BA. The clock drawing test in primary care: sensitivity in dementia detection and specificity against normal and depressed elderly. Int J Geriatr Psychiatry 2001; 16: 935–40.

Klassen BT, Hentz JG, Shill HA, Driver-Dunckley E, Evidente VGH, Sabbagh MN, et al. Quantitative EEG as a predictive biomarker for Parkinson disease dementia. Neurology 2011; 77: 118–24.

Klein LK. Vergleichende neuropsychologische Untersuchungen bei älteren Patienten mit früh und spät beginnenden depressiven Störungen unter besonderer Berücksichtigung von Uhrentests, Universität Tübingen.

Kobal G, Hummel T, Sekinger B, Barz S, Roscher S, Wolf S. ‘Sniffin’ sticks’: screening of olfactory performance. Rhinology 1996; 34: 222–6.

Kornhuber HH. Prävention von Demenz (einschließlich Alzheimer-Krankheit). Gesundheitswesen 2004; 67: 346–51.

Krawczyk B. Learning from imbalanced data: open challenges and future directions. Prog Artif Intell 2016; 5: 221–32.

Kuhn M. The caret Package [Internet]. [cited 2019 Mar 7] Available from: http://topepo.github.io/caret/index.html

Laatu S, Revonsuo A, Pihko L, Portin R, Rinne JO. Visual object recognition deficits in early Parkinson’s disease. Parkinsonism Relat Disord 2004; 10: 227–33.

Lanciego JL, Luquin N, Obeso JA. Functional Neuroanatomy of the Basal Ganglia [Internet]. Cold Spring Harb Perspect Med 2012; 2[cited 2019 Aug 13] Available from: https://www.ncbi.nlm.nih.gov/pmc/articles/PMC3543080/

Lanskey JH, McColgan P, Schrag AE, Acosta-Cabronero J, Rees G, Morris HR, et al. Can neuroimaging predict dementia in Parkinson’s disease? Brain 2018; 141: 2545–60.

de Lau LML, Giesbergen PCLM, de Rijk MC, Hofman A, Koudstaal PJ, Breteler MMB. Incidence of parkinsonism and Parkinson disease in a general population: the Rotterdam Study. Neurology 2004; 63: 1240–4.

Lawson RA, Yarnall AJ, Duncan GW, Breen DP, Khoo TK, Williams-Gray CH, et al. Stability of mild cognitive impairment in newly diagnosed Parkinson’s disease. J Neurol Neurosurg Psychiatry 2017; 88: 648–52.

Lee DY, Seo EH, Choo IH, Kim SG, Lee JS, Lee DS, et al. Neural Correlates of the Clock Drawing Test Performance in Alzheimer's Disease: A FDG-PET Study. Dement Geriatr Cogn Disord 2008; 26: 306–13.

Levin BE, Llabre MM, Reisman S, Weiner WJ, Sanchez-Ramos J, Singer C, et al. Visuospatial impairment in Parkinson's disease. Neurology 1991; 41: 365.

Levy G, Schupf N, Tang M-X, Cote LJ, Louis ED, Mejia H, et al. Combined effect of age and severity on the risk of dementia in Parkinson's disease. Ann Neurol 2002; 51: 722–9.

Li D-H, He Y-C, Liu J, Chen S-D. Diagnostic Accuracy of Transcranial Sonography of the Substantia Nigra in Parkinson's disease: A Systematic Review and Meta-analysis. Sci Rep 2016; 6: 20863.

Liaw, A. & Wiener, M. Classification and Regression by randomForest., R News: The Newsletter of the R Project 2 (3) , 18-22 . 2002

Liepelt I, Behnke S, Schweitzer K, Wolf B, Godau J, Wollenweber F, et al. Pre-motor signs of PD are related to SN hyperechogenicity assessed by TCS in an elderly population. Neurobiol Aging 2011; 32: 1599–606.

Liepelt-Scarfone I, Brändle B, Yilmaz R, Gauss K, Schaeffer E, Timmers M, et al. Progression of prodromal motor and non-motor symptoms in the premotor phase study - 2-year follow-up data. Eur J Neurol 2017; 24: 1369–74.

Liepelt-Scarfone I, Gauss K, Maetzler W, Müller K, Bormann C, Berger MF, et al. Evaluation of Progression Markers in the Premotor Phase of Parkinson's Disease: The Progression Markers in the Premotor Phase Study. Neuroepidemiology 2013; 41: 174–82.

Liepelt-Scarfone I, Gauss K, Maetzler W, Müller K, Bormann C, Fruhmann Berger M, et al. Evaluation of progression markers in the premotor phase of Parkinson's disease: the progression markers in the premotor phase study. Neuroepidemiology 2013; 41: 174–82.

Liepelt-Scarfone I, Lerche S, Behnke S, Godau J, Gaenslen A, Pausch C, et al. Clinical characteristics related to worsening of motor function assessed by the Unified Parkinson's Disease Rating Scale in the elderly population. J Neurol 2015; 262: 451–8.

Litvan I, Goldman JG, Tröster AI, Schmand BA, Weintraub D, Petersen RC, et al. Diagnostic criteria for mild cognitive impairment in Parkinson's disease: Movement Disorder Society Task Force guidelines. Mov Disord 2012; 27: 349–56.

Lötsch J, Schiffmann S, Schmitz K, Brunkhorst R, Lerch F, Ferreiros N, et al. Machine-learning based lipid mediator serum concentration patterns allow identification of multiple sclerosis patients with high accuracy [Internet]. Sci Rep 2018; 8[cited 2019 Jan 29] Available from: https://www.ncbi.nlm.nih.gov/pmc/articles/PMC6173715/

Lovinger DM. Communication Networks in the Brain. Alcohol Res Health 2008; 31: 196–214.

Magrinelli F, Picelli A, Tocco P, Federico A, Roncari L, Smania N, et al. Pathophysiology of Motor Dysfunction in Parkinson's Disease as the Rationale for Drug Treatment and Rehabilitation [Internet]. Park Dis 2016[cited 2019 May 23] Available from: https://www.hindawi.com/journals/pd/2016/9832839/

Mahlknecht P, Gasperi A, Djamshidian A, Kiechl S, Stockner H, Willeit P, et al. Performance of the Movement Disorders Society criteria for prodromal Parkinson's disease: A population-based 10-year study: MDS Criteria Performance for Prodromal PD. Mov Disord 2018; 33: 405–13.

Mahlknecht P, Gasperi A, Willeit P, Kiechl S, Stockner H, Willeit J, et al. Prodromal Parkinson's disease as defined per MDS research criteria in the general elderly community: Prodromal PD in the Community. Mov Disord 2016; 31: 1405–8.

Mahlknecht P, Seppi K, Poewe W. The Concept of Prodromal Parkinson's Disease. J Park Dis 2015; 5: 681–97.

Manuel AL, Nicastro N, Schnider A, Guggisberg AG. Resting-state connectivity after visuo-motor skill learning is inversely associated with offline consolidation in Parkinson's disease and healthy controls. Cortex 2018; 106: 237–47.

Marder K, Tang MX, Mejia H, Alfaro B, Côté L, Louis E, et al. Risk of Parkinson's disease among first-degree relatives: A community-based study. Neurology 1996; 47: 155–60.

Matsuoka T, Narumoto J, Okamura A, Taniguchi S, Kato Y, Shibata K, et al. Neural correlates o. The components o. The clock drawing test. Int Psychogeriatr 2013; 25: 1317–23.

Matsuoka T, Narumoto J, Shibata K, Okamura A, Nakamura K, Nakamae T, et al. Neural correlates of performance on the different scoring systems of the clock drawing test. Neurosci Lett 2011; 487: 421–5.

Mavaddat N, Michailidou K, Dennis J, Lush M, Fachal L, Lee A, et al. Polygenic Risk Scores for Prediction of Breast Cancer and Breast Cancer Subtypes. Am J Hum Genet 2019; 104: 21–34.

Melgari J-M, Curcio G, Mastrolilli F, Salomone G, Trotta L, Tombini M, et al. Alpha and beta EEG power reflects L-dopa acute administration in parkinsonian patients. Front Aging Neurosci 2014; 6: 302.

Melrose RJ, Harwood D, Khoo T, Mandelkern M, Sultzer DL. Association between cerebral metabolism and Rey–Osterrieth Complex Figure Test performance in Alzheimer's disease. J Clin Exp Neuropsychol 2013; 35: 246–58.

Memory Clinic NPZ. Memory Clinic NPZ [Internet]. Consort Establ Regist Alzheimers Dis CERAD-Plus[cited 2019 May 24] Available from: https://www.memoryclinic.ch/de/main-navigation/neuropsychologen/cerad-plus/

Meng X, D'Arcy C. Education and Dementia in the Context of the Cognitive Reserve Hypothesis: A Systematic Review with Meta-Analyses and Qualitative Analyses [Internet]. PLoS ONE 2012; 7[cited 2019 Oct 17] Available from: https://www.ncbi.nlm.nih.gov/pmc/articles/PMC3366926/

Meyer D, Wien TU. Support Vector Machines. The Interface to libsvm in package e1071. Online-Documentation of the package e1071 for "R. 2001

Miley AÅ, Kecklund G, Åkerstedt T. Comparing two versions of the Karolinska Sleepiness Scale (KSS). Sleep Biol Rhythms 2016; 14: 257–60.

Miller AM, Miocinovic S, Swann NC, Rajagopalan SS, Darevsky DM, Gilron R, et al. Effect of levodopa on electroencephalographic biomarkers of the parkinsonian state. J Neurophysiol 2019; 122: 290–9.

Mirelman A, Saunders-Pullman R, Alcalay RN, Shustak S, Thaler A, Gurevich T, et al. Application of the Movement Disorder Society prodromal criteria in healthy *G2019S - LRRK2* carriers: Prodromal Criteria Nonmanifesting LRRK2 Carriers. Mov Disord 2018; 33: 966–73.

Mitchell TM. Machine Learning. 1st ed. New York, NY, USA: McGraw-Hill, Inc.; 1997

Monastero R, Cicero CE, Baschi R, Davì M, Luca A, Restivo V, et al. Mild cognitive impairment in Parkinson's disease: the Parkinson's disease cognitive study (PACOS). J Neurol 2018; 265: 1050–8.

Morgan ML, Witte EA, Cook IA, Leuchter AF, Abrams M, Siegman B. Influence of age, gender, health status, and depression on quantitative EEG. Neuropsychobiology 2005; 52: 71–6.

Morita A, Kamei S, Serizawa K, Mizutani T. The Relationship Between Slowing EEGs and the Progression of Parkinson's Disease. J Clin Neurophysiol 2009; 26: 426.

Morley JF, Cohen A, Silveira-Moriyama L, Lees AJ, Williams DR, Katzenschlager R, et al. Optimizing olfactory testing for the diagnosis of Parkinson's disease: item analysis of the university of Pennsylvania smell identification test. Npj Park Dis 2018; 4: 1–7.

Morris JC, Heyman A, Mohs RC, Hughes JP, van Belle G, Fillenbaum G, et al. The Consortium to Establish a Registry for Alzheimer's Disease (CERAD). Part I. Clinical and neuropsychological assessment of Alzheimer's disease. Neurology 1989; 39: 1159–65.

Mostile G, Giuliano L, Monastero R, Luca A, Cicero CE, Donzuso G, et al. Electrocortical networks in Parkinson's disease patients with Mild Cognitive Impairment. The PaCoS study. Parkinsonism Relat Disord 2019

Moustafa AA, Chakravarthy S, Phillips JR, Gupta A, Keri S, Polner B, et al. Motor symptoms in Parkinson's disease: A unified framework. Neurosci Biobehav Rev 2016; 68: 727–40.

Movement Disorder Society Task Force on Rating Scales for Parkinson's D. The Unified Parkinson's Disease Rating Scale (UPDRS): Status and recommendations. Mov Disord 2003; 18: 738–50.

Musaeus CS, Engedal K, Høgh P, Jelic V, Mørup M, Naik M, et al. Oscillatory connectivity as a diagnostic marker of dementia due to Alzheimer's disease. Clin Neurophysiol 2019; 130: 1889–99.

Muslimović D, Post B, Speelman JD, Schmand B. Cognitive profile of patients with newly diagnosed Parkinson disease. Neurology 2005; 65: 1239.

Nichols E, Szoeke CEI, Vollset SE, Abbasi N, Abd-Allah F, Abdela J, et al. Global, regional, and national burden of Alzheimer's disease and other dementias, 1990–2016: a systematic analysis for the Global Burden of Disease Study 2016. Lancet Neurol 2019; 18: 88–106.

Nick TG, Campbell KM. Logistic regression. Methods Mol Biol Clifton NJ 2007; 404: 273–301.

Nombela C, Rowe JB, Winder-Rhodes SE, Hampshire A, Owen AM, Breen DP, et al. Genetic impact on cognition and brain function in newly diagnosed Parkinson's disease: ICICLE-PD study. Brain 2014; 137: 2743–58.

Noyce AJ, Bestwick JP, Silveira-Moriyama L, Hawkes CH, Knowles CH, Hardy J, et al. PREDICT-PD: Identifying risk of Parkinson's disease in the community: methods and baseline results. J Neurol Neurosurg Psychiatry 2014; 85: 31–7.

Noyce AJ, Dickson J, Rees RN, Bestwick JP, Isaias IU, Politis M, et al. Dopamine reuptake transporter-single-photon emission computed tomography and transcranial sonography as imaging markers of prediagnostic Parkinson's disease: Dat-Spect and TCS in subjects at risk of PD. Mov Disord 2018; 33: 478–82.

Noyce AJ, Lees AJ, Schrag A-E. The prediagnostic phase of Parkinson's disease. J Neurol Neurosurg Psychiatry 2016; 87: 871–8.

Ogawa T, Fujii S, Kuya K, Kitao S, Shinohara Y, Ishibashi M, et al. Role of Neuroimaging on Differentiation of Parkinson's Disease and Its Related Diseases. Yonago Acta Med 2018; 61: 145–55.

Olde Dubbelink KTE, Hillebrand A, Stoffers D, Deijen JB, Twisk JWR, Stam CJ, et al. Disrupted brain network topology in Parkinson's disease: a longitudinal magnetoencephalography study. Brain 2014; 137: 197–207.

Olde Dubbelink KTE, Stoffers D, Deijen JB, Twisk JWR, Stam CJ, Hillebrand A, et al. Resting-state functional connectivity as a marker of disease progression in Parkinson's disease: A longitudinal MEG study. NeuroImage Clin 2013; 2: 612–9.

Özyurt IB, Brown GG. Knowledge Discovery via Machine Learning for Neurodegenerative Disease Researchers. In: Astakhov V, editor(s). Biomedical Informatics. Totowa, NJ: Humana Press; 2009. p. 173–96

Pak K, Kim K, Lee MJ, Lee JM, Kim BS, Kim S-J, et al. Correlation between the availability of dopamine transporter and olfactory function in healthy subjects. Eur Radiol 2018; 28: 1756–60.

Pascual-Marqui RD. Standardized low-resolution brain electromagnetic tomography (sLORETA): technical details. Methods Find Exp Clin Pharmacol 2002; 24 Suppl D: 5–12.

Pedersen KF, Larsen JP, Tysnes O-B, Alves G. Natural course of mild cognitive impairment in Parkinson disease. Neurology 2017; 88: 767.

Pellecchia MT, Picillo M, Santangelo G, Longo K, Moccia M, Erro R, et al. Cognitive performances and DAT imaging in early Parkinson's disease with mild cognitive impairment: a preliminary study. Acta Neurol Scand 2015; 131: 275–81.

Pena D, Barman A, Suescun J, Jiang X, Schiess MC, Giancardo L, et al. Quantifying Neurodegenerative Progression With DeepSymNet, an End-to-End Data-Driven Approach [Internet]. Front Neurosci 2019; 13[cited 2019 Nov 20] Available from: https://www.frontiersin.org/articles/10.3389/fnins.2019.01053/full

Pereira JB, Junqué C, Martí M-J, Ramirez-Ruiz B, Bargalló N, Tolosa E. Neuroanatomical substrate of visuospatial and visuoperceptual impairment in Parkinson's disease. Mov Disord 2009; 24: 1193–9.

Petersen RC, Caracciolo B, Brayne C, Gauthier S, Jelic V, Fratiglioni L. Mild cognitive impairment: a concept in evolution. J Intern Med 2014; 275: 214–28.

Pfeiffer RF. Non-motor symptoms in Parkinson's disease. Parkinsonism Relat Disord 2016; 22: S119–22.

Ph.D DAC. E. Strauss, E. M. S. Sherman, & O. Spreen, A Compendium of Neuropsychological Tests: Administration, Norms, and Commentary. Appl Neuropsychol 2007; 14: 62–3.

Pilotto A, Heinzel S, Suenkel U, Lerche S, Brockmann K, Roeben B, et al. Application of the movement disorder society prodromal Parkinson's disease research criteria in 2 independent prospective cohorts: Application of Research Criteria For Prodromal PD. Mov Disord 2017; 32: 1025–34.

Pinto E, Peters R. Literature Review of the Clock Drawing Test as a Tool for Cognitive Screening. Dement Geriatr Cogn Disord 2009; 27: 201–13.

Ploenes C, Sharp S, Martin M. [The Clock Test: drawing a clock for detection of cognitive disorders in geriatric patients]. Z Gerontol 1994; 27: 246–52.

Pochet NLMM, Suykens J a. K. Support vector machines versus logistic regression: improving prospective performance in clinical decision-making. Ultrasound Obstet Gynecol 2006; 27: 607–8.

Poewe W, Gauthier S, Aarsland D, Leverenz JB, Barone P, Weintraub D, et al. Diagnosis and management of Parkinson's disease dementia. Int J Clin Pract 2008; 62: 1581–7.

Pohlert T. PMCMRplus: Calculate Pairwise Multiple Comparisons of Mean Rank Sums Extended [Internet]. 2018[cited 2019 Feb 4] Available from: https://CRAN.R-project.org/package=PMCMRplus

Ponsen MM, Stam CJ, Bosboom JLW, Berendse HW, Hillebrand A. A three dimensional anatomical view of oscillatory resting-state activity and functional connectivity in Parkinson's disease related dementia: An MEG study using atlas-based beamforming. NeuroImage Clin 2013; 2: 95–102.

Postuma RB, Berg D. Advances in markers of prodromal Parkinson disease. Nat Rev Neurol 2016; 12: 622–34.

Postuma RB, Iranzo A, Hu M, Högl B, Boeve BF, Manni R, et al. Risk and predictors of dementia and parkinsonism in idiopathic REM sleep behaviour disorder: a multicentre study. Brain 2019; 142: 744–59.

Purves D, Augustine GJ, Fitzpatrick D, Katz LC, LaMantia A-S, McNamara JO, et al. Excitatory and Inhibitory Postsynaptic Potentials [Internet]. Neurosci 2nd Ed 2001[cited 2019 Aug 21] Available from: https://www.ncbi.nlm.nih.gov/books/NBK11117/

Quinlan JR. Induction of decision trees. Mach Learn 1986; 1: 81–106.

Quinlan JR. Simplifying decision trees. Int J Man-Mach Stud 1987; 27: 221–34.

Quinn CR, Harris A, Felmingham K, Boyce P, Kemp A. The impact of depression heterogeneity on cognitive control in major depressive disorder. Aust N Z J Psychiatry 2012; 46: 1079–88.

R Core Team. R: A language and environment for statistical computing. R Foundation for Statistical Computing, Vienna, Austria. URL https://www.R-project.org/. [Internet]. 2018Available from: http://www.R-project.org/.

Rana AQ, Ghouse AT, Govindarajan R. Basics of Electroencephalography (EEG). In: Rana AQ, Ghouse AT, Govindarajan R, editor(s). Neurophysiology in Clinical Practice. Cham: Springer International Publishing; 2017. p. 3–9

Ranganathan P, Pramesh CS, Aggarwal R. Common pitfalls in statistical analysis: Logistic regression. Perspect Clin Res 2017; 8: 148–51.

Raymond JL, Medina JF. Computational Principles of Supervised Learning in the Cerebellum. Annu Rev Neurosci 2018; 41: 233–53.

Refaeilzadeh P, Tang L, Liu H. Cross-Validation. In: LIU L, ÖZSU MT, editor(s). Encyclopedia of Database Systems. Boston, MA: Springer US; 2009. p. 532–8

Regard M, Strauss E, Knapp P. Children's production on verbal and non-verbal fluency tasks. Percept Mot Skills 1982; 55: 839–44.

Reiman EM, Quiroz YT, Fleisher AS, Chen K, Velez-Pardo C, Jimenez-Del-Rio M, et al. Brain imaging and fluid biomarker analysis in young adults at genetic risk for autosomal dominant Alzheimer's disease in the presenilin 1 E280A kindred: a case-control study. Lancet Neurol 2012; 11: 1048–56.

Reitan RM. The relation of the trail making test to organic brain damage. J Consult Psychol 1955; 19: 393–4.

Revelle W. psych: Procedures for Psychological, Psychometric, and Personality Research [Internet]. 2018[cited 2018 Oct 18] Available from: https://CRAN.R-project.org/package=psych

Riedel O, Klotsche J, Förstl H, Wittchen H-U. Clock Drawing Test: Is It Useful for Dementia Screening in Patients Having Parkinson Disease With and Without Depression? J Geriatr Psychiatry Neurol 2013; 26: 151–7.

Rietdijk CD, Perez-Pardo P, Garssen J, van Wezel RJA, Kraneveld AD. Exploring Braak's Hypothesis of Parkinson's Disease [Internet]. Front Neurol 2017; 8[cited 2019 Aug 2] Available from: https://www.ncbi.nlm.nih.gov/pmc/articles/PMC5304413/

de la Riva P, Smith K, Xie SX, Weintraub D. Course of psychiatric symptoms and global cognition in early Parkinson disease. Neurology 2014; 83: 1096–103.

Rokach L, Maimon O. Decision Trees. In: Maimon O, Rokach L, editor(s). Data Mining and Knowledge Discovery Handbook. Boston, MA: Springer US; 2005. p. 165–92

Rosenow F, Klein KM, Hamer HM. Non-invasive EEG evaluation in epilepsy diagnosis. Expert Rev Neurother 2015; 15: 425–44.

Ross GW, Abbott RD, Petrovitch H, Tanner CM, White LR. Pre-motor features of Parkinson's disease: the Honolulu-Asia Aging Study experience. Parkinsonism Relat Disord 2012; 18: S199–202.

Ruffini G, Ibañez D, Castellano M, Dubreuil-Vall L, Soria-Frisch A, Postuma R, et al. Deep Learning With EEG Spectrograms in Rapid Eye Movement Behavior Disorder. Front Neurol 2019; 10: 806.

Salzberg SL. C4.5: Programs for Machine Learning by J. Ross Quinlan. Morgan Kaufmann Publishers, Inc., 1993. Mach Learn 1994; 16: 235–40.

Sanyal J, Banerjee TK, Rao VR. Dementia and Cognitive Impairment in Patients With Parkinson's Disease From India: A 7-Year Prospective Study. Am J Alzheimers Dis Other Demen 2014; 29: 630–6.

Sarapas C, Shankman SA, Harrow M, Goldberg JF. Parsing trait and state effects of depression severity on neurocognition: Evidence from a 26-year longitudinal study. J Abnorm Psychol 2012; 121: 830–7.

Sarica A, Cerasa A, Quattrone A. Random Forest Algorithm for the Classification of Neuroimaging Data in Alzheimer's Disease: A Systematic Review [Internet]. Front Aging Neurosci 2017; 9[cited 2019 Jan 29] Available from: https://www.frontiersin.org/articles/10.3389/fnagi.2017.00329/full

Savica R, Rocca WA, Ahlskog JE. When Does Parkinson Disease Start? [Internet]. Arch Neurol 2010; 67[cited 2016 Jul 6] Available from: http://archneur.jamanetwork.com/article.aspx?doi=10.1001/archneurol.2010.135

Schmidt MT, Kanda PAM, Basile LFH, da Silva Lopes HF, Baratho R, Demario JLC, et al. Index of Alpha/Theta Ratio of the Electroencephalogram: A New Marker for Alzheimer's Disease [Internet]. Front Aging Neurosci 2013; 5[cited 2016 Jan 13] Available from: http://journal.frontiersin.org/article/10.3389/fnagi.2013.00060/abstract

Schneider A, Hommel G, Blettner M. Linear Regression Analysis. Dtsch Ärztebl Int 2010; 107: 776–82.

Schrag A, Barone P, Brown RG, Leentjens AFG, McDonald WM, Starkstein S, et al. Depression rating scales in Parkinson's disease: Critique and recommendations. Mov Disord 2007; 22: 1077–92.

Schrag A, Jahanshahi M, Quinn N. What contributes to quality of life in patients with Parkinson's disease? J Neurol Neurosurg Psychiatry 2000; 69: 308–12.

Schrag A, Siddiqui UF, Anastasiou Z, Weintraub D, Schott JM. Clinical variables and biomarkers in prediction of cognitive impairment in patients with newly diagnosed Parkinson's disease: a cohort study. Lancet Neurol 2017; 16: 66–75.

Schubach M, Re M, Robinson PN, Valentini G. Imbalance-Aware Machine Learning for Predicting Rare and Common Disease-Associated Non-Coding Variants. Sci Rep 2017; 7: 2959.

Seifert KD, Wiener JI. The impact of DaTscan on the diagnosis and management of movement disorders: A retrospective study. Am J Neurodegener Dis 2013; 2: 29–34.

Serizawa K, Kamei S, Morita A, Hara M, Mizutani T, Yoshihashi H, et al. Comparison of quantitative EEGs between Parkinson disease and age-adjusted normal controls. J Clin Neurophysiol Off Publ Am Electroencephalogr Soc 2008; 25: 361–6.

Shobha G, Rangaswamy S. Chapter 8 - Machine Learning. In: Gudivada VN, Rao CR, editor(s). Handbook of Statistics. Elsevier; 2018. p. 197–228

Shon JM, Lee DY, Seo EH, Sohn BK, Kim JW, Park SY, et al. Functional neuroanatomical correlates of the executive clock drawing task (CLOX) performance in Alzheimer's disease: A FDG-PET study. Neuroscience 2013; 246: 271–80.

Shulman KI. Clock-drawing: Is it the ideal cognitive screening test? Int J Geriatr Psychiatry 2000; 15: 548–61.

Shulman LM, Gruber-Baldini AL, Anderson KE, Fishman PS, Reich SG, Weiner WJ. The Clinically Important Difference on the Unified Parkinson's Disease Rating Scale. Arch Neurol 2010; 67: 64–70.

Signaevsky M, Prastawa M, Farrell K, Tabish N, Baldwin E, Han N, et al. Artificial intelligence in neuropathology: deep learning-based assessment of tauopathy. Lab Invest 2019; 99: 1019–29.

Sing T, Sander O, Beerenwinkel N, Lengauer T. ROCR: visualizing classifier performance in R. Bioinformatics 2005; 21: 3940–1.

Singal AG, Mukherjee A, Joseph Elmunzer B, Higgins PDR, Lok AS, Zhu J, et al. Machine Learning Algorithms Outperform Conventional Regression Models in Predicting Development of Hepatocellular Carcinoma. Am J Gastroenterol 2013; 108: 1723–30.

Singh A, Richardson SP, Narayanan N, Cavanagh JF. Mid-frontal theta activity is diminished during cognitive control in Parkinson's disease. Neuropsychologia 2018; 117: 113–22.

Singh G, Vadera M, Samavedham L, Lim EC-H. Multiclass Diagnosis of Neurodegenerative Diseases: A Neuroimaging Machine-Learning-Based Approach. Ind Eng Chem Res 2019; 58: 11498–505.

Smajlovic D, Ibrahimagic OC. Transcranial Brain Sonography in Parkinson's Disease and Other Parkinsonian Disorders: a Hospital Study from Tuzla, Bosnia and Herzegovina. Med Arch 2017; 71: 261–4.

Sperandei S. Understanding logistic regression analysis. Biochem Medica 2014; 24: 12–8.

Sporns O, Tononi G, Kötter R. The Human Connectome: A Structural Description of the Human Brain. PLOS Comput Biol 2005; 1: e42.

Spreen O, Strauss E. A compendium of neuropsychological tests. New York: Oxford University Press; 1998

Stam CJ, Nolte G, Daffertshofer A. Phase lag index: assessment of functional connectivity from multi channel EEG and MEG with diminished bias from common sources. Hum Brain Mapp 2007; 28: 1178–93.

Steffens DC, Potter GG. Geriatric depression and cognitive impairment. Psychol Med 2008; 38: 163–75.

Stern Y. Cognitive reserve. Neuropsychologia 2009; 47: 2015–28.

Stiasny-Kolster K, Mayer G, Schäfer S, Möller JC, Heinzel-Gutenbrunner M, Oertel WH. The REM sleep behavior disorder screening questionnaire--a new diagnostic instrument. Mov Disord Off J Mov Disord Soc 2007; 22: 2386–93.

Stoffers D, Bosboom JLW, Deijen JB, Wolters EC, Berendse HW, Stam CJ. Slowing of oscillatory brain activity is a stable characteristic of Parkinson's disease without dementia. Brain 2007; 130: 1847–60.

Stoffers D, Bosboom JLW, Deijen JB, Wolters ECh, Stam CJ, Berendse HW. Increased cortico-cortical functional connectivity in early-stage Parkinson's disease: An MEG study. NeuroImage 2008; 41: 212–22.

Strimbu K, Tavel JA. What are Biomarkers? Curr Opin HIV AIDS 2010; 5: 463–6.

Strobl C, Boulesteix A-L, Zeileis A, Hothorn T. Bias in random forest variable importance measures: Illustrations, sources and a solution. BMC Bioinformatics 2007; 8: 25.

Sturm W. Willmes K. Horn W. LPS 50+ - Leistungsprüfsystem für 50-bis 90-Jährige – Hogrefe, Verlag für Psychologie [Internet]. 1993[cited 2019 May 24] Available from: https://www.testzentrale.de/shop/leistungspruefsystem-fuer-50-bis-90-jaehrige.html

Suchowersky O, Reich S, Perlmutter J, Zesiewicz T, Gronseth G, Weiner WJ, et al. Practice Parameter: diagnosis and prognosis of new onset Parkinson disease (an evidence-based review): report of the Quality Standards Subcommittee of the American Academy of Neurology. Neurology 2006; 66: 968–75.

Suenderhauf C, Hammann F, Huwyler J. Computational prediction of blood-brain barrier permeability using decision tree induction. Mol Basel Switz 2012; 17: 10429–45.

Sunwoo J-S, Lee S, Kim J-H, Lim J-A, Kim T-J, Byun J-I, et al. Altered Functional Connectivity in Idiopathic Rapid Eye Movement Sleep Behavior Disorder: A Resting-State EEG Study [Internet]. Sleep 2017; 40[cited 2019 Jun 21] Available from: https://academic.oup.com/sleep/article-lookup/doi/10.1093/sleep/zsx058

Sveinbjornsdottir S. The clinical symptoms of Parkinson's disease. J Neurochem 2016; 139: 318–24.

Talabis MRM, McPherson R, Miyamoto I, Martin JL, Kaye D. Chapter 1 - Analytics Defined. In: Talabis MRM, McPherson R, Miyamoto I, Martin JL, Kaye D, editor(s). Information Security Analytics. Boston: Syngress; 2015. p. 1–12

Tewes U. HAWIE-R: Hamburg-Wechsler-Intelligenztest für Erwachsene ; Revision 1991. Bern: Huber; 1991

Thalmann B, Spiegel R, Staehelin H. Dementia screening in general practice: Optimised scoring for the clock drawing test. Brain Aging 2002; 2: 36–43.

Thurstone LL. Primary mental abilities. Science 1948; 108: 585.

Tibshirani R. Regression Shrinkage and Selection via the Lasso. J R Stat Soc Ser B Methodol 1996; 58: 267–88.

Tibshirani R. Regression Shrinkage and Selection via the Lasso. J R Stat Soc Ser B Methodol 1996; 58: 267–88.

Tibshirani R. THE LASSO METHOD FOR VARIABLE SELECTION IN THE COX MODEL. Stat Med 1997; 16: 385–95.

Tin Kam Ho. The random subspace method for constructing decision forests. IEEE Trans Pattern Anal Mach Intell 1998; 20: 832–44.

Tomlinson CL, Stowe R, Patel S, Rick C, Gray R, Clarke CE. Systematic review of levodopa dose equivalency reporting in Parkinson's disease. Mov Disord 2010; 25: 2649–53.

Tong S, Chang E. Support Vector Machine Active Learning for Image Retrieval. In: Proceedings of the Ninth ACM International Conference on Multimedia. New York, NY, USA: ACM; 2001. p. 107–118

Tripoliti EE, Fotiadis DI, Argyropoulou M. A supervised method to assist the diagnosis and monitor progression of Alzheimer's disease using data from an fMRI experiment. Artif Intell Med 2011; 53: 35–45.

Tucha O. Lange KW. TL-D - Turm von London – Deutsche Version – Hogrefe, Verlag für Psychologie [Internet]. 2004[cited 2019 May 24] Available from: https://www.testzentrale.ch/shop/turm-von-london-deutsche-version.html

Tysnes O-B, Storstein A. Epidemiology of Parkinson's disease. J Neural Transm 2017; 124: 901–5.

Tzourio-Mazoyer N, Landeau B, Papathanassiou D, Crivello F, Etard O, Delcroix N, et al. Automated Anatomical Labeling of Activations in SPM Using a Macroscopic Anatomical Parcellation of the MNI MRI Single-Subject Brain. NeuroImage 2002; 15: 273–89.

Ungerleider LG, Haxby JV. 'What' and 'where' in the human brain. Curr Opin Neurobiol 1994; 4: 157–65.

United Nations, Department of Economic and Social Affairs,Population Division. World Population Prospects 2019: Ten Key Findings. [Internet]. 2019Available from: https://population.un.org/wpp/Publications/Files/WPP2019_10KeyFindings.pdf

Van Den Eeden SK, Tanner CM, Bernstein AL, Fross RD, Leimpeter A, Bloch DA, et al. Incidence of Parkinson's disease: Variation by age, gender, and race/ethnicity. Am J Epidemiol 2003; 157: 1015–22.

Vecchio F, Miraglia F, Maria Rossini P. Connectome: Graph theory application in functional brain network architecture. Clin Neurophysiol Pract 2017; 2: 206–13.

Veropoulos K, Campbell C, Cristianini N. Controlling the Sensitivity of Support Vector Machines. In: Proceedings of the International Joint Conference on AI. 1999. p. 55–60

Walczak TS, Chokroverty S. Chapter 12 - Electroencephalography, Electromyography, and Electro-Oculography: General Principles and Basic Technology. In: Chokroverty S, editor(s). Sleep Disorders Medicine (Third Edition). Philadelphia: W.B. Saunders; 2009. p. 157–81

Walker Z, Possin KL, Boeve BF, Aarsland D. Non-Alzheimer's dementia 2. Lancet Lond Engl 2015; 386: 1683–97.

Wang H, Xu Q, Zhou L. Large Unbalanced Credit Scoring Using Lasso-Logistic Regression Ensemble [Internet]. PLoS ONE 2015; 10[cited 2019 Oct 12] Available from: https://www.ncbi.nlm.nih.gov/pmc/articles/PMC4338292/

Warden C, Hwang J, Marshall A, Fenesy M, Poston KL. The effects of dopamine on digit span in Parkinson's disease. J Clin Mov Disord 2016; 3: 5.

Warrington EK, James M, Maciejewski C. The WAIS as a lateralizing and localizing diagnostic instrument: A study of 656 patients with unilateral cerebral lesions. Neuropsychologia 1986; 24: 223–39.

Watson GS, Cholerton BA, Gross RG, Weintraub D, Zabetian CP, Trojanowski JQ, et al. Neuropsychological assessment in collaborative Parkinson's disease research. Alzheimers Dement J Alzheimers Assoc 2013; 9: 609–14.

Watson GS, Leverenz JB. Profile of Cognitive Impairment in Parkinson Disease. Brain Pathol Zurich Switz 2010; 20: 640–5.

Wechsler D, Härting C. Wechsler-Gedächtnistest - revidierte Fassung: WMS-R ; deutsche Adaptation der revidierten Fassung der Wechsler Memory scale von David Wechsler. Bern: Huber; 2004

Weil RS, Costantini AA, Schrag AE. Mild Cognitive Impairment in Parkinson's Disease—What Is It? Curr Neurol Neurosci Rep 2018; 18: 17.

Welch P. The use of fast Fourier transform for the estimation of power spectra: A method based on time averaging over short, modified periodograms. IEEE Trans Audio Electroacoustics 1967; 15: 70–3.

Wen M-C, Chan LL, Tan LCS, Tan EK. Mild cognitive impairment in Parkinson's disease: a distinct clinical entity? [Internet]. Transl Neurodegener 2017; 6[cited 2019 Mar 19] Available from: https://www.ncbi.nlm.nih.gov/pmc/articles/PMC5596909/

Wenning GK, Tison F, Seppi K, Sampaio C, Diem A, Yekhlef F, et al. Development and validation of the Unified Multiple System Atrophy Rating Scale (UMSARS). Mov Disord 2004; 19: 1391–402.

WHO International Programme on Chemical Safety Biomarkers in Risk Assessment: Validity and Validation. Biomarkers In Risk Assessment: Validity And Validation (EHC 222, 2001) [Internet]. 2001[cited 2019 Nov 28] Available from: http://www.inchem.org/documents/ehc/ehc/ehc222.htm#1.0

Wilde MC, Boake C, Sherer M. Wechsler adult intelligence scale-revised block design broken configuration errors in nonpenetrating traumatic brain injury. Appl Neuropsychol 2000; 7: 208–14.

Williams-Gray CH, Foltynie T, Brayne CEG, Robbins TW, Barker RA. Evolution of cognitive dysfunction in an incident Parkinson's disease cohort. Brain 2007; 130: 1787–98.

Williams-Gray CH, Mason SL, Evans JR, Foltynie T, Brayne C, Robbins TW, et al. The CamPaIGN study of Parkinson's disease: 10-year outlook in an incident population-based cohort. J Neurol Neurosurg Psychiatry 2013; 84: 1258–64.

Wood K-L, Myall DJ, Livingston L, Melzer TR, Pitcher TL, MacAskill MR, et al. Different PD-MCI criteria and risk of dementia in Parkinson's disease: 4-year longitudinal study. NPJ Park Dis 2016; 2: 15027.

World Health Organization. The ICD-10 classification of mental and behavioural disorders : diagnostic criteria for research [Internet]. 1992[cited 2019 May 24] Available from: https://apps.who.int/iris/handle/10665/37108

World Health Organization. Dementia Fact Sheet 2019 [Internet]. [cited 2019 Aug 7] Available from: https://www.who.int/news-room/fact-sheets/detail/dementia

World Medical Association Declaration of Helsinki. Recommendations Guiding Physicians in Biomedical Research Involving Human Subjects | JAMA | JAMA Network [Internet]. 1997[cited 2019 May 24] Available from: https://jamanetwork.com/journals/jama/fullarticle/414713

Wu G, Chang EY. Adaptive feature-space conformal transformation for imbalanced-data learning. In: in The Twentieth International Conference on Machine Learning (ICML-2003), (Washington DC. 2003. p. 816–823

Wu TT, Chen YF, Hastie T, Sobel E, Lange K. Genome-wide association analysis by lasso penalized logistic regression. Bioinformatics 2009; 25: 714–21.

Wyss-Coray T. Ageing, neurodegeneration and brain rejuvenation. Nature 2016; 539: 180–6.

Xu J, Zhang Y, Qiu C, Cheng F. Global and regional economic costs of dementia: a systematic review. The Lancet 2017; 390: S47.

Yaar I, Shapiro MB. A quantitative study of the electroencephalographic response to levodopa treatment in parkinsonian patients. Clin EEG Electroencephalogr 1983; 14: 82–5.

Yarnall AJ, Rochester L, Burn DJ. Mild cognitive impairment in Parkinson's disease. Age Ageing 2013; 42: 567–76.

Zaltieri M, Longhena F, Pizzi M, Missale C, Spano P, Bellucci A. Mitochondrial Dysfunction and α-Synuclein Synaptic Pathology in Parkinson's Disease: Who's on First? Park Dis 2015; 2015: 108029.

Zhang H, Alberts E, Pongratz V, Mühlau M, Zimmer C, Wiestler B, et al. Predicting conversion from clinically isolated syndrome to multiple sclerosis–An imaging-based machine learning approach [Internet]. NeuroImage Clin 2018[cited 2019 Jan 29] Available from: http://www.sciencedirect.com/science/article/pii/S2213158218303413

Zimmermann P. Fimm B. Testbatterie zur AufmerksamkeitsprUfung (Version 1.7). Herzogenrath: Psytests; 2002. [Internet]. 2002[cited 2019 May 24] Available from: https://www.psytest.net/index.php?page=TAP-2-2&hl=de_DE

Zimmermann P, Fimm B. Testbatterie zur Aufmerksamkeitsprüfung. Herzogenrath: Psytest Psychologische Testsysteme; 2007

Zimmermann R, Gschwandtner U, Hatz F, Schindler C, Bousleiman H, Ahmed S, et al. Correlation of EEG Slowing with Cognitive Domains in Nondemented Patients with Parkinson's Disease. Dement Geriatr Cogn Disord 2015; 39: 207–14.

Zimmermann R, Gschwandtner U, Hatz F, Schindler C, Bousleiman H, Ahmed S, et al. Correlation of EEG Slowing with Cognitive Domains in Nondemented Patients with Parkinson's Disease. Dement Geriatr Cogn Disord 2015; 39: 207–14.

Zou J, Weng R-H, Chen Z-Y, Wei X-B, Wang R, Chen D, et al. Position Emission Tomography/Single-Photon Emission Tomography Neuroimaging for Detection of Premotor Parkinson's Disease. CNS Neurosci Ther 2016; 22: 167–77.

The Unified Parkinson's Disease Rating Scale (UPDRS): Status and recommendations. Mov Disord 2003; 18: 738–50.

Sniffin' Sticks & Taste Strips - Tobacco industry, Medical devices & Prototype construction [Internet]. [cited 2019 Aug 13] Available from: https://www.burghart-mt.de/en/medical-devices/sniffin-sticks-taste-strips.html